8-19-2015 12:00 AM

Metal-Ligand Cooperative Catalysis and Methods for Metal Removal from Organic Transformations

John-Paul J. Bow
The University of Western Ontario

Supervisor
Johanna M. Blacquiere
The University of Western Ontario

Graduate Program in Chemistry
A thesis submitted in partial fulfillment of the requirements for the degree in Master of Science

METAL-LIGAND COOPERATIVE CATALYSIS AND METHODS FOR METAL REMOVAL FROM ORGANIC TRANSFORMATIONS

by

John-Paul James Bow

Graduate Program in Chemistry

A thesis submitted in partial fulfillment
of the requirements for the degree of
Master of Science

The School of Graduate and Postdoctoral Studies
The University of Western Ontario
London, Ontario, Canada

Abstract

Organometallic catalysis has revolutionized the synthesis of complex organic molecules. Methods for C-C, C-X and C-H bond formation and cleavage are exploited throughout the areas of fine chemicals synthesis, with major applications for pharmaceuticals. This situation raises duel challenges: 1) high-performance catalysts for environmentally and economically sustainable synthesis and 2) efficient methods of catalyst (i.e. metal) removal must be identified. This work tackles both of these areas. The highly tunable cooperative $P^{R}{}_{2}N^{R'}{}_{2}$ ligands have been implemented for the first time for catalytic organic transformations. I show that $[Ru(Cp)(P^{tBu}{}_{2}N^{Bn}{}_{2})(MeCN)][PF_6]$ is an effective catalyst for the cyclization of alkynyl alcohols and have characterized a deactivated species, $[Ru(Cp)(P^{tBu}{}_{2}N^{Bn}{}_{2})(-C{=}CHPh)][PF_6]$, from the attempted hydration of alkynes. Directions in metal removal from catalytic reactions have been investigated, using both a solid-supported catalyst and an insoluble metal scavenger.

Keywords

Inorganic, Chemistry, Organometallic, Catalysis, Homogeneous, Ruthenium, Rhodium, Palladium, Polymer, and Scavenger.

Co-Authorship Statement

Sections 3.1-3.7 have been published by John-Paul Bow and all work was performed by him except for the X-ray crystallographic analysis, which was performed by Paul D. Boyle.

John-Paul J. Bow, Paul D. Boyle, Johanna M. Blacquiere*, European Journal of Inorganic Chemistry, 2015, Accepted.

Section 4.2 The metal scavenging work was initiated by Erin Evoy, a joint Chem 4491 student with the Blacquiere and Ragogna groups. All work reported here was completed by John-Paul Bow.

Acknowledgments

First and foremost I would like to express my extreme gratitude to my supervisor Johanna M. Blacquiere. Under Johanna's supervision I have become a much better chemist both in and out of the lab. Without Johanna's help much of what I have written would be an incomprehensive mess. Johanna told me at the beginning of my degree that there are a lot of downs in grad school so you have to make sure to celebrate the little victories when you can. These words are very important to live by not just in grad school, but in life.

I would like to express my gratitude to John F. Corrigan and Paul J. Ragogna for sharing their instruments and lab space with us in our early days. The chemistry department's research staff are thanked greatly for their assistance: Mat Willans for his assistance with NMR spectroscopy, Paul Boyle for his X-ray expertise, Doug Hairsine for allowing me to commandeer his GC-MS; Kristina Jurcic and Jasmine Wang are thanked for acquiring MALDI data. Everyone in the electronics shop is thanked for building a good portion of our equipment without which some experiments would have been very tedious.

The Puddephatt lab (or Chemstores 2.0 as the Blacquiere group calls it) is thanked for lending us chemicals and glassware on a regular basis. I'm grateful that Richard, James, and Jeremy were always up for sharing a pint on those tough days. The Blacquiere group members Richard, James, and Ava are thanked for their constructive criticism, helpful suggestions and an enjoyable day-to-day life in the lab. My friends are thanked for all the enjoyable and unforgettable adventures, which allowed me to get through this degree without completely hating my life.

Finally, I would like to thank my parents for always supporting me even though they told me I wasn't allowed to become a professional student and stay in school forever. Without your support and inspiration none of this would have been possible.

Abbreviations

Bn	Benzyl
bipy	2,2'-bipyridine
COSY	Correlation spectroscopy
Cp	Cyclopentadienyl
Cp*	Pentamethylcyclopentadienyl
2D	Two-dimensional
DCM	Dichloromethane
dppm	1,1-Bis(diphenylphosphino)methane
dppp	1,3-Bis(diphenylphosphino)propane
E	Element
EMEA	European Medicines Agency
GC-FID	Gas chromatography flame ionization detection
GC-MS	Gas chromatography mass spectrometry
H_2IMes	1,3-Bis(2,4,6-trimethylphenyl)-4,5-dihydroimidazol-2-ylidene
HDMF	Protonated dimethylformamide
HMBC	Heteronuclear multiple bond correlation
HSQC	Heteronuclear single quantum coherence
Hz	Hertz
I	Intermediate

ICH	The International Conference on Harmonisation of Technical Requirements for Registration of Pharmaceuticals for Human Use
ICP-MS	Inductively coupled plasma mass spectrometry
IR	Infrared
L	Ligand
M	Metal
MALDI-TOF	Matrix assisted laser desorption ionization-time of flight
MeCN	Acetonitrile
MLC	Metal-ligand cooperative
MS	Mass spectrometry
m/z	Mass-to-charge ratio
NMR	Nuclear magnetic resonance
ORTEP	Oak ridge thermal ellipsoid plot program
OTf	Trifluoroacetate
P	Product
ppm	Parts per million (μg/g)
$P^{R}{}_{2}N^{R'}{}_{2}$	(1,5-R'-3,7-R-1,5-diaza-3,7-diphosphacyclooctane)
PTFE	Polytetrafluoroethylene
S	Substrate
^{t}Bu	tert-Butyl

THF	Tetrahydrofuran
TOF	Turnover frequency
TON	Turnover number
UV-Vis	Ultraviolet-visible
XRD	X-ray diffraction

Table of Contents

List of Tables

List of Schemes

List of Figures

List of Appendices

Chapter 1

1 Introduction

1.1 Organometallic Catalysis

A catalyst is any substance that changes the rate of a reaction and is not consumed by the progression of the reaction.[1] A catalyst mediates the conversion of a substrate molecule to the product, but then must be regenerated to the active catalyst form. The catalyst is then primed to turnover more substrate to product. A catalyst can either be heterogeneous such as palladium on carbon or homogeneous such as the Grubbs catalyst $RuCl_2(H_2IMes)(PCy_3)$. A heterogeneous catalyst is in a different phase than that of the reactants and products whereas a homogeneous catalyst is in the same phase. Approximately 80% of all chemical processes involve a catalyst.[2] Not only do catalysts facilitate the synthesis of many chemicals they also reduce large amounts of chemical waste by reducing the need for stoichiometric reagents. The pharmaceutical and fine chemical industries rely heavily on catalysts.[3] Many reactions would not be possible without the presence of a catalyst or would be too costly for large-scale production. There is still a need for new catalysts because many uncatalyzed processes are wasteful, inefficient or inaccessible.[4]

There are many types of catalysts including biological, acid/base, organic, and organometallic catalysts. Organometallic compounds contain a metal centre and a hydrocarbon-metal bond. These organic fragment bonded to the metal centre are known as ligands. Ligands can affect the sterics and electronics of a metal, which affect how a substrate interacts with the catalyst. Ligands can be highly functionalized allowing for tunability of the sterics and electronics around the metal centre. This tunability allows for many catalysts to be developed for different purposes. In a traditional organometallic catalytic cycle the first step is binding of substrate to the metal centre. Following binding of substrate it can be converted to a reaction intermediate either by the catalyst or an

additive that may be present. Finally, the product is made and it is kicked out of the catalytic cycle regenerating the active catalyst, which can then interact with substrate again (Scheme 1).

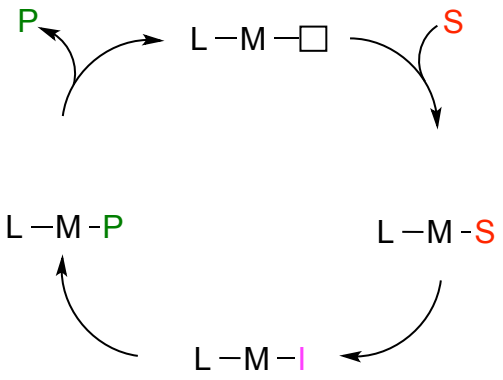

Scheme 1. Traditional organometallic catalytic cycle: S = Substrate, P = Product, I = Intermediate, M = Metal, L = Ligand, □ = Empty Coordination Site

1.2 Metal-Ligand Cooperative Catalysis

Metal-ligand cooperative (MLC) catalysis is where both the metal and the ligand are involved in the formation of product (Scheme 2). Some ligands can interact with the substrate and if this interaction assists in the turnover it is considered a cooperative effect. Ligand-mediated interactions can assist in certain steps of the reaction, which may have required an additive to proceed in traditional organometallic catalysis. These ligand-mediated interactions are intramolecular[5] allowing for faster reactions to occur. Cooperative ligands can assist in proton transfer, hydrogen bonding, dynamic coordination, and redox non-innocence.

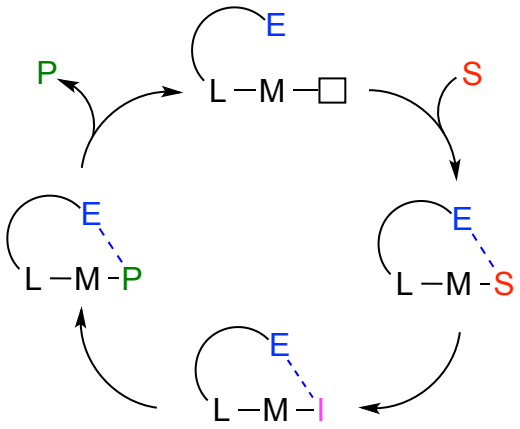

Scheme 2. Metal-ligand cooperative catalytic cycle: S = Substrate, P = Product, I = Intermediate, M = Metal, L = Ligand, E = Element, □ = Empty Coordination Site

1.2.1 Proton Transfer MLC

Proton transfer is a common subset of MLC catalysis with many examples in hydrogenation, dehydrogenation, dehydrogenative coupling, and hydration reactions. Noyori[6], Morris[7], Milstein[8], and others have designed catalysts that are capable of proton transfer for hydrogenation or dehydrogenation (Figure 1).

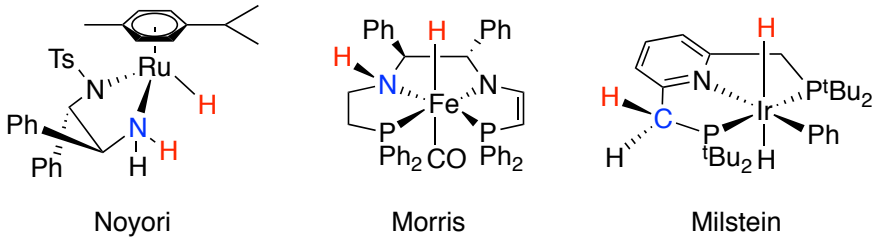

Figure 1. A subset of known proton transfer metal-ligand cooperative catalysts where the acidic/basic site is shown in blue

The acidic/basic site of the ligand mediates the proton transfer steps in MLC catalysis. Altering the basicity or sterics of the site may affect catalyst reactivity in either a positive or negative way. Effective MLC catalysts can be challenging to design because a balance

of the sterics, electronics of the primary coordination sphere and the properties of the acidic/basic sites must be found.

1.2.2 $P^{R}_{2}N^{R'}_{2}$ Ligands

The cooperative family of $P^{R}_{2}N^{R'}_{2}$ (1,5-R'-3,7-R-1,5-diaza-3,7-diphosphacyclooctane) ligands[9] are an eight membered ring that contain two amines and two phosphines. The $P^{R}_{2}N^{R'}_{2}$ ligands[9,10,11,12,13] bind to late metals through the two phosphines in a κ^2-fashion creating two pendant amines capable of proton shuttling (Figure 2).

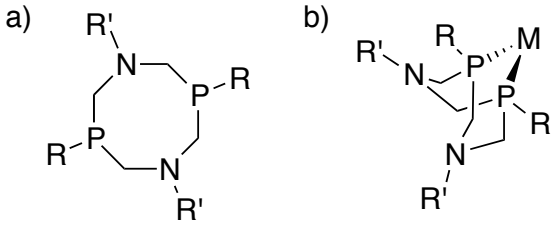

Figure 2. General structure of a) the $P^{R}_{2}N^{R'}_{2}$ ligand family; and b) κ^2-P,P coordination of the $P^{R}_{2}N^{R'}_{2}$ ligand to a metal centre

The ligand framework is flexible allowing for the amines to come close to the metal centre. The R groups of the ligand allow for modularity of the steric and electronics which can effect the metal by either altering the electron-density at the metal or the steric protection at the metal. The basicity and sterics of the pendant amines can directly be influenced by altering[14] the R' groups of the ligand. Extensive work with the $P^{R}_{2}N^{R'}_{2}$ ligands has been done in electrocatalytic processes for fuel generation and use. There have been many examples of $[Ni(P^{R}_{2}N^{R'}_{2})_2]^{2+}$ complexes for the oxidation and production of H_2[15], reduction of CO_2[16], oxidation of alcohols[17], and oxidation of formate[18], all of which involve a proton transfer step. However, the $P^{R}_{2}N^{R'}_{2}$ ligands have not yet been used for catalytic organic transformations. I postulate that they will be capable of proton transfer steps in organic transformations and because of the high modularity very useful for catalyst design and performance assessment.

1.2.3 Catalytic Hydration of Alkynes

The selective hydration of terminal alkynes is an attractive process because it allows for an atom-economic synthesis of the anti-Markovnikov aldehyde product (Scheme 3). The hydration of alkynes is performed using water as a green reagent where there are no byproducts from the catalytic cycle.

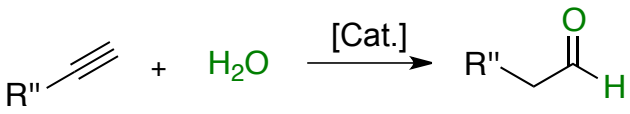

Scheme 3. Catalytic hydration of terminal alkynes

Hydroboration, a common alternative synthesis of aldehydes from alkynes, produces stoichiometric boron-containing byproducts. The hydroboration[19] method consumes more reagents and produces more waste than the direct catalytic hydration reaction. The first reported catalysts for the anti-Markovnikov hydration of alkynes were the ruthenium chloride cyclopentyldienyl(dppm) complexes, **A**, developed by Wakatsuki[20] (Figure 3). These complexes did not contain a pendant base and gave only moderate conversion. A new generation of catalysts were discovered by Grotjahn and co-workers; these complexes contained a pendant amine capable of cooperative catalysis. These new ruthenium cyclopentyldienyl complexes, **B**, had two imidazolyl-phosphine ligands with a bulky R group on the imidazolyl, **C**. These ligands were capable of proton transfer and greatly outperformed the previously known systems. The bulky R group on the ligand prevented the coordination of the pendant amine to the metal centre, which subsequently deactivates the complex. Hintermann and co-workers[5,21,22,23] showed that only one imidazolyl-phosphane ligand, **D**, is required for the catalytic hydration but the bulky R groups were still required to prevent deactivation (Figure 3).

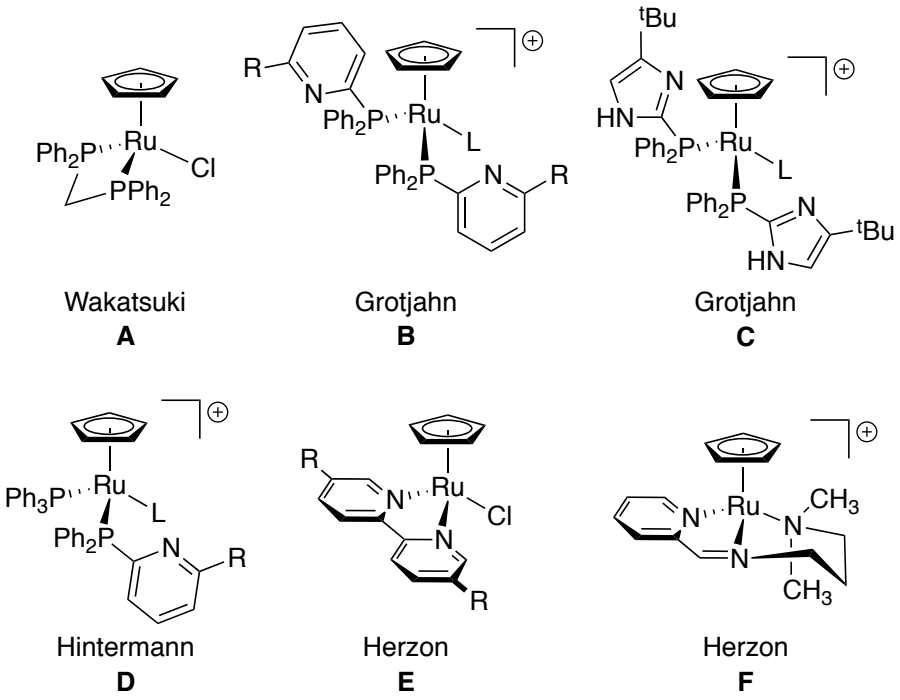

Figure 3. Subset of catalysts for the hydration of terminal alkynes

The proposed catalytic cycle for the cooperative hydration of alkynes first involves alkyne coordination to the ruthenium centre (Scheme 4). This is followed by isomerization to generate a vinylidene intermediate. The metal-vinylidene can then undergo nucleophilic attack by water at the alpha carbon. Through a series of proton transfer steps the aldehyde product is then generated along with the active catalyst. In each of the steps of the catalytic cycle a proton transfer step occurs in which the pendant amine can assist. Grotjahn[24] has reported that to reduce the deactivation of the complex bulky R groups are important to prevent the binding of the pendant amine on the metal centre and to the substrate. Smaller substrates can be attacked by the pendant amine during the catalytic cycle. However, increasing the bulk on the ligands hinders the attack by water and catalyst deactivation.[24] The P-donor catalysts designed by Grotjahn[25] and Hintermann[19,26,27] are limited in their tunability of sterics and electronics.

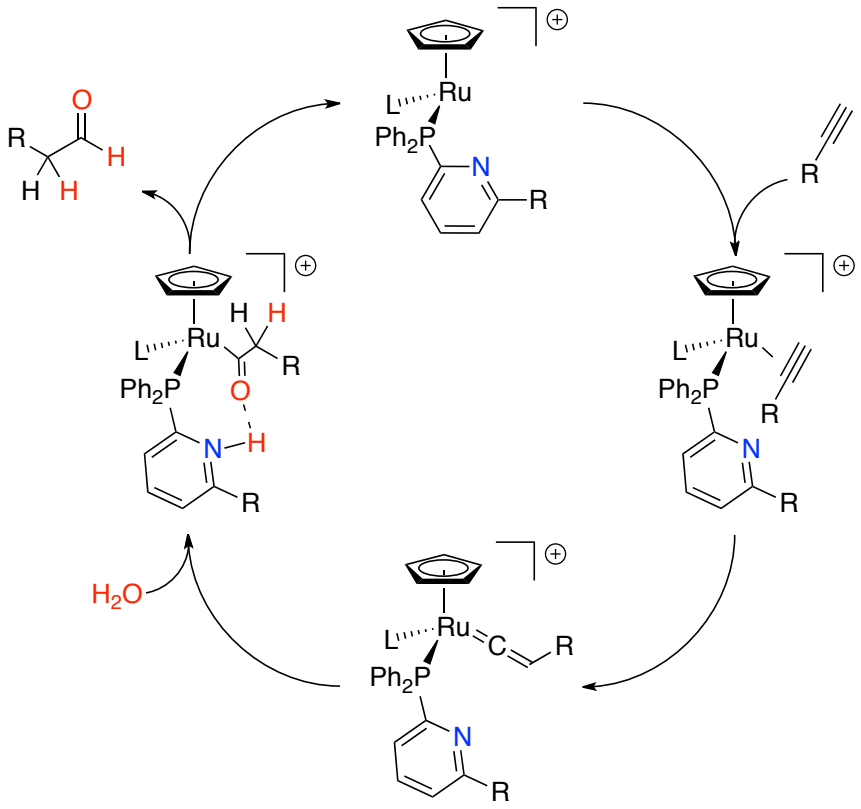

Scheme 4. Proposed catalytic cycle for the hydration of alkynes

The reactivity of metal-vinylidene species is greatly affected by the electron donating ability of the ancillary ligands on the metal.[28,29] If the ancillary ligands are strong electron donors the metal centre becomes more electron rich, which increases back bonding into the vinylidene moiety. However, if the metal centre is electron-deficient the α-carbon of the vinylidene becomes very electrophilic and more susceptible to nucleophilic attack. During the course of this work Herzon *et al.* [31,32,33] developed an N-donor catalyst, which dramatically outperforms the previous catalysts systems in both activity and scope. The initial bipy style catalyst Herzon[31] developed, **E**, is not thought to proceed through a cooperative mechanism but allows for a large variety of tuning of the sterics and electronics by functionalization of the bipy ligand. However, a second catalyst, **F**, was developed that is thought to proceed though a cooperative mechanism.[32]

1.2.4 Catalytic Cyclization of Alkynyl Alcohols

The synthesis of heterocyclic biaryl compounds is highly desirable for pharmaceuticals because they can be easily mapped onto more complex compounds of interest. Benzofurans and indoles are often common frameworks for pharmaceuticals and natural products.[33] An interesting method for synthesizing these compounds is through the cyclization of alkynyl alcohols or amines. These cyclization reactions can be a convenient and easy method for the synthesis of high value organic compounds. Varying the length of the linker between the alkyne and alcohol or amine functionality, products with different ring sizes can be accessed. Previous methods for cyclizing alkynyl alcohols include transition metal catalyzed cyclization, metal-free Lewis and Brønsted acid/base catalysts, and enantioselective organo-catalysts.[34] The metal catalyzed synthesis of these biaryl compounds is similar to the hydration of terminal alkynes. But instead of having an intermolecular nucleophilic attack by water, an intramolecular attack by the alcohol or amine affords the cyclized product. Saa *et al.*[35] proposed that a catalytic cycle for the cyclization of alkynyl alcohols involves very similar steps to the catalytic hydration of alcohols (Scheme 5).

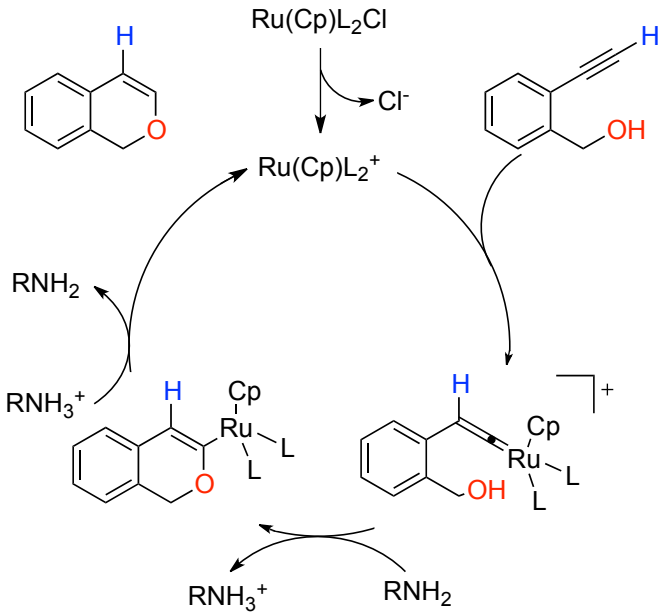

Scheme 5. Catalytic cycle for the cyclization of alkynyl alcohols

Grotjahn *et al.*[36] reports the probable mechanism of the reaction starts with the formation of the ruthenium-vinylidene, followed by attack of the electrophilic alpha carbon by the pendant amine or alcohol and loss of the proton on the heteroatom is facilitated by an acidic/basic site on the ligand. The product then dissociates from the metal regenerating the active catalyst and giving the heterocyclic product. Many hydration catalysts (see Figure 3, catalyst **B**) are also used in these cyclization reactions. Saa[35] *et al.* reports the use of a non-cooperative catalyst capable of cyclizing alkynyl alcohols; however, a base must be present in the reaction for it to occur.

1.3 Metal Removal from High Value Products

The use of metal catalysts for organic transformations creates the problem of having products contaminated with metal. Removal of the metal to an acceptable level can be challenging. However, many pharmaceuticals cannot be synthesized without the use of transition metal catalysts. Traditional purification methods, including column chromatography, crystallization, and extraction may not be efficient enough to remove

the metal to an acceptable standard.[37] Crystallization and extraction are the main industrial techniques used for the purification of large scale reactions.[38] However, these may not be suitable for some chemicals and the alternative method of chromatography can be very challenging and expensive on industrial-scale reactions.[38] Acceptable levels in pharmaceuticals must have an oral concentration lower than 5 ppm for platinum group metals in order to meet EMEA and ICH (European Medicines Agency, The International Conference on Harmonisation of Technical Requirements for Registration of Pharmaceuticals for Human Use) guidelines.[39] Residual metal from early synthetic steps can create side reactions or give low yields in later stages of the synthesis.[38, 39] The use of palladium has become very popular for cross-coupling reactions allowing for a wide variety of products to be synthesized.[3] Without the use of palladium many pharmaceuticals would not be accessible. With this wide-scale implementation of transition metal catalysts efficient metal removal is very important in order to meet the acceptable levels.[3] Ruthenium- or molybdenum-catalyzed olefin metathesis is also a very powerful synthetic tool for carbon-carbon bond formation in both organic synthesis and polymerization reactions.[40, 41] However, due to the difficulty of removing the ruthenium-based catalysts it has not been widely implemented in industry.[42]

Certain catalysts have been specially designed to ease metal removal by methods such as filtration or extraction. For example, a catalyst can be designed with a ligand that binds irreversibly to silica.[42] However, since the ligand mediates the removal, this method requires non-trivial modification of each catalyst employed. In order for these specialty catalysts to be implemented they must be capable of giving high turnover numbers (TONs), promote reactivity in low activity substrates, and preferable work at lower temperatures, if not they cannot compete with the catalysts that are already in place.

1.3.1 Solid Supported Catalysis

Solid-supported catalysts are becoming more attractive because they utilize the strengths of heterogeneous and homogeneous catalysts. The ability to tune the catalyst properties

through ligand structure is a major advantage of homogeneous catalysts over heterogeneous systems. However, catalyst separation from target products is significantly easier in the latter systems. Mechanistic studies of homogenous molecular catalysts are performed more readily than heterogeneous catalysts. Mechanistic insight to catalytic cycles can provide very useful information on how to make a catalyst better to produce higher yields or purer products. Xiao *et al.* report a group of diphosphine-containing polymers capable of binding a rhodium catalyst that is a pertinent example of a supported homogeneous catalyst. The solid supported catalysts demonstrate high activity for the hydroformylation of olefins, are highly selective and are easily separated from the reaction mixture. Xiao *et al.* propose the catalysts are acting in a homogeneous fashion but are heterogeneous in nature.[43]

1.3.2 Metal Scavenging

Typical problems associated with solid supported catalysts include lower performance, they are not commercially available, they are much more expensive, and leeching of metal can be problematic.[37,44] These drawbacks have helped lead to the development of metal scavengers. Development of scavengers for easy homogeneous catalyst removal has become a large field for the separation of precious metals from high-value products. There are different types of scavengers; for example, phosphines can be bound to an insoluble resin that, after binding to a metal, are easily separated from soluble organics by filtration.[44] An ideal scavenger would be capable of binding to different metals, remove all the metal quickly, and be regenerated for multiple uses. Some mesoporous silicates have been shown to be highly effective at removing palladium from solution.[37] The QuadraPure scavengers are commercially available and are functionalized macroporous polystyrene beads.[45] Depending on the functionalization of the bead, different metals can be scavenged with very high removal.[45] However, there is still a need to design more scavengers that are cheaper, have broader applicability, and can be regenerated.

1.4 References

(1) Hartwig, J. *Organotransition Metal Chemistry: From Bonding to Catalysis*, 1st ed.; University Science Books: Sausilito, California: **2010**.

(2) Behr, A., Neubert, P. *Applied Homogeneous Catalysis,* 1st ed.; Wiley-VCH: New York: **2012**.

(3) Magano, J.; Dunetz, J. R. *Chem. Rev.* **2011**, 111, 2177–2250.

(4) Adams C. *Chem. Ind. Lond.* **1999**, 740–742.

(5) Grotjahn, D. B. *Dalton Trans.* **2008**, 6497–6508.

(6) Haack, K. J.; Hashiguchi, S.; Fujii, A.; Ikariya, T.; Noyori, R. *Angew. Chem. Int. Ed.* **1997**, *36*, 285–288.

(7) Zuo, W.; Lough, A. J.; Li, Y. F.; Morris, R. H. *Science.* **2013**, *342*, 1080–1083.

(8) Ben-Ari, E.; Leitus, G.; Shimon, L. J. W.; Milstein, D. *J. Am. Chem. Soc.* **2006**, *128*, 15390–15391.

(9) DuBois, D. L.; Bullock, R. M. *Eur. J. Inorg. Chem.* **2011**, *2011*, 1017–1027.

(10) Tronic, T. A.; Rakowski DuBois, M.; Kaminsky, W.; Coggins, M. K.; Liu, T.; Mayer, J. M. *Angew. Chem. Int. Ed.* **2011**, *50*, 10936–10939.

(11) Tronic, T. A.; Kaminsky, W.; Coggins, M. K.; Mayer, J. M. *Inorg. Chem.* **2012**, *51*, 10916–10928.

(12) Wiedner, E. S.; Yang, J. Y.; Dougherty, W. G.; Kassel, W. S.; Bullock, R. M.; DuBois, M. R.; DuBois, D. L. *Organometallics* **2010**, *29*, 5390–5401.

(13) Kilgore, U. J.; Roberts, J. a S.; Pool, D. H.; Appel, A. M.; Stewart, M. P.; DuBois, M. R.; Dougherty, W. G.; Kassel, W. S.; Bullock, R. M.; DuBois, D. L. *J. Am. Chem. Soc.* **2011**, *133*, 5861–5872.

(14) Weiss, C. J.; Wiedner, E. S.; Roberts, J. a S.; Appel, A. M. *Chem. Commun.* **2015**, *51*, 6172–6174.

(15) a) Bullock R. M.; Appel A.M; Helm M. L.; *Chem. Commun.* **2014**, *50*, 3125-3143; b) Kilgore U. J.; Roberts J. A. S.; Pool D. H.; Appel A. M.; Stewart M. P.; DuBois M. R.; Dougherty W. G.; Kassel W. S.; Bullock R. M.; DuBois D. L.; *J. Am. Chem. Soc.* **2011**, *133*, 5861-5872; c) Kilgore U. J.; Stewart M. P.; Helm M. L.;

Dougherty W. G.; Kassel W. S.; DuBois M. R.; Bullock R. M.; *Inorg. Chem.* **2011**, *50*, 10908-10918.

(16) Seu C. S.; Ung D.; Doud M. D.; Moore C. E.; Rheingold A. L.; Kubiak C. P.; *Organometallics* **2013**, *32*, 4556-4563.

(17) a) Weiss C. J.; Das P.; Miller D. L.; Helm M. L.; Appel A. M. *ACS Catalysis* **2014**, *4*, 2951-2958; b) Weiss C. J.; Wiedner E. S.; Roberts J. A. S.; Appel A. M. *Chem. Commun.* **2015**, *51*, 6172-6174.

(18) Galan B. R.; Schöffel J.; Linehan J. C.; Seu C.; Appel A. M.; Roberts J. A. S.; Helm M. L.; Kilgore U. J.; Yang J. Y.; DuBois D. L.; Kubiak C. P. *J. Am. Chem. Soc.* **2011**, *133*, 12767-12779.

(19) Hintermann, L.; Labonne, A. *Synthesis* **2007**, *2007*, 1121–1150.

(20) Tokunaga, M.; Wakatsuki, Y. *Angew. Chemie Int. Ed.* **1998**, 2867–2869.

(21) Grotjahn, D. B.; Incarvito, C. D.; Rheingold, A. L. *Angew. Chem. Int. Ed.* **2001**, *585*, 3884–3887.

(22) Grotjahn, D. B. *Top. Catal.* **2010**, *53*, 1009–1014.

(23) Grotjahn, D. B. *Pure Appl. Chem.* **2010**, *82*, 635–647.

(24) Grotjahn, D. B. *Chem. Eur. J.* **2005**, *11*, 7146–7153.

(25) Grotjahn, D. B.; Lev, D. *J. Am. Chem. Soc.* **2004**, *126*, 12232–12233.

(26) Hintermann, L.; Dang, T. T.; Labonne, A.; Kribber, T.; Xiao, L.; Naumov, P. *Chem. Eur. J.* **2009**, *15*, 7167–7179.

(27) Boeck, F.; Kribber, T.; Xiao, L.; Hintermann, L. *J. Am. Chem. Soc.* **2011**, *133*, 8138–8141

(28) Chang, L.-H.; Yeh, C.-W.; Ma, H.-W.; Liu, S.-Y.; Lin, Y.-C.; Wang, Y.; Liu, Y.-H. *Organometallics* **2010**, *29*, 1092–1099.

(29) (a) Dixneuf, P. H. *Acc. Chem. Res.* **1999**, *32*, 311–323. (b) Mutoh, Y.; Kimura, Y.; Ikeda, Y.; Tsuchida, N.; Takano, K. *Organometallics* **2012**, *31*, 5150–5158. (c) Trost, B. M.; Frederiksen, M. U.; Rudd, M. T. *Angew. Chem. Int. Ed.* **2005**, *44*, 6630–6666.

(30) Li, L.; Herzon, S. B. *Nat. Chem.* **2014**, *6*, 22–27.

(31) Li, L.; Zeng, M.; Herzon, S. B. *Angew. Chem. Int. Ed.* **2014**, *53*, 7892–7895.

(32) Zeng, M.; Li, L.; Herzon, S. B. *J. Am. Chem. Soc.* **2014**, *136*, 7058–7067.

(33) Horton, D. a; Bourne, G. T.; Smythe, M. L. *Chem. Rev.* **2003**, *103*, 893–930.

(34) Majumdar, N.; Paul, N. D.; Mandal, S.; de Bruin, B.; Wulff, W. D. *ACS Catal.* **2015**, *5*, 2329–2366.

(35) Varela-Fernández, A.; González-Rodríguez, C.; Varela, J. A.; Castedo, L.; Saá, C. *Org. Lett.* **2009**, *11*, 5350–5353.

(36) Nair, R. N.; Lee, P. J.; Grotjahn, D. B. *Top. Catal.* **2010**, *53*, 1045–1047.

(37) McEleney, K.; Allen, D. P.; Holliday, A. E.; Crudden, C. M. *Org. Lett.* **2006**, *8*, 2663–2666.

(38) Welch, C. J.; Albaneze-Walker, J.; Leonard, W. R.; Biba, M.; DaSilva, J.; Henderson, D.; Laing, B.; Mathre, D. J.; Spencer, S.; Bu, X.; Wang, T. *Org. Process Res. Dev.* **2005**, *9*, 198–205.

(39) (a) Recho, J.; Black, R. J. G.; North, C.; Ward, J. E.; Wilkes, R. D. *Org. Process Res. Dev.* **2014**, *18*, 626–635. (b) For, U.; Step, C.; Step, A.; Process, I. C. H.; Expert, I. C. H.; Group, W.; Committee, I. C. H. S.; Union, E. "Guideline for Elemental Impurities Q3D" **2013**.

(40) Galan, B. R.; Kalbarczyk, K. P.; Szczepankiewicz, S.; Keister, J. B.; Diver, S. T. *Org. Lett.* **2007**, *9*, 1203–1206.

(41) Vougioukalakis, G. C. *Chem. Eur. J.* **2012**, *18*, 8868–8880.

(42) Skowerski, K.; Wierzbicka, C.; Szczepaniak, G.; Gułajski, Ł.; Bieniek, M.; Grela, K. *Green Chem.* **2012**, *14*, 3264.

(43) Sun, Q.; Dai, Z.; Liu, X.; Sheng, N.; Deng, F.; Meng, X.; Xiao, F.-S. *J. Am. Chem. Soc.* **2015**, *137*, 5204–5209.

(44) Westhus, M.; Gonthier, E.; Brohm, D.; Breinbauer, R. *Tetrahedron Lett.* **2004**, *45*, 3141–3142.

(45) Hinchcliffe, a.; Hughes, C.; Pears, D. a.; Pitts, M. R. *Org. Process Res. Dev.* **2007**, *11*, 477–481.

Chapter 2

2 Experimental

2.1 General Considerations

2.1.1 Chemical

All manipulations were carried out under an inert nitrogen atmosphere using standard glovebox or Schlenk techniques unless otherwise stated. Solvents were obtained from an Innovative Technologies 400-5 Solvent Purification System and were stored over activated 4 Å molecular sieves unless otherwise stated. Acetone was dried with calcium sulfate and deoxygenated by sparging with nitrogen. Acetone and acetonitrile were not stored with sieves. Reagents were purchased from Alfa Aesar or Sigma Aldrich and used without further purification unless otherwise stated. $RuCl_3 \cdot 3H_2O$ was purchased from Pressure Chemical Company. Phenylacetylene, 1-octyne, and styrene were sparged with nitrogen and stored over 4 Å molecular sieves. Vinylmagnesium bromide was used without further purification. Water was deoxygenated by sparging with nitrogen before use. [HDMF][OTf],[1] $[Ru(Cp)(naph)][PF_6]$,[2] and $[Ru(Cp)(MeCN)_3][PF_6]$[2] were synthesized according to literature procedures. $CDCl_3$ and CD_2Cl_2 were purchased from Cambridge Isotope Laboratories and were sparged with nitrogen and stored over 4Å molecular sieves before use. Acetone-d_6 and MeCN-d_3 were purchased in ampules from Cambridge Isotope Laboratories and used without further purification.

2.1.2 Instrumentation

NMR spectra were recorded at 298K on a Varian INOVA 600 or 400 spectrometer and ^1H and ^{13}C spectra were referenced using residual solvent signals to TMS at 0.00 ppm.[3] $^{31}P\{^1H\}$ spectra were referenced externally to 85% phosphoric acid at 0.0 ppm. Peak multiplicities are designated as: s = singlet, d = doublet, t = triplet, m = multiplet, sept = septet, br = broad. Reaction aliquots from catalytic experiments were analyzed using a calibrated Shimadzu GCMS-QP2010 Ultra GC with a DB-5 column or a calibrated

Agilent 7890A GC-FID with an HP-5 column. Styrene and ethylbenzene were quantified relative to an internal standard by GC-FID analysis. Area counts for ethylbenzene were corrected using a response factor obtained by calibration of styrene and ethylbenzene over the concentration range 1 to 5 mM. A linear response for both species was found in this range. Authentic samples of each were used to construct calibration curves. Scanning Electron Microscopy (SEM) was performed using a Hitachi S-4500 field emission SEM with a Quartz XOne EDX system. MALDI-TOF mass spectra were collected using an AB Sciex 5800 TOF/TOF mass spectrometer using pyrene as the matrix in a 20:1 molar ratio with the sample. Spectra were simulated using www.chemcalc.org.[4] ICP-MS samples were first digested in aqua-regia for 2 hours then data was collected on an Agilent 7700 Series ICP-MS.

2.2 Synthesis of Ru(Cp)($P^{tBu}_2N^{Bn}_2$)Cl

Ru(Cp)($P_2^{tBu}N_2^{Bn}$)Cl was prepared following the literature procedure.[5]

Yield: 130 mg (65%). ^{1}H NMR ($CDCl_3$): δ 7.34−7.26 (m, 10H, Ph-*H*), 4.67 (s, 5H, Cp-*H*), 3.67 (s, 2H, PhCH_2N), 3.62 (s, 2H, PhCH_2N), 3.42 (m, 2H, PCH_2N), 2.70 (m, 2H, PCH_2N), 2.52 (m, 2H, PCH_2N), 2.42 (m, 2H, PCH_2N), 1.06 (m, 18H, tBu-CH_3) ^{31}P{^{1}H}: δ 51.6 (s).

2.3 Synthesis of [Ru(Cp)($P^{tBu}_2N^{Bn}_2$)(MeCN)][PF_6], **1**

[Ru(Cp)($MeCN)_3$][PF_6] (500 mg, 1.15 mmol) and $P^{tBu}_2N^{Bn}_2$ (509 mg, 1.15 mmol) were added to a 100 mL Schlenk flask containing a stir bar and acetonitrile (~ 40 mL). The reaction mixture was heated at 70 ˚C for 3 hours under a flow of N_2. The solvent was then removed under vacuum and the remaining solids were returned to the glovebox. The solid was washed with Et_2O (3 × 10 mL) giving a yellow powder.

Yield: 731 mg (81%). ^{1}H and ^{31}P{^{1}H} NMR spectra match previously reported values.[5] Reported spectra in CD_2Cl_2 ^{1}H NMR($CDCl_3$): δ ^{1}H: 7.27−7.18 (m, 8H, Ph-*H*), 7.07 (d,

2H, Ph-*H*), 4.72 (s, 5H, Cp-*H*), 3.63 (d, 4H, PhCH_2N), 2.97 (m, 2H, PCH_2N), 2.63−2.38 (m, 6H, PCH_2N), 2.27 (s, 3H, NCCH_3), 0.95 (m, 18H, tBu-CH_3) $^{31}P\{^1H\}$: δ 52.4 (s), −144.3 (m).

2.4 Synthesis of [Ru(Cp)($P^{tBu}{}_2N^{Bn}{}_2$)(-C=CHPh)][PF_6], **2**

1 (175 mg, 0.222 mmol) and phenylacetylene (41.0 mg, 0.222 mmol) were combined in a 20 mL vial containing a stir bar with acetone (3.0 mL). The vial was capped, and the solution was allowed to stir at room temperature for 20 hours. The acetone solution was concentrated to a minimum amount (ca. 1 mL) and was layered with Et_2O (ca. 8 mL) and placed in a –33˚C freezer for 2 days. A yellow solid precipitated, the mother liquor was removed by pipette and the solid was washed with Et_2O and hexanes (5 × 2.0 mL each). Excess Et_2O and hexanes were removed under vacuum to give **2** as a yellow-orange solid. For full atom label assignment see Appendix 1.

Yield: 140 mg (87%). ^1H NMR ($CDCl_3$, 600.0 MHz): δ 7.67 (d, $^3J_H{}^M{}_{-H}{}^N$ = 6.9 Hz, 1H, H^M), 7.61-7.59 (m, 2H, H^N), 7.56 – 7.51 (m, 1H, H^O), 7.39 (s, 1H, H^A), 7.33-7.31 (m, 2H, H^C), 7.27-7.24 (m, 1H, H^D), 7.22-7.19 (m, 1H, H^R), 7.13-7.10 (m, 2H, H^Q), 6.99 (d, $^3J_H{}^B{}_{-H}{}^C$ = 7.4 Hz, 2H, H^B), 6.60 (d, $^3J_H{}^P{}_{-H}{}^Q$ = 6.7 Hz, 2H, H^P), 4.83 (s, 2H, H^E), 4.40 (s, 5H, H^T), 3.43 (s, 2H, H^F), 3.27-3.23 (m, 2H, $H^{K/L}$), 3.17-3.14 (m, 2H, $H^{I/J}$), 2.98-2.95 (m, 2H, $H^{I/J}$), 2.28-2.24 (m, 2H, $H^{K/L}$), 1.08-1.05 (m, 18H, H^S). $^{13}C\{^1H\}$ NMR ($CDCl_3$, 150.8 MHz): δ 195.7 (observed through correlation, C^6), 141.6 (s, C^8), 136.4 (s, C^{18}), 132.7 (s, C^{15}), 131.7 (s, C^{14}), 130.3 (s, C^{17}), 129.9 (s, C^9), 129.6 (s, C^{16}), 129.3 (s, C^{19}), 128.9 (s, C^{20}), 128.3 (s, $C^{7 \text{ and } 10}$), 128.1 (s, C^{21}), 126.6 (s, C^{11}), 81.9 (s, C^5), 68.7 (m, C^{12}), 67.0 (m, C^{13}), 58.7 (m, $C^{3/4}$), 50.9 (m, $C^{1/2}$), 26.3 (s, C^{22}). $^{31}P\{^1H\}$ NMR ($CDCl_3$, 161.8 MHz): δ 71.5 (s, $P^{tBu}{}_2N^{Bn}{}_2$), –144.2 (sept, PF_6). MALDI MS (pyrene matrix): Calc. *m/z* 711.3 [(Ru(Cp)($P^{tBu}{}_2N^{Bn}{}_2$)(-C=CHPh)]$^+$), Obs. m/z 711.3. Anal. Calc. for $C_{39}H_{51}F_6N_2P_3Ru$: C, 54.73; H, 6.01; N, 3.27. Found: C, 52.99; H, 6.01; N, 3.49.

2.5 In situ Synthesis of [Ru(Cp)($P^{tBu}{}_2N^{Bn}{}_2$)(-C=CHPh)(H)][PF_6][OTf], **3**

To an NMR tube containing **2** (8.0 mg, 0.0094 mmol) was added with 1.25 eq of [HDMF][OTf] (2.6 mg, 0.0117 mmol) and CD_2Cl_2 (1.0 mL). The resulting product was analyzed after 1 hour by $^{31}P\{^1H\}$ NMR spectroscopy indicating complete conversion from **2** to **3**. For full atom label assignment see Appendix 5.

^1H NMR (CD_2Cl_2, 600.0 MHz): δ 7.72 (s, 1H, H^A), 7.68-7.66 (m, 2H, Ar-*H*), 7.55-7.33 (m, 11H, Ar-*H*), 7.01 (d, *J* = 7.6 Hz, 2H, H^B), 6.33 (br s, 1H, H^Z), 4.96 (s, 2H, H^E), 4.87 (d, *J* = 5.9 Hz, 2H, H^F), 4.70 (s, 5H, H^T), 3.81 – 3.68 (m, 2H, $H^{I/J}$), 3.66 – 3.53 (m, 2H, $H^{K/L}$), 3.45 – 3.35 (m, 2H, $H^{K/L}$), 3.27 – 3.15 (m, 2H, $H^{I/J}$), 1.18 – 0.93 (m, 18H, H^S). $^{13}C\{^1H\}$ NMR (CD_2Cl_2, 150.8 MHz): δ 189.9 (observed through correlation, C^6), 132.6 (s, Ar-*C*), 131.7 (s, Ar-*C*), 131.4 (s, Ar-*C*), 130.5 (s, Ar-*C*), 130.4 (s, Ar-*C*), 129.7 (s, Ar-*C*), 129.2 (s, Ar-*C*), 127.9 (s, Ar-*C*), 83.6 (s, C^5), 67.9 (m, C^{12}), 64.9 (m, C^{13}), 61.6 (m, $C^{3/4}$), 46.4 (m, $C^{1/2}$), 26.1 (s, C^{22}). $^{31}P\{^1H\}$ NMR (CD_2Cl_2, 161.8 MHz): δ 83.1 (s, $P^{tBu}{}_2N^{Bn}{}_2$), –144.0 (sept, PF_6).

2.6 VT NMR Analysis of **2**

To an NMR tube, **2** (10 mg, 0.117 mmol) and MeCN-d_3 (ca. 0.7 mL) were added and the solution was analyzed by VT NMR spectroscopy. The NMR probe was raised in 20 degree intervals to a max of 70 ˚C running both ^1H and $^{31}P\{^1H\}$ experiments at each interval. No changes were observed in the NMR spectra (Appendix 10). This procedure was repeated with acetone-d_6 as the solvent to a max temperature of 40 ˚C. No changes were observed in the NMR spectra (Appendix 11).

2.7 Addition of Vinylmagnesium Bromide to **2**:

2 (10 mg, 0.117 mmol) and vinylmagnesium bromide (1.05 eq, 12.3 µL, 0.123 mmol) were added to a 20 ml vial with 10 mL of THF. After 1 hour of stirring, the solvent was removed under vacuum and the solids were dissolved in $CDCl_3$ and analyzed by ^1H and

$^{31}P\{^{1}H\}$ NMR spectroscopy. There were no new signals observed through $^{31}P\{^{1}H\}$ NMR spectroscopy (Appendix 13).

2.8 Addition of Water to **2**:

2 (10 mg, 0.117 mmol) and acetone were added to an NMR tube fitted with a septum. Degassed water (5.0 μL, 0.278 mmol) was injected by syringe through the septum and the solution was shaken. The sample was analyzed by $^{31}P\{^{1}H\}$ NMR spectroscopy after 10 minutes, 1 hour, and 24 hours and no new signals were observed (Appendix 14).

2.9 Representative Procedure for the Attempted Catalytic Hydration

The following stock solutions were prepared: 1-Octyne (303 mg, 2.75 mmol, 416.7 mM) and tetradecane (109 mg, 0.55 mmol) in acetone (6.600 mL) and $[Ru(Cp)(P^{tBu}{}_2N^{Bn}{}_2)(MeCN)][PF_6]$, **1**, (19.6 mg, 0.0249 mmol, 25 mM) in acetone (1.100 mL). To a set of 5 vials containing stir bars the 1-octyne/tetradecane stock solution (300.0 μL $[Ru(Cp)(P^{tBu}{}_2N^{Bn}{}_2)(MeCN)][PF_6]$ (100.0 μL) solution and acetone (100.0 μL) were added to give a final volume of 500 μL. The vials were sealed with a screw cap fitted with a PTFE septum, removed from the glovebox and degassed water (5.0 μL) was injected into each vial by syringe. The vials were heated to 70 ˚C with stirring. After 2, 4, 6, 24, and 48 hours one vial from the set was removed from heat, cooled, and exposed to air to quench. An aliquot (100.0 μL) was removed and diluted with acetone (1.0 mL) giving final concentrations of 25 mM for octyne and 5 mM for tetradecane and the diluted samples were analyzed by calibrated GC-MS.

2.10 General Procedure for the Catalytic Hydration of 1-Octyne

In a glovebox, the following stock solutions were prepared: 1-Octyne (303 mg, 2.75 mmol, 416.7 mM) and tetradecane (109 mg, 0.55 mmol) in acetone (6.600 mL); $Ru(Cp)(P^{tBu}{}_2N^{Bn}{}_2)Cl$ (17.6 mg, 0.0275 mmol, 25 mM) in acetone (1.100 mL);

Ru(Cp*)($P^{tBu}_2N^{Bn}_2$)Cl (19.6 mg, 0.0275 mmol, 25 mM) in acetone (1.100 mL). To two sets of 5 vials containing stir bars the 1-octyne/tetradecane stock solution (300.0 μL), catalyst stock solution (set 1= Ru(Cp)($P_2{}^{tBu}N_2{}^{Bn}$)Cl; set 2= Ru(Cp*)($P^{tBu}_2N^{Bn}_2$)Cl)) (100.0 μL) and acetone (100.0 μL) were added to give a final volume of 500 μL and sealed with a screw cap fitted with a PTFE septum. The vials were removed from the glovebox and degassed water (5.0 μL) was injected into each vial. The vials were heated to 70 ˚C with stirring. After 2, 4, 6, 24, and 48 hours one vial from each set was removed from heat, cooled, and exposed to air to quench. An aliquot (100.0 μL) was removed and diluted with acetone (1.0 mL) giving final concentrations of 25 mM for octyne and 5 mM for tetradecane and the diluted samples were analyzed by calibrated GC-MS.

2.11 NMR Scale Ligand Exchange Reactions of [Ru(Cp)($P^{tBu}_2N^{Bn}_2$)Cl][PF_6]

In a glovebox Ru(Cp)($P^{tBu}_2N^{Bn}_2$)Cl (10 mg, 0.016 mmol) and $TlPF_6$ (6 mg, 0.018 mmol) were weighed into a 1 dram vial with a stir bar. Acetone (0.7 mL) was added and the reaction was stirred for 30 minutes. The suspension was filtered through a glass microfiber plug to remove the TlCl salt. A portion of the filtrate was analyzed by $^{31}P\{^1H\}$ NMR spectroscopy (unlocked). To the NMR tube containing Ru(Cp)($P^{tBu}_2N^{Bn}_2$)$^+$ degassed water (5.0 μL) was added through the septum and the solution was analyzed by $^{31}P\{^1H\}$ NMR. Octyne (1.72 mg, 0.016 mmol) was injected into the NMR tube containing the aqua complex and the reaction mixture was analyzed by $^{31}P\{^1H\}$ NMR spectroscopy. The remaining reaction mixture was removed from the glovebox and exposed to air and analyzed by $^{31}P\{^1H\}$ NMR spectroscopy.

2.12 General Procedure for the Catalytic Cyclization of 2-Ethynylbenzyl Alcohol

In a glovebox, the following stock solutions were prepared: 2-Ethynylbenzyl alcohol (218 mg, 1.65 mmol, 0.75 M) and dimethyl terephthalate (53 mg, 0.27 mmol, 0.12 M) in acetone (2.200 mL); [Ru(Cp)($P^{tBu}_2N^{Bn}_2$)(MeCN)][PF_6], **1**, (65 mg, 0.08 mmol, 74.9 mM)

in acetone (1.100 mL). Four sets, A-D, of 5 vials (20 vials total) containing stir bars were charged with the 2-ethynylbenzyl alcohol/dimethyl terephthalate stock solution (100 μL). To each vial of set A was added the catalyst stock solution (50 μL) and additional acetone (350 μL) giving a final volume of 500 μL. The solvent was removed from vial sets B-D *in vacuo* leaving a substrate/internal standard residue. To each of these vials (sets B-D) the catalyst stock solution (50 μL) was added along with the reaction solvents: acetonitrile (450 μL to set B), THF (450 μL, to set C) and CH_2Cl_2 (450 μL, to set D). The final concentrations for all vials were 0.150 M in substrate. A final vial was charged with substrate/internal standard stock solution (100 μL) for use as the time = 0 sample, required for accurate quantification of substrate and product. The vials were capped and removed from the glove box and heated to 40 ˚C (sets A, C and D) or 60 ˚C (set B) with stirring. After 0.167, 0.5, 1, 6, and 24 hours one vial from each of the sets was removed from heat, cooled, and exposed to air to quench. The solvent was then removed *in vacuo*; the remaining residue was dissolved in $CDCl_3$ and analyzed by ^{1}H NMR spectroscopy.

2.13 Optimization of Catalyst Loading for Cyclization Reactions

In a glovebox, the following stock solutions were prepared: 2-ethynylbenzyl alcohol (119 mg, 0.9 mmol, 0.75 M) and dimethyl terephthalate (29 mg, 0.15 mmol, 0.125 M) in acetone (1.200 mL); [Ru(Cp)($P^{tBu}{}_2N^{Bn}{}_2$)(MeCN)][PF_6], **1**, (10 mg, 0.013 mmol, 3.85 mM) in acetone (3.381 mL). Two sets, A & B, of 5 vials (11 vials total) containing stir bars were charged with the 2-ethynylbenzyl alcohol/dimethyl terephthalate stock solution (100 μL) and a final vial was charged with substrate/internal standard stock solution (100 μL) for use as the control sample. The first set of vials, A, were loaded with catalyst stock solution (200 μL) resulting in a catalyst loading of 1 mol%, the vials were then topped off with acetone (200 μL) giving a final volume of 500 μL in each vial. The second set of vials, B, were loaded with catalyst stock solution (20 μL) resulting in a catalyst loading of 0.1 mol%, the vials were then topped off with acetone (380 μL) giving a final volume of 500 μL in each vial. The final concentration of substrate for all vials was 0.15 M. All

vials were capped and removed from the glove box, heated to 40 ˚C, and analyzed as described in Section 2.12.

2.14 NMR Scale Cyclization of 2-Ethynylbenzyl Alcohol

In a glovebox [Ru(Cp)($P^{tBu}{}_2N^{Bn}{}_2$)(MeCN)][PF_6], **1**, (20 mg, 0.026 mmol) and 2-ethynyl alcohol (3.4 mg, 0.026 mmol) were weighed into a 1 dram vial with a stir bar. Acetone-d_6 (ca. 1.0 mL) was added to the vial and the reaction was stirred. The reaction mixture was analyzed by ^{1}H and ^{31}P{^{1}H} NMR spectroscopy at 10 minute, 1 hour, and 24 hour timepoints.

2.15 General Procedure for Suzuki Cross-Coupling Reactions

In a glovebox, the following stock solutions were prepared: bromobenzene (208.5 mg, 1.328 mmol, 0.86 M) and tetrahydronaphthalene (70.2 mg, 0.5312 mmol) in DMF (1600 µL); 4-methylboronic acid (189.6 mg, 1.394 mmol) in DMF (1600 µL); $Pd(OAc)_2$ (**A**) (2.8 mg, 0.00249 mmol) in DMF (500 µL); PCy_3 (8.8 mg, 0.0314 mmol) in DMF (500.0 µL).[6] $PdCl_2$ Polymer (**B**) (1.8 mg, 0.00249 mmol) was added to one set of 5 vials containing stir bars and K_2CO_3 (22.9 mg, 0.166 mmol) was added to each vial. $Pd(OAc)_2$ Polymer (**C**) (1.6 mg, 0.00249 mmol) and K_2CO_3 (22.9 mg, 0.166 mmol) were added to a second set of 5 vials containing stir bars. To each vial containing the polymer based catalysts 100.0 µL of bromobenzene/tetrahydronaphthalene stock solution, 100.0 µL of 4-methylboronic acid stock solution, and 300 µL of DMF were added to give a final volume of 500 µL. To a third set of 5 vials containing stir bars and K_2CO_3 (22.9 mg, 0.166 mmol) the following was added: 100.0 µL of bromobenzene/tetrahydronaphthalene, 100.0 µL of 4-methylboronic acid, 100.0 µL of $Pd(OAc)_2$, and 100.0 µL of PCy_3. An additional 100 µL of DMF was added to the third set of vials to give a final volume of 500 µL. All vials were sealed, removed from the glovebox and placed on a hotplate at 110 ˚C with stirring. At time points of 0.5, 1, 2, 5, and 20 hours one vial from each of the 3 sets was removed from the heat, cooled, opened

to air and an aliquot (30.0 μL) was removed and diluted with acetone (1.0 mL) to give a final concentration of 5 mM for bromobenzene. These diluted samples were analyzed by GC-MS on a Shimadzu GCMS-QP2010S Ultra with a DB-5 Column. Each sample was injected twice and the median area count was used.

2.16 Procedure for Filtration of Catalytic Suzuki Cross-Coupling Reactions

Stock solutions for this reaction were prepared in the same manner as the general Suzuki cross-coupling procedure. The three sets of 5 vials were placed on the hotplate at 110 ˚C and after 0.5 h all vials were removed from the hot plate. One vial from each set was allowed to cool, opened to air, diluted, and analyzed by GC-MS. The remaining vials were returned to the glovebox and the solids were removed by filtration though a glass microfiber plug. The filtration process took approximately half an hour; this time was not included in the reaction time since heat is required to achieve conversion. The filtrate from each vial was injected into a new vial pre-loaded with a stir bar and K_2CO_3 (22.9 mg, 0.166 mmol). These vials were removed from the glovebox and heated to 110 ˚C; after 1, 2, 5, and 20 hours from the initial time a vial from each set was cooled and exposed to air. An aliquot (30.0 μL) was removed and diluted with acetone (1.0 mL) and analyzed by GC-MS.

2.17 Suzuki Coupling Mercury Poisoning Test

Stock solutions for these reactions were prepared in the same manner as in the general Suzuki cross-coupling procedure. Three sets of 5 vials were charged with a stir bar, polymer catalyst, base and removed from the glove box and exposed to air. A drop of mercury was added to each vial, which was then fitted with a screw cap fitted with a PTFE septum. The vials were deoxygenated under a flow of nitrogen. Stock solutions of bromobenzene and tetrahydronaphthalene were injected into the vials through the septa and the vials heated to 110 ˚C on a hot plate with stirring. At 0.5, 1, 2, 5, and 20 hour

time points, one vial from each set was removed from heat, cooled, diluted (procedure as described in Section 2.15) and analyzed by GC-MS.

2.18 General Procedure for the Catalytic Hydrogenation of Styrene

In a glovebox, the following stock solutions were prepared: styrene (104 mg, 1 mmol, 500 mM) in toluene (2.00 mL); cyclodecane (70 mg, 0.25 mmol, 250 mM) in toluene (2.00 mL); $RhCl(PPh_3)_3$ (9.3 mg , 0.01 mmol, 10 mM) in dichloromethane (1.00 mL). To a 100 mL Schlenk flask containing a stir bar, the catalyst stock solution was added (200 μL), and dichloromethane was removed *in vacuo*. Added to the same flask was the styrene stock (400 μL) and cyclodecane stock (400 μL). Toluene was added (5.20 mL) to give a final volume of 6.00 mL and the flask was sealed with a rubber septum. The final concentrations of the reaction mixture were 33.0 mM styrene, 8.3 mM cyclodecane, and 0.33 mM $RhCl(PPh_3)_3$ (1 mol%). The flask was removed from the glovebox and H_2 gas was bubbled into solution for 2 minutes using a needle pierced through the rubber septum of the Schlenk flask. The contents were allowed to stir at room temperature and every 10 minutes for 90 minutes, 200 μL aliquots were taken from the flask and exposed to air to quench. From each aliquot, 150 μL was removed and diluted with acetone (850 μL) giving final concentrations of 5 mM for styrene and tetradecane and the diluted samples were analyzed by calibrated GC-FID.

2.19 General Procedure for the Quenching of the Hydrogenation of Styrene

The procedure for the catalytic hydrogenation of styrene was followed as outlined in Section 2.18. Added to the reaction set-up was an excess of polymer (32 mg, 0.04 mmol), or ca. 1.5 equivalents of phosphine by mol. The polymer was present from the outset and 200 μL aliquots taken at 10 minutes intervals, up to 50 minutes. From each aliquot 150 μL was removed and diluted with acetone (850 μL) giving final concentrations of 5 mM for styrene and tetradecane and the diluted samples were analyzed by calibrated GC-FID.

After the final aliquot for GC-FID analysis was taken from the quenched reaction, the mixture was allowed to stir for 24 hours. The mixture was then taken up in a syringe and filtered through a syringe filter (Promax Syringe Filter, 13 mm, 0.22 μm PTFE) into a preweighed vial. Solvent was removed *in vacuo* leaving a residue. The residue was submitted for ICP-MS analysis. Additionally, a control reaction to which no polymer was added was submitted for ICP-MS analysis, for a comparison of the trace metal amounts in each sample.

2.20 Incubation Time of Polymer

The procedure for making the stock solutions used for the incubation time of the polymer was followed as outlined in Section 2.18. Two Schlenk flasks were set up containing an excess of polymer (32 mg, 0.04 mmol), or ca. 1.5 equivalents of phosphine repeat units to metal. The stock solutions were added and the Schlenk flasks were capped with septa. The flasks were removed from the glovebox and H_2 gas was bubbled into solution for 2 minutes using a needle pierced through the rubber septum of the Schlenk flask. The contents were allowed to stir at room temperature. One flask was allowed to stir for 20 minutes and the other for 24 hours before filtration. The mixture was then taken up in a syringe and filtered through a syringe filter (Promax Syringe Filter, 13 mm, 0.22 μm polytetrafluoroethylene) into a preweighed vial. Solvent was removed *in vacuo* leaving a residue and was submitted for ICP-MS analysis.

2.21 Equivalents of Polymer in the Hydrogenation of Styrene

In a glovebox, the following stock solutions were prepared: styrene (125 mg, 1.2 mmol, 500 mM) in toluene (2.40 mL); cyclodecane (84 mg, 0.6 mmol, 250 mM) in toluene (2.40 mL); $RhCl(PPh_3)_3$ (11.1 mg , 1.2×10^{-2} mmol, 10 mM) in dicloromethane (1.20 mL). Five Schlenk flasks were set up containing different equivalents of polymer: 0 equivalents, 1/10 equivalent (1.6 mg, 2×10^{-6} mol), 1 equivalents (8.0 mg, 1×10^{-5} mol), 2 equivalents (24.1 mg, 3×10^{-5} mol), and 4 equivalents (48.12 mg, 6×10^{-5} mol). To each of the 100 mL Schlenk flasks containing a stir bar and polymer the catalyst stock solution was added

(200 μL), and dichloromethane was removed *in vacuo*. Added to the same flask was the styrene stock (400 μL) and cyclodecane stock (400 μL). Toluene was added (5.20 mL) to give a final volume of 6.00 mL and the flask was sealed with a rubber septum. The final concentrations of the reaction mixture were 33 mM styrene, 8.3 mM cyclodecane, and 0.33 mM $RhCl(PPh_3)_3$ (1 mol%). The flask was removed from the glovebox and H_2 gas was bubbled into solution for 2 minutes using a needle pierced through the rubber septum of the Schlenk flask. The contents were allowed to stir at room temperature. Every 10 minutes for 90 minutes, 200 μL aliquots were taken from the flask and exposed to air to quench. From each aliquot 150 μL was removed and diluted with acetone (850 μL) giving final concentrations of 5 mM for styrene and tetradecane and the diluted samples were analyzed by calibrated GC-FID. The reaction of hydrogenation of styrene using free $RhCl(PPh_3)_3$ was monitored using GC-FID. All flasks containing polymer were allowed to incubate for 24 hours. The mixture was then taken up in a syringe and filtered through a syringe filter (Promax Syringe Filter, 13 mm, 0.22 μm polytetrafluoroethylene) into a preweighed vial. Solvent was removed *in vacuo* leaving a residue that was submitted for ICP-MS analysis.

2.22 References

(1) Favier, I.; Duñach, E. *Tetrahedron Lett.* **2004**, *45*, 3393–3395.

(2) Kündig, E. P.; Monnier, F. R. *Adv. Synth. Catal.* **2004**, *346*, 901–904.

(3) Fulmer, G. R.; Miller, A. J. M.; Sherden, N. H.; Gottlieb, H. E.; Nudelman, A.; Stoltz, B. M.; Bercaw, J. E.; Goldberg, K. I. *Organometallics* **2010**, *29*, 2176–2179.

(4) Patiny, L.; Borel, A. *J. Chem. Inf. Model.* **2013**, *53*, 1223–1228.

(5) Tronic, T. A.; Kaminsky, W.; Coggins, M. K.; Mayer, J. M. *Inorg. Chem.* **2012**, 51, 10916–10928.

(6) Catalytic conditions adapted from (a) Fu, G. C.; Littke, A. F. *Angew. Chem. Int. Ed.* **1998**, *2*, 3387–3388. (b) Buchwald, S. L.; Old, D. W.; Wolfe, J. P. *Angew. Chem. Int. Ed.* **1998**, 9722–9723. (c) Kudo, N.; Perseghini, M.; Fu, G.

C. *Angew. Chem. Int. Ed.* **2006**, *45*, 1282–1284. (d) Littke, A. F.; Dai, C.; Fu, G. C. *J. Am. Chem. Soc.* **2000**, 4020–4028.

Chapter 3

3 [Ru(Cp)($P^{tBu}_2N^{Bn}_2$)MeCN)][PF_6] Complexes as Possible Metal-Ligand Cooperative Catalysts for Organic Transformations

I postulated that metal complexes with $P^{R}_2N^{R'}_2$ ligands will be efficient MLC catalysts for organic transformations. The improved synthesis of [Ru(Cp)($P^{tBu}_2N^{Bn}_2$)MeCN)][PF_6], and its use as a catalyst for the hydration of terminal alkynes and the cyclization of alkynyl alcohols, is reported herein.

3.1 Alternative synthesis of [Ru(Cp)($P^{tBu}_2N^{Bn}_2$)(MeCN)][PF_6]

The reported synthesis of [Ru(Cp)($P^{tBu}_2N^{Bn}_2$)(MeCN)][PF_6] was performed by synthesizing [Ru(Cp)($P^{tBu}_2N^{Bn}_2$)(Cl)], which is accessed by first performing a ligand exchange on RuCp(PPh_3)Cl with ($P^{tBu}_2N^{Bn}_2$) to give the desired the chloro- complex.[1] This method for synthesizing [Ru(Cp)($P^{tBu}_2N^{Bn}_2$)(Cl)] results in a low yield, and to access the acetonitrile complex a toxic thallium reagent must be used making this an undesirable method. Alternatively, [Ru(Cp)($P^{tBu}_2N^{Bn}_2$)(MeCN)][PF_6][2] was synthesized from [Ru(Cp)(η^6-naphthalene)][PF_6] by allowing [Ru(Cp)(η^6-naphthalene)][PF_6] to stir in acetonitrile for 72 hours. After isolating the [Ru(Cp)($MeCN)_3$][PF_6] complex, 1 equivalent of the ligand ($P^{tBu}_2N^{Bn}_2$) was added in acetonitrile and heated to 75 ˚C with stirring for 4 hours yielding [Ru(Cp)($P^{tBu}_2N^{Bn}_2$)(MeCN)][PF_6] (81%) (Scheme 6). This synthesis resulted in an overall combined yield of 60%. This is a much-improved route over the initial synthesis, which has an overall yield of ca. 20% through a two-step ligand exchange followed by a chloride abstraction using $TlPF_6$. This new pathway through [Ru(Cp)(η^6-naphthalene)][PF_6] is beneficial because of its higher yield and it avoids the use of a toxic thallium reagent.

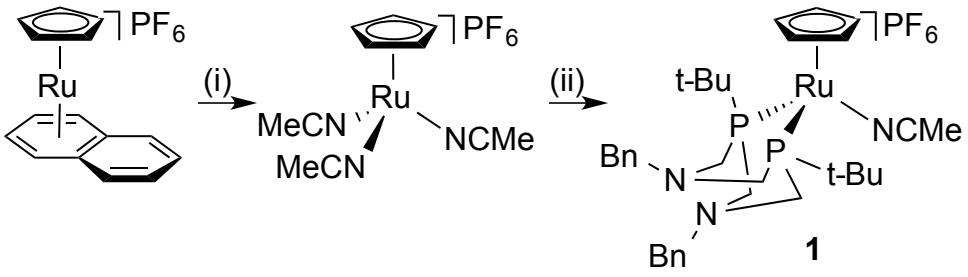

Scheme 6. Alternative synthesis of known [Ru(Cp)($P^{tBu}{}_2N^{Bn}{}_2$)(MeCN)][PF_6] complex **1**. Reaction conditions: (i) MeCN for 72 h (74%); (ii) 1 equiv. $P^{tBu}{}_2N^{Bn}{}_2$ in MeCN for 4 h at 75 ˚C (81%).

3.2 Attempted Catalytic Hydration of Terminal Alkynes

The hydration of both 1-octyne and phenylacetylene was attempted using [Ru(Cp)($P^{tBu}{}_2N^{Bn}{}_2$)(MeCN)][PF_6], **1**, and [Ru(Cp)($P^{tBu}{}_2N^{Bn}{}_2$)(Cl)] as a catalyst and was carried out in acetone at 70 ˚C with 5 equivalents of water as standard conditions, other conditions were tested as well (Scheme 7; Table 1). Unfortunately, no conversion to product or consumption of starting material was seen in the catalytic reactions by GC/MS. Upon addition of formic acid, no desired product was observed by GC/MS. The literature suggests that the addition of formic acid in THF would assist in the formation of product; however, the reported catalysts are not cooperative in nature and likely proceed through a different mechanism.[3,4,5] However, this low reactivity provides a unique opportunity to investigate the individual steps of the mechanism in detail.

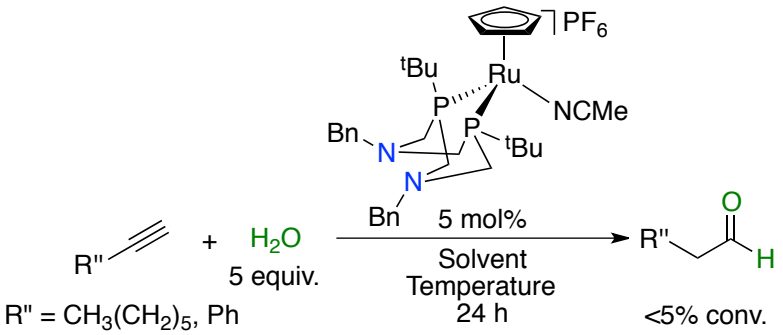

Scheme 7. Attempted catalytic hydration of terminal alkynes using Ru(Cp)($P^{tBu}_2N^{Bn}_2$)(MeCN)][PF_6], **1**.

Table 1. Performance of **1** toward anti-Markovnikov hydration of 1-octyne and phenylacetylene[a]

Entry	Substrate	Solvent	Additive	Temperature (˚C)	Conversion (%) GC[b]	Yield (%) GC[b]
1[c]	1-Octyne	Acetone	None	70	0	0
2	Phenylacetylene	Acetone	None	70	0	0
3	1-Octyne	THF	None	65	0	0
4	Phenylacetylene	THF	None	65	0	0
5	1-Octyne	THF	Formic Acid[d]	65	2	2
6	1-Octyne	DMF	None	70	0	0
7	1-Octyne	DMF	None	110	0	0

[a] 5 mol% **1**, 250 mM alkyne, 5 equiv. H_2O, 48 h; [b] Calibrated GC yield of Anti-Markovnikov aldehyde product; [c] Analyzed by ^{1}H NMR spectroscopy and no product was observed; [d] 1.5 equiv. formic acid.

3.3 Reactivity of [Ru(Cp)($P^{tBu}_2N^{Bn}_2$)Cl] Following Halide Abstraction

The ligand exchange reactivity of [Ru(Cp)($P^{tBu}_2N^{Bn}_2$)MeCN][PF_6], **1**, was assessed through small-scale probe reactions which were analyzed by $^{31}P\{^1H\}$ NMR spectroscopy (Scheme 8). In all cases, the acetonitrile solvate complex [Ru(Cp)($P^{tBu}_2N^{Bn}_2$)MeCN][PF_6], **1**, was generated *in situ* following treatment of [Ru(Cp)($P^{tBu}_2N^{Bn}_2$)Cl] with $TlPF_6$. To [Ru(Cp)($P^{tBu}_2N^{Bn}_2$)MeCN][PF_6], **1**, was added 1.0 equivalents of degassed water and a colour change to orange was observed immediately. The ^{31}P NMR singlet resonance shifted ca. 10 ppm upfield to 46 ppm. The new product is tentatively assigned as [Ru(Cp)($P^{tBu}_2N^{Bn}_2$)(H_2O)][PF_6]. Attempts to isolate the product (*vide infra*) were unsuccessful, which hampered characterization efforts. To the [Ru(Cp)($P^{tBu}_2N^{Bn}_2$)(H_2O)][PF_6] complex was added 1.0 equivalent of acetonitrile and there was an immediate formation of a new signal at 54.4 ppm and the peak for [Ru(Cp)($P^{tBu}_2N^{Bn}_2$)H_2O][PF_6] was absent. This indicates that water is a weak ligand and is easily displaced by acetonitrile, which is consistent with ligand field theory. It was hypothesized that the water adduct may participate in a hydrogen-bonding interaction to the pendant tertiary amine. If this is the case, the interaction is weak and does not inhibit ligand exchange. To [Ru(Cp)($P^{tBu}_2N^{Bn}_2$)MeCN][PF_6], 1.0 equivalents of phenylacetylene was added and a colour change from yellow to yellowish orange was observed over a long reaction time (ca. 20 hours) and, upon heating to 50 ˚C, the reaction occured much faster (2 hours). A downfield shift from 54.4 ppm to 71.5 ppm was observed with the complete disappearance of the signal at 54.4 ppm with no other peaks observed (Table 2). This indicates that acetonitrile is displaced by phenylacetylene and that formation of the product is favorable. Phenylacetylene was also added to the water complex and water was displaced just as with the acetonitrile complex. The reaction of octyne proceeded slightly faster than with phenylacetylene, indicating that the steric bulk on the ligands and substrate does affect the rate of formation. The product following phenylacetylene addition was opened to air and the complex did not degrade and was stable even after one

week. However, when the aceto- and aqua- complexes were exposed to air they degraded in a very short period of time (ca. 1 hour) to give the peroxo-species that was previously reported.[1,6]

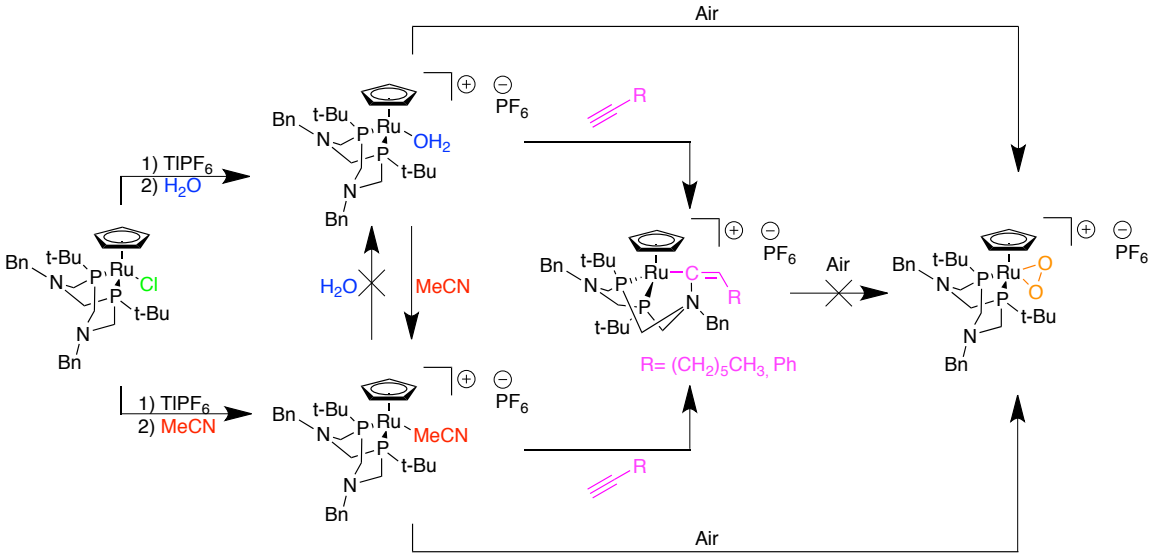

Scheme 8. Reactivity of [Ru(Cp)($P^{tBu}_2N^{Bn}_2$)Cl]

Table 2. $^{31}P\{^{1}H\}$ shifts of the Ru(Cp)($P^{tBu}{}_2N^{Bn}{}_2$) complexes

Compound	$^{31}P\{^{1}H\}$ (acetone unlocked)[a]
[Ru(Cp)($P^{tBu}{}_2N^{Bn}{}_2$)Cl]	51.1
[Ru(Cp)($P^{tBu}{}_2N^{Bn}{}_2$)MeCN][PF_6]	54.4
[Ru(Cp)($P^{tBu}{}_2N^{Bn}{}_2$)H_2O][PF_6]	46.1
[Ru(Cp)($P^{tBu}{}_2N^{Bn}{}_2$)O_2][PF_6]	30.2
[Ru(Cp)($P^{tBu}{}_2N^{Bn}{}_2$) (Octyne)][PF_6]	73.3
[Ru(Cp)($P^{tBu}{}_2N^{Bn}{}_2$)(–C=CHC_6H_5)][PF_6]	71.5

[a] Values externally referenced to H_3PO_4 at 0.0 ppm

3.4 Attempted Synthesis of [Ru(Cp)($P^{tBu}{}_2N^{Bn}{}_2$)(H_2O)][PF_6]

Following halide abstraction of Ru(Cp)($P^{tBu}{}_2N^{Bn}{}_2$)(Cl) in CH_2Cl_2 addition of 1.1 equivalents of degassed water afforded an orange/brown solution (Scheme 9). An NMR scale experiment (*vide infra*) indicated that a new species, presumably the aqua complex, was generated in quantitative yield. Attempted isolation by precipitation yielded a black oil, which is indicative of decomposition.

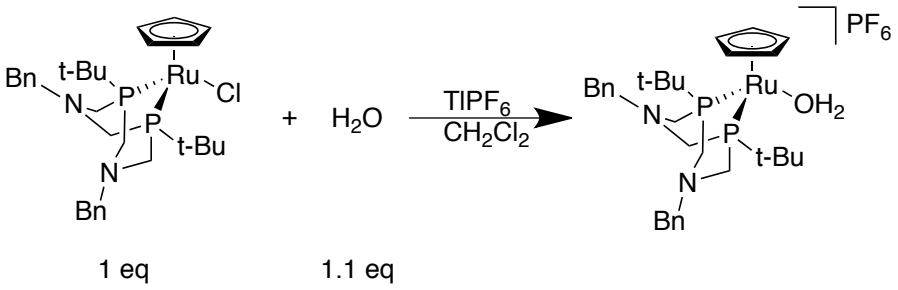

Scheme 9. Attempted synthesis of the water complex from Ru(Cp)($P^{tBu}{}_2N^{Bn}{}_2$)(Cl)

3.5 Synthesis and Characterization of [Ru(Cp)($P^{tBu}_2N^{Bn}_2$)(–C=CPh)][PF_6], **2**

The complex [Ru(Cp)($P^{tBu}_2N^{Bn}_2$)(–C=CPh)][PF_6], **2**, was synthesized by adding 1.0 equivalent of phenylacetylene to [Ru(Cp)($P^{tBu}_2N^{Bn}_2$)(MeCN)][PF_6], **1**, in acetone at room temperature (Scheme 10).

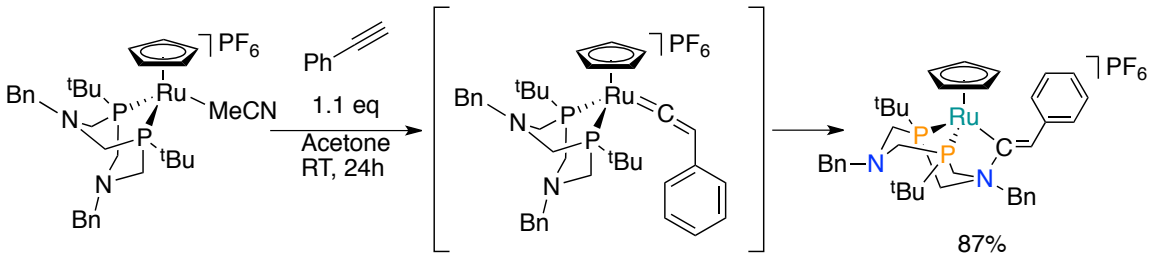

Scheme 10. Synthesis of the complex [Ru(Cp)($P^{tBu}_2N^{Bn}_2$)(–C=CPh)][PF_6], **2**, showing postulated vinylidene intermediate

After 20 hours, complete conversion to the product was observed as judged by $^{31}P\{^1H\}$ NMR analysis of a reaction aliquot. Pure product was obtained by concentration of solvent to a minimum and layered with diethyl ether and placed in a –33˚C freezer. A yellow solid precipitated and was washed with Et_2O and hexanes excess solvents were removed *in vacuo* giving a yellow-orange solid. The product was analyzed by MALDI-MS using pyrene as the matrix. The observed spectrum had an isotope pattern and monoisotopic mass of *m/z* 711.3 that is consistent with simulated values that are consistent with a vinylidene complex, Ru(Cp)($P^{tBu}_2N^{Bn}_2$)(=C=CPh)$]^+$, or a vinyl ammonium species, [Ru(Cp)($P^{tBu}_2N^{Bn}_2$)(–C=CPh)$]^+$ (Figure 4). The complex was also submitted for elemental analysis the calculated and found values match except there is a small but significant difference in the calculated and found value for carbon.

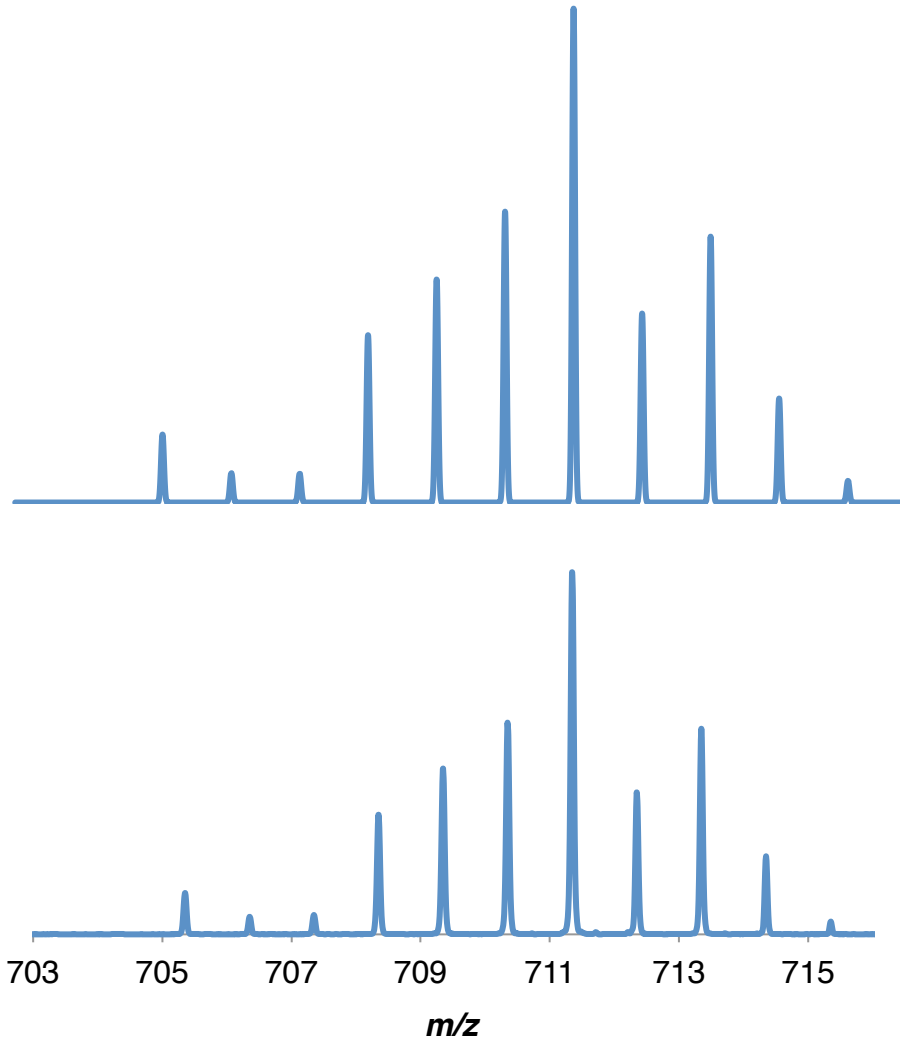

Figure 4. MALDI-MS of [Ru(Cp)($P^{tBu}{}_2N^{Bn}{}_2$)(–C=CPh)][PF_6], **2**, acquired with a pyrene matrix. The top spectrum shows [Ru(Cp)($P^{tBu}{}_2N^{Bn}{}_2$)(–C=CPh)]$^+$ (*m/z* 711.3) is the collected data and the bottom is the simulated[6] spectrum for [Ru(Cp)($P^{tBu}{}_2N^{Bn}{}_2$)(–C=CPh)]$^+$ (*m/z* 711.3).

Crystalline product was obtained for X-ray analysis by slow vapor diffusion in acetone with diethyl ether. An X-ray crystal structure was obtained of the product and it was

determined that the structure is a vinyl ammonium, where the pendant amine of the ligand has attacked the alpha carbon of the phenylacetylene (Figure 5). The bond length between Ru1 and C6 is characteristic of a single Ru-C bond at 2.0721(16) Å.[8] This bond is ca. 0.3 Å longer than the typically expected ruthenium-vinylidene bond length (Table 3).[9,10] The bond length between C6 and C7 is 1.340(2) Å is characteristic of a C=C bond. The bond length between N1 and C6 is 1.591(2) Å, within the range expected for a N-C single bond. The bond angle between Ru1-C6-C7 is 135.05˚, which is wider than the typical 120˚ for an sp^2 hybridized carbon atom. These distorted angles may be caused by the sterics of ligand and phenylacetylene or because of the interaction between the C6-N1. The tertiary nitrogen of the P_2N_2 ligand is not extremely basic therefore other stronger bases or nucleophiles may be able to compete with this interaction.

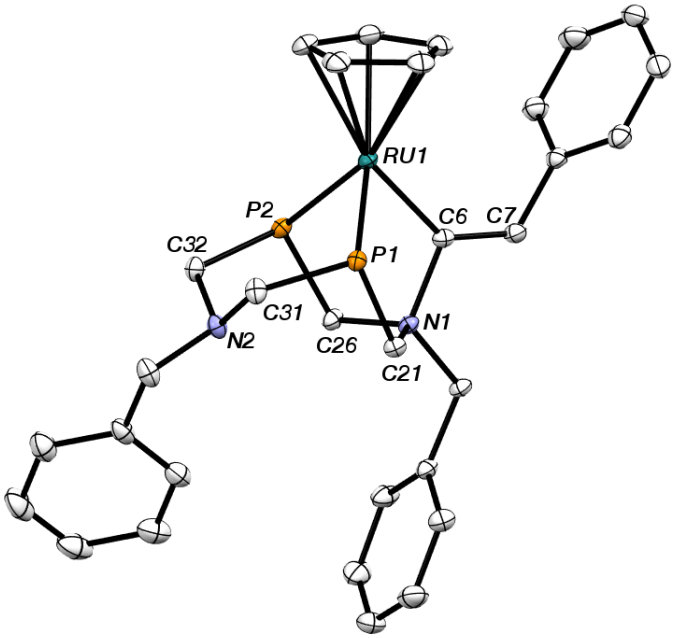

Figure 5. ORTEP of [Ru(Cp)($P^{tBu}{}_2N^{Bn}{}_2$)(-C=CPh)][PF_6], **2**. Thermal ellipsoids are shown at a 50% probability. Hydrogen atoms, ^{t}Bu groups (on the $P^{tBu}{}_2N^{Bn}{}_2$ ligand) and the PF_6 anion were removed for clarity.

Table 3. Table of selected bond lengths for complex **2**

Entry	Selected Bonds	Length (Å)	Bond Character	Typical Bond Length (Å)
1	Ru1-C6	2.0721(16)	Single Bond	1.841[a] 2.251[b]
2	C6-C7	1.340(2)	Double Bond	1.33
3	N1-C6	1.591(2)	Single Bond	1.469

[a] Double Bond [b] Single Bond

A combination of ^{1}H, $^{31}P\{^{1}H\}$, $^{13}C\{^{1}H\}$, and 2D NMR spectroscopy experiments were performed on isolated $[Ru(Cp)(P^{tBu}{}_2N^{Bn}{}_2)(-C{=}CPh)][PF_6]$, **2**, and all of the ^{1}H and ^{13}C for the complex have been assigned. The ^{1}H NMR signal for the vinyl proton H^A (see Figure 6 for atom labels) was found at 7.39 ppm by a ^{1}H-^{13}C HMBC correlation to the adjacent aryl group and through correlations the Cα was found at 195.7 ppm in the ^{1}H-^{13}C HMBC NMR spectrum. Typically Cα of a vinylidene functionality is found at ca. 350 ppm; however, the vinyl ammonium Cα is significantly upfield. This is in agreement with similar Ru-vinyl species, which have a shift at ca. 190 ppm.[9,11] A ^{1}H-^{1}H COSY correlation was also observed between the H^A to the methylene (H^E) of the proximal benzyl group of the $P^{tBu}{}_2N^{Bn}{}_2$ ligand at 4.83 ppm. The proximal benzyl group was shifted downfield by 1.4 ppm relative to the methylene of the distal benzyl (H^F). The data indicates that the vinyl ammonium, N1-C6 bond, is retained in the solution state.

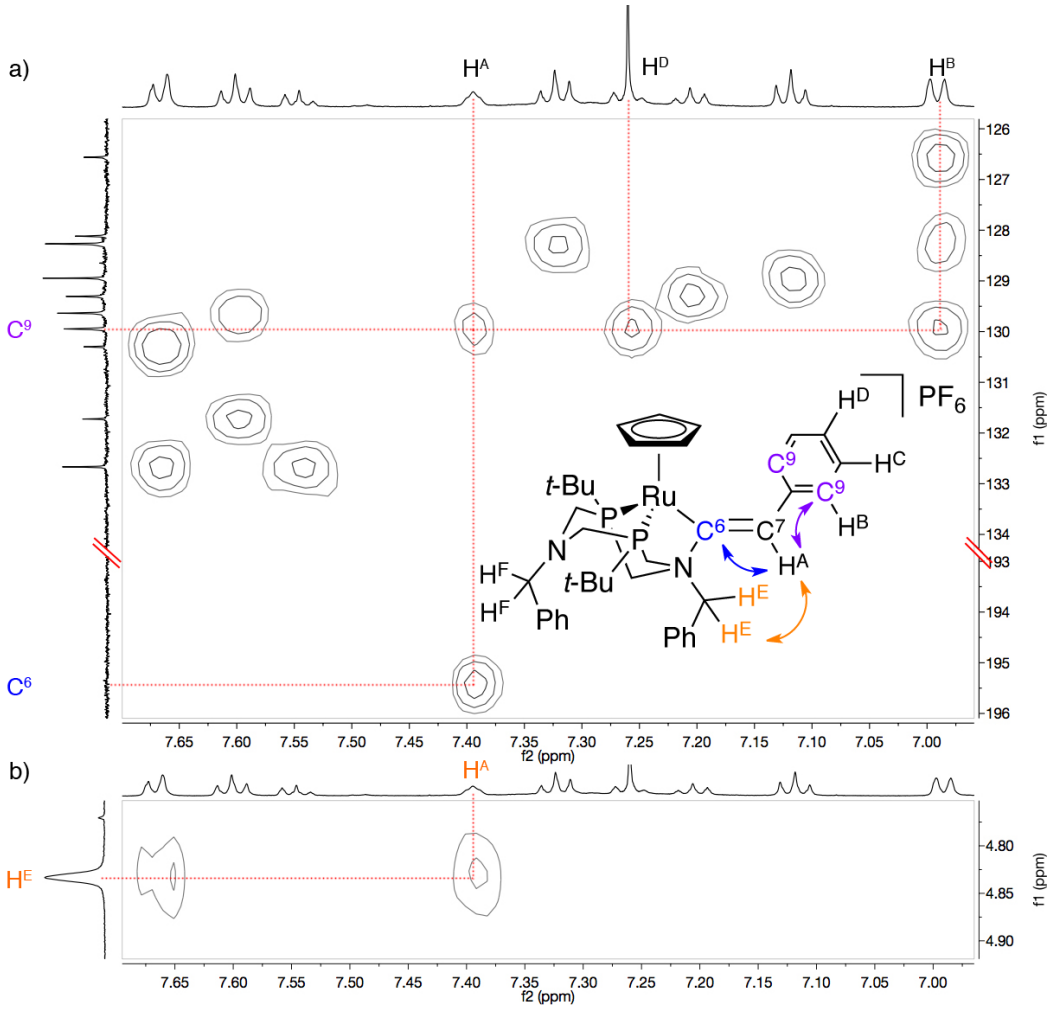

Figure 6. Relevant portions of correlation NMR spectra for complex **2**, for atom labels see the inset structure. a) ^{1}H-^{13}C HMBC spectrum correlations from H^{A} (purple and blue arrows on the inset structure); b) ^{1}H-^{1}H COSY NMR spectrum of H^{A} to the benzyl methylene H^{E} of the P$^{tBu}{}_2$N$^{Bn}{}_2$ ligand (orange arrow on the inset structure).

It is postulated that a vinylidene is initially formed but is rapidly attacked by the pendant base of the P$^{tBu}{}_2$N$^{Bn}{}_2$ ligand forming the vinyl ammonium species. This deactivation pathway has been reported for other ruthenium-vinylidene species containing a pendant amine.[11] This is because the Cα is electrophilic and presumably the vinyl ammonium

species is a lower energy product. It is possible that in solution an equilibrium exists between the vinyl ammonium and vinylidene (Scheme 11).[13]

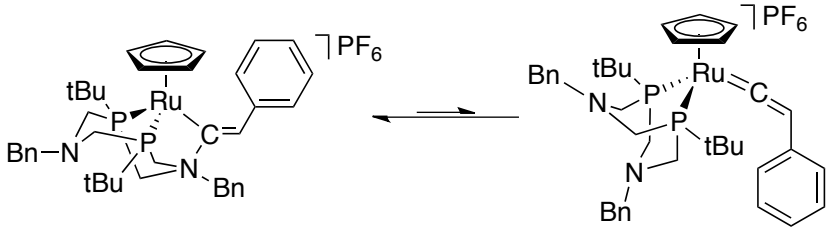

Scheme 11. Possible equilibrium between vinyl ammonium, **2**, and vinylidene moiety.

3.6 Attempts to Break Lewis Acid-Base Interaction

To understand the inactivity of [Ru(Cp)($P^{tBu}{}_2N^{Bn}{}_2$)(–C=CPh)][PF_6], **2**, better, the isolated complex's stability and possible equilibrium were assessed with a variety of probe reactions (Scheme 11). In similar ruthenium-vinyl systems an equilibrium between the vinylidene and a vinyl enolester is present in the solution state.[13] Using variable temperature NMR spectroscopy, the vinyl ammonium complex, **2**, was heated to 70˚C in acetonitrile and monitored by $^{31}P\{^1H\}$ NMR spectroscopy (Figure 7). Heating of the vinyl ammonium could possibly push the equilibrium to form the vinylidene complex; however, no changes were observed in the spectra.

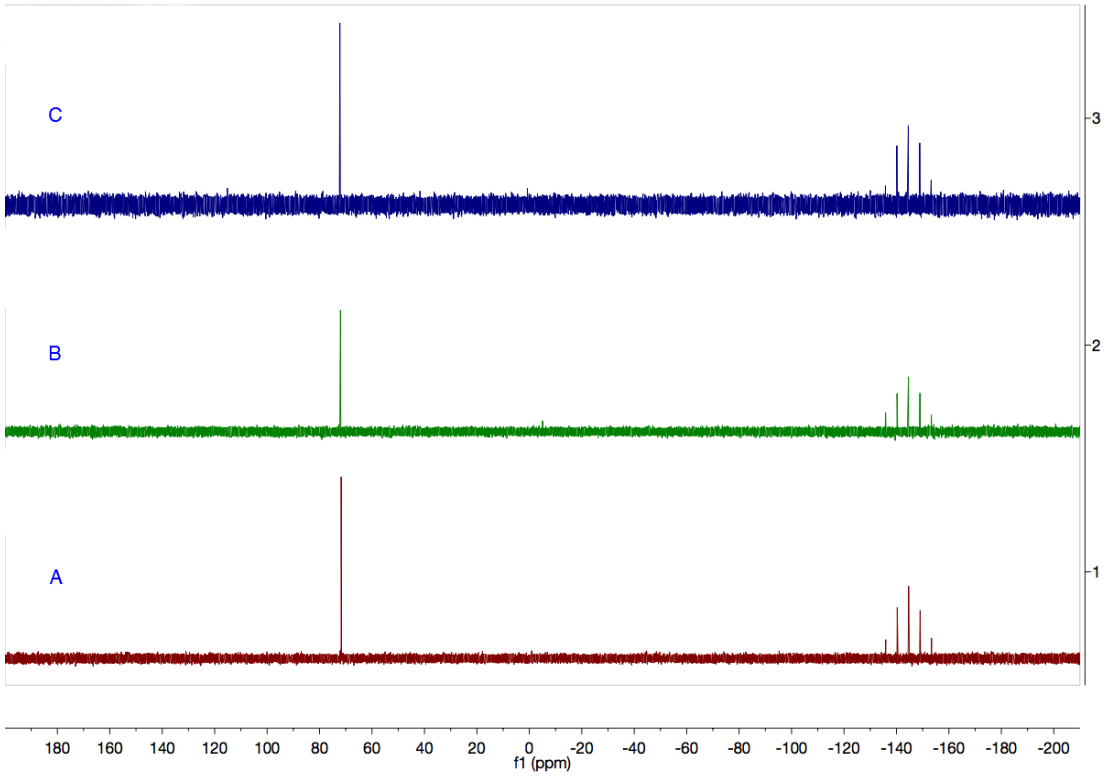

Figure 7. Variable Temperature $^{31}P\{^{1}H\}$ NMR spectra (161.8 MHz) of complex **2** in MeCN-d_3 at: A. 25 ˚C, B. 50 ˚C, and C. 70 ˚C.

Water was chosen as a weak nucleophile to assess the equilibrium of the vinyl ammonium moiety and the vinylidene (Scheme 12). However, upon treatment with one equivalent no changes were observed. Using vinylmagnesium bromide as a stronger nucleophile the complex still showed no changes by $^{31}P\{^{1}H\}$ NMR spectroscopy, indicating that the Lewis acid-base interaction is very strong and that the nucleophiles added were not sufficiently strong enough to compete with the formation of the C-N bond and that no equilibrium between the vinyl ammonium and vinylidene exists.

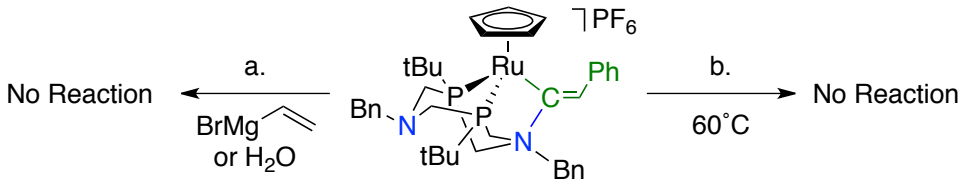

Scheme 12. Attempts to cleave the Lewis acid-base interaction of the vinyl ammonium complex **2** with a) nucleophiles or b) by heating.

3.7 Protonation of Vinyl Ammonium Complex

A small excess (1.25 equiv.) of [HDMF]OTf ($pK_{a(MeCN)}$ = 6.1) was added to [Ru(Cp)($P^{tBu}{}_2N^{Bn}{}_2$)(–C=CPh)][PF_6], **2**, in hopes of breaking the Lewis acid-base interaction (Scheme 13). Upon addition of acid a new species was formed with δ_P = 80.8, ca. 9 ppm downfield of the signal for [Ru(Cp)($P^{tBu}{}_2N^{Bn}{}_2$)(–C=CPh)][PF_6], **2**. Attempts to isolate the new complex were unsuccessful however the new species was characterized in situ by NMR spectroscopy. Through correlation NMR spectroscopy the protons on the distal methylene of the benzyl group, H^F, were shown to be correlating to a new broad singlet at 6.35 ppm (Figure 8). This signal was also shown to correlate to $H^{K/L}$, the distal methylene protons of the P_2N_2 ring, indicating that the distal nitrogen was protonated. Correlation of H^A (of the vinyl ammonium moiety) to the proximal benzyl protons, H^E, was still observed indicating that the Lewis acid-base interaction remained intact. Through correlations, Cα was found at 189.9 ppm consistent with a vinyl ammonium species.[9,13] Through correlation NMR spectroscopy it was observed that the proton from the new protonated site, H^Z, was correlating to the distal methylene protons of the benzyl group, H^F, and to the distal protons of the methylene's in the P_2N_2 ring, $H^{K/L}$. There was also a correlation between H^A and H^E, the protons of the proximal benzyl methylene, indicating that the C6-N1 bond of the vinyl ammonium remained intact. The correlation NMR spectroscopy data all suggest that the site of protonation is the distal nitrogen of the $P^{tBu}{}_2N^{Bn}{}_2$ ligand and the Lewis acid-base interaction remained intact. Upon addition of

2.0 equivalents of [HDMF]OTf, there is no sign of protonation other than the on the distal nitrogen of the P_2N_2 ligand.

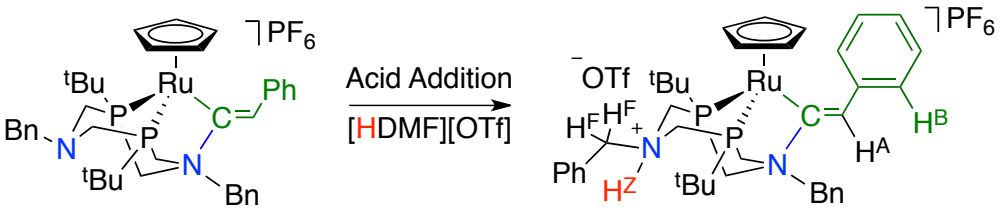

Scheme 13. Attempt to break the LAB interaction in complex **2** using [HDMF][OTf]

Through heating, addition of nucleophiles, and addition of acid it was observed that the Lewis acid-base interaction in for [Ru(Cp)($P^{tBu}{}_2N^{Bn}{}_2$)(–C=CPh)][PF_6], **2**, is strong and that a vinylidene is not present as a minor equilibrium species.

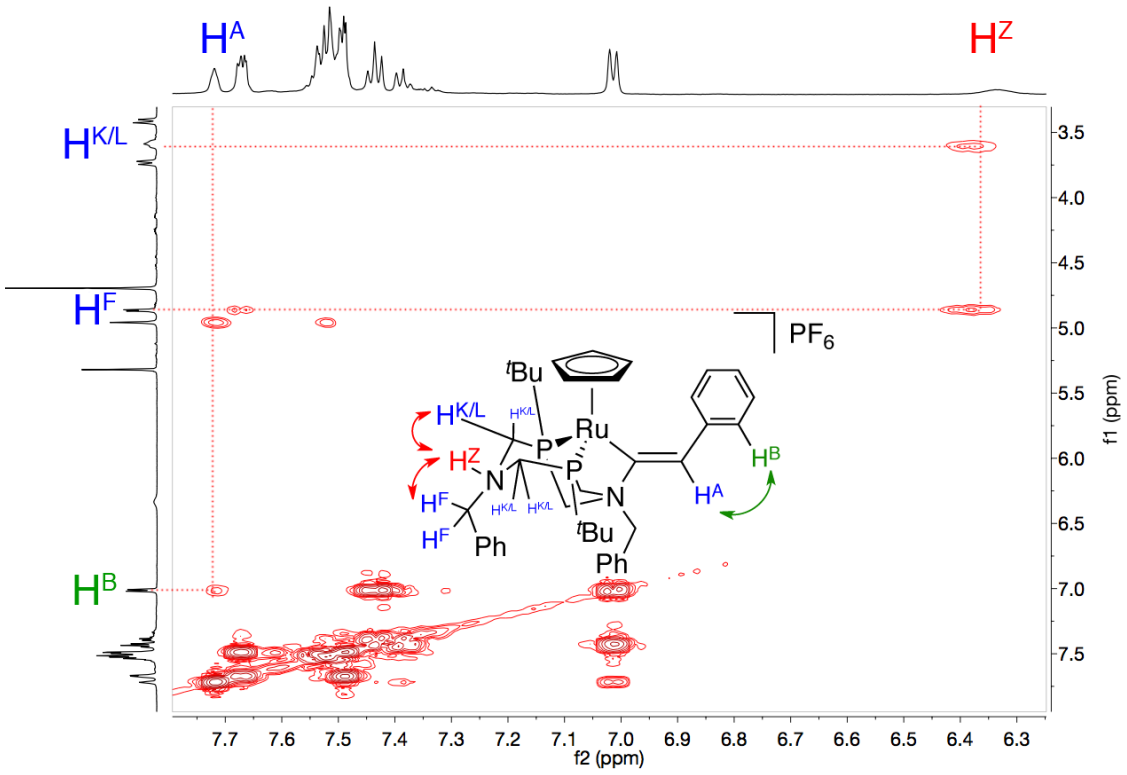

Figure 8. Relevant portions of correlation NMR spectra for complex **3**, for atom labels see the inset structure. ^{1}H-^{1}H COSY NMR spectrum in CD_2Cl_2 (600 MHz).

3.8 Cyclization of Alkynyl Alcohols

The vinyl ammonium complex has a strong Lewis acid-base interaction that is unreactive to acid, nucleophiles, and heating. I postulate that the intermolecular attack of water in the hydration reactions could not compete with the intramolecular deactivation. The intermolecular attack of water was not sufficiently fast. To prevent the formation of the deactivated species, a new substrate, 2-ethynylbenzyl alcohol, was chosen (Scheme 14). The new substrate may be capable of competing with the intramolecular deactivation because the cyclization would occur through the intramolecular attack of the alcohol, to form a favourable 6-membered heterocycle. To assess this hypothesis the reactivity of the new substrate was tested in an NMR spectroscopy probe reaction where 1 equivalent of 2-ethynylbenzyl alcohol was reacted with 1 equivalent of

[Ru(Cp)($P^{tBu}_2N^{Bn}_2$)(MeCN)][PF_6], **1**, in acetone-d_6 (Scheme 14). After 24 hours there was a decrease in the organic starting material and a new peak was observed in the ^1H spectrum at 5.86 ppm, which is consistent with the ring closed organic product, 1*H*-isochromene.[14] No changes were observed in $^{31}P\{^1H\}$ NMR spectra suggesting the starting [Ru(Cp)($P^{tBu}_2N^{Bn}_2$)(MeCN)][PF_6] complex was not deactivated, but instead regenerated after product formation. This indicates that the intramolecular nucleophilic attack of the alcohol is competitive with the attack of the pendant base. In this reaction, formation of the product is faster than the formation of a deactivated vinyl ammonium species.

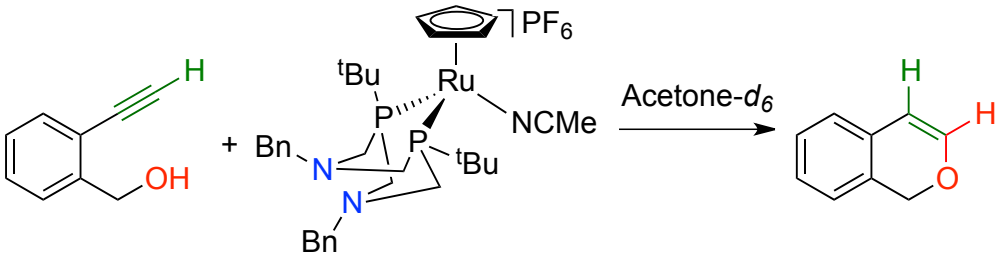

Scheme 14. Stoichiometric addition of 2-ethynylbenzyl alcohol to **1** analyzed at 10 minutes, 1 hour and 24 hours.

3.9 Optimization of Catalytic Cyclization Conditions

With successful cyclization of 2-ethynylbenzyl alcohol under stoichiometric conditions, the reaction could then be tested under catalytic conditions where 5 mol% of [Ru(Cp)($P^{tBu}_2N^{Bn}_2$)(MeCN)][PF_6], **1**, is used with 0.15 M 2-ethynylbenzyl alcohol. To establish the optimal reaction conditions, four different solvents were assessed (acetone, acetonitrile, THF, and CH_2Cl_2)(Scheme 15). All reactions were heated at 40˚C with the exception of acetonitrile, which was heated to 60˚C, and monitored over 24 hours (Figure 9). Acetone was the best solvent for the reaction giving a maximum substrate consumption of 99% and conversion to product of 82%. The difference in mass balance suggests that a minor amount of an unidentified side-product was formed (15%). DCM gave comparable conversions (83%) to acetone but was slower to reach maximum

conversion and there was a larger amount of the side-product being formed (20%). When THF was used as the solvent there was a significant amount of side-product formed and the overall conversion to product reached a maximum of only 72%. Acetonitrile gave the lowest conversion to product with a maximum of 10%, which is not unexpected because acetonitrile is a coordinating ligand that competes with substrate binding. With a massive excess of acetonitrile present the rate of binding of the phenylacetylene would be very low.

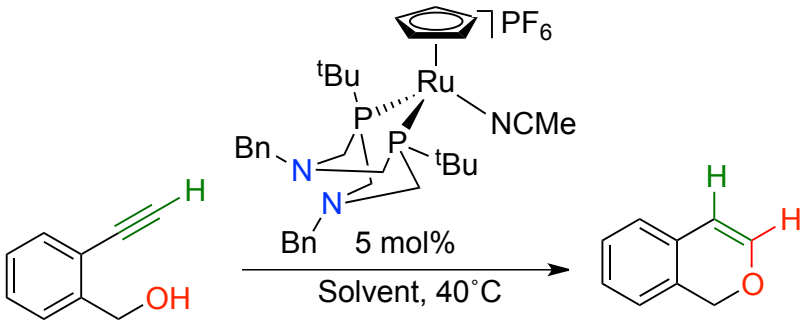

Scheme 15. General Conditions for the catalytic cyclization of 2-ethynylbenzyl alcohol using **1**

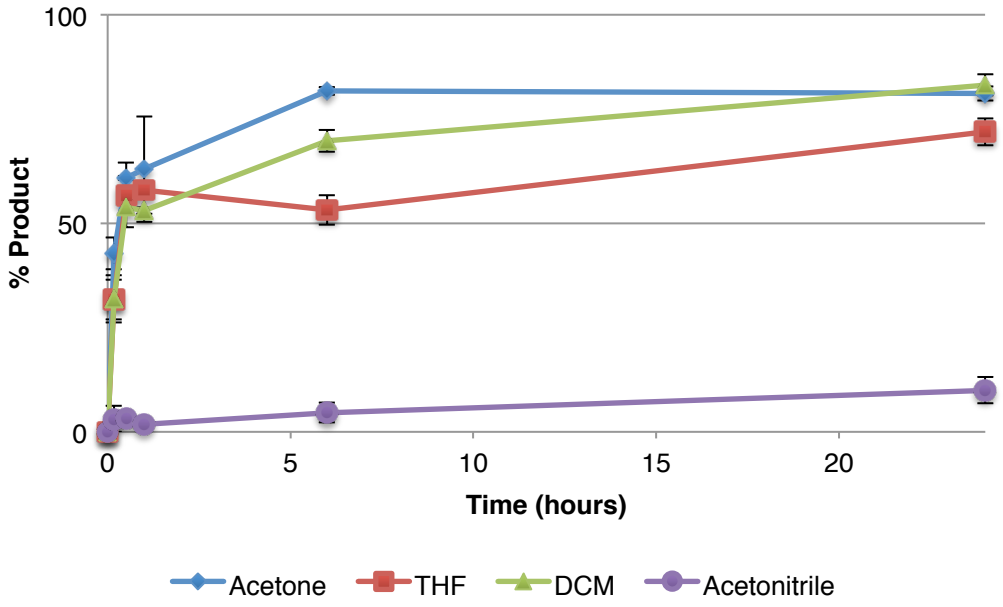

Figure 9. Conversion curve for the formation of 1*H*-isochromene in different solvents with complex **1** as the catalyst. Reactions were performed in duplicate and the error bars represent the spread in the conversion values.

With acetone established as the optimal solvent the catalyst loading was dropped to 1 mol% and 0.1 mol% and followed the same procedure as above. The maximum conversion to product observed in the 1 mol% catalyst loading reactions was 68% after 24 hours. With a catalyst loading of 5 mol% the conversion from starting material to product is quick, with 63% conversion after 1 hour and a maximum conversion of 82% achieved by 6 hours (Figure 10). When the catalyst loading is dropped to 1 mol% the reaction is slowed down slightly but the overall conversion is very similar to the 5 mol% reaction. Dropping the catalyst loading to 0.1 mol% resulted in very slow reaction times and low conversion. The optimal loading for this reaction is 1 mol% because less catalyst was used and the slower reaction times allowed for easier catalyst comparisons.

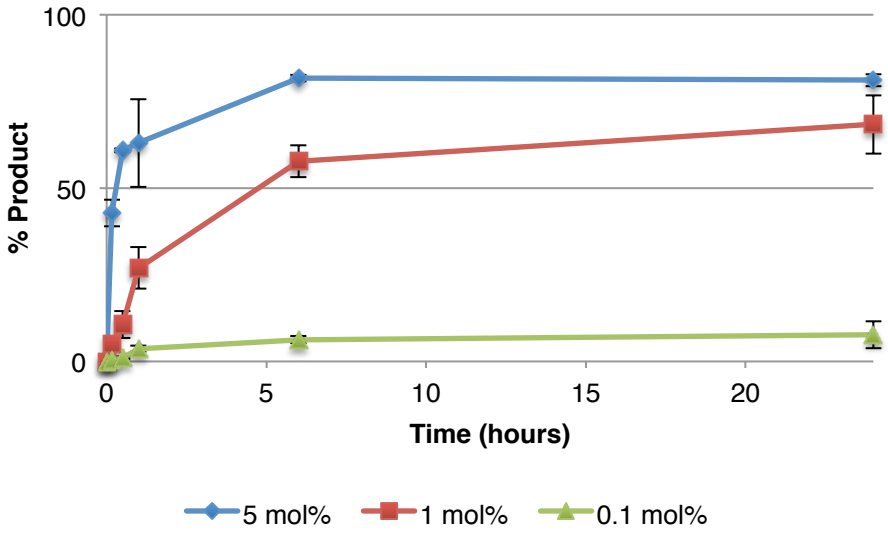

Figure 10. Conversion curve for the formation of 1*H*-isochromene using different catalyst loadings of Ru(Cp)($P^{tBu}{}_2N^{Bn}{}_2$)MeCN][PF_6], **1**.

3.10 References

(1) Tronic, T. A.; Kaminsky, W.; Coggins, M. K.; Mayer, J. M. *Inorg. Chem.* **2012**, *51*, 10916–10928.

(2) Kundig, E. P.; Monnier F. R. *Adv. Synth. Catal.* **2004**, *346*, 901–904.

(3) Li, L.; Herzon, S. B. *Nat. Chem.* **2014**, *6*, 22–27.

(4) Li, L.; Zeng, M.; Herzon, S. B. *Angew. Chem. Int. Ed.* **2014**, *53*, 7892–7895.

(5) Zeng, M.; Li, L.; Herzon, S. B. *J. Am. Chem. Soc.* **2014**, *136*, 7058–7067.

(6) Tronic, T. A.; Rakowski DuBois, M.; Kaminsky, W.; Coggins, M. K.; Liu, T.; Mayer, J. M. *Angew. Chem. Int. Ed.* **2011**, *50*, 10936–10939.

(7) Patiny, L.; Borel, A. *J. Chem. Inf. Model.* **2013**, *53*, 1223–1228.

(8) Sung, H. L.; Her, T. M.; Su, W. H.; Cheng, C. P. *Molecules* **2012**, *17*, 8533–8553.

(9) Bruce M. I. *Chem. Rev.* **1991**, *91*, 197-257.

(10) Bruce M. I.; Cifuentes M. P.; Humphrey M. G.; Poczman E.; Snow M. R.; Tiekink E. R. T. *J. Organomet. Chem.* **1988**, *338*, 237-248.

(11) Johnson D. G.; Lynam J. M.; Slattery J. M.; Welby C. E. *Dalton Trans.* **2010**, *39*, 10432-10441.

(12) Grotjahn, D. B. *Chem. Eur. J.* **2005**, *11*, 7146–7153.

(13) Smith, E. J.; Pridmore, N. E.; Whitwood, A. C.; Lynam, J. M. *Organometallics* **2014**, *33*, 7260–7269.

(14) Varela-Fernández, A.; González-Rodríguez, C.; Varela, J. A.; Castedo, L.; Saá, C. *Org. Lett.* **2009**, *11*, 5350–5353.

Chapter 4

4 Pd-Loaded Polymer Catalysis and Metal Scavenging with Polymer

A phosphine rich polymer has been designed by Ragogna[1] *et al.* that has been shown to bind to metals effectively (Scheme 16). The many alkyl phosphines in the backbone of the polymer can act as ligands to a metal. The insolubility of the polymer in many solvents makes this ideal for metal scavenging or a solid supported catalyst because when the reaction is complete the polymer can easily be separated from the reaction through a simple filtration.

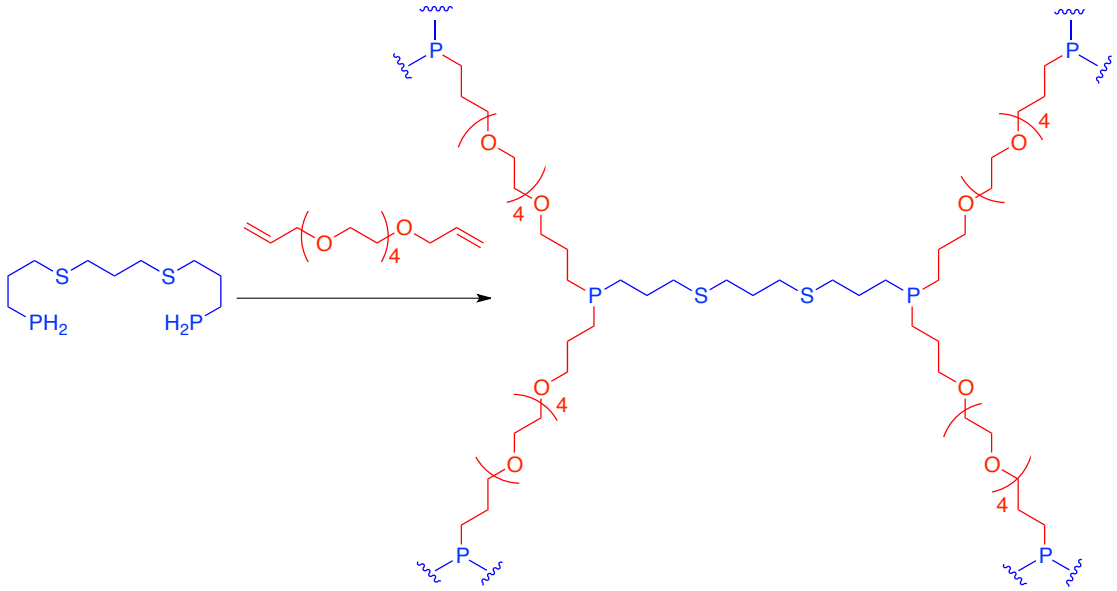

Scheme 16. Phosphine containing polymer developed by Ragogna *et al.*[1]

Herein, I assess the performance of this polymer as a solid support for a homogeneous catalyst and as a scavenger for spent catalyst species.

4.1 Solid Supported Catalysis

4.1.1 Methodology for Suzuki Coupling Reactions

Catalytic studies of the Pd-loaded polymers involve three main sets of experiments: 1) Test the performance in generic Suzuki cross-coupling reactions. The performance is benchmarked relative to structurally analogous molecular complexes acting as control catalysts. 2) Establish heterogeneity of the catalyst though filtration tests to determine if the catalytic species is immobilized on the polymer support. 3) Establish if the catalyst is a single-site palladium species. Mercury tests are used as a common method to establish if the catalytic species is of a molecular nature or heterogeneous (i.e. solid palladium, nanoparticulate).[2] In all cases, performance was assessed through the quantification of the product *p*-methylbiphenyl. The Pd-loaded polymer was made with either $PdCl_2$ or $Pd(OAc)_2$ and the polymeric structure contains primarily alkyl phosphines. Therefore $PdCl_2$ and $Pd(OAc)_2$ with PCy_3 were chosen as inexpensive and easily handled molecular analogues to the polymer as control catalysts. These molecular analogues allow performance of the polymers to be tested accurately. Quantification of the catalytic runs was done based only on the product formed because the aryl halide substrate could not be accurately quantified with the GC/MS method employed.

4.1.2 Optimization of Suzuki Coupling Conditions

An aryl halide, 1.05 equivalents boronic acid, 2 equivalents of a base, and 1.5 mol% Pd catalyst were added to a vial with solvent (Scheme 17). Optimal conditions were established by varying the parameters (Table 4, Entry 15).

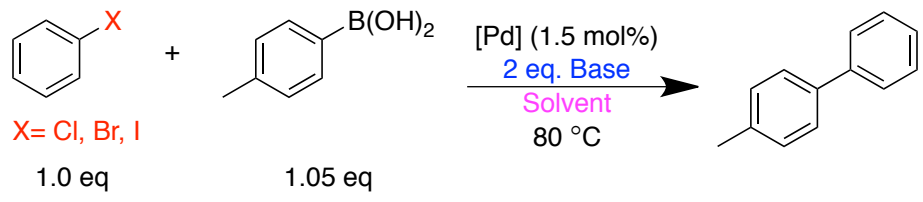

Scheme 17. General conditions for the optimization of Suzuki coupling reaction

All reactions were carried out at 80 ˚C except for Entry 8, Table 4, which was carried out at 120 ˚C. All reactions were carried out using *p*-methylphenylboronic acid except for entry 2, which used *p*-methoxyphenylboronic acid. The initial conditions were chosen to be similar to conditions found in the literature.[3] Initial testing was done with both *p*-methyl and *p*-methoxyphenylboronic acids (Table 4, Entries 1 and 2); however, because there was no initial activity with either substrate, only *p*-methylphenylboronic acid was used for optimization. Using chlorobenzene as the substrate there was no conversion to product or consumption of starting material observed by GC-MS (Table 4, Entries 1 and 2). Because there was no conversion with PhCl it was thought that the C-X bond was too strong and there was no activation of the substrate. Iodobenzene was chosen as a substrate due to its weaker C-X bond. There was no product observed, but there was full consumption of the iodobenzene (Table 4, Entry 3). This indicated that PhI was too easy of a substrate to activate; therefore, in subsequent tests bromobenzene was used as the aryl halide, which has a C-X bond energy between the other two aryl halides. It was also thought that Cs_2CO_3 may not have been a strong enough base, so KO^tBu was employed (Table 4, Entries 4-9). Despite changing the base and aryl halide there was no product formed. Because no conversion was observed with $PdCl_2$, the metal was changed to $Pd(OAc)_2$ (Table 4, Entries 14-19), which was assessed with the bases KO^tBu, K_2CO_3 and Na_2CO_3 (Table 4, Entries 15, 16, 18-23). With the change in base and metal source, product was finally observed and K_2CO_3 gave higher conversion than Na_2CO_3 (Table 4, Entries 15, 20, 22). The solvent mixture of DMF/H_2O was used in some cases but when analyzed by GC/MS there were no peaks observed, which may have been caused by water solubility issues (Table 4, Entries 9, 12, 13, 17-19). With the optimal base and solvent established, the polymer samples were tested and limited conversion was observed but on par with $Pd(OAc)_2/PCy_3$. It was seen that the K_2CO_3 gave higher yields (Table 4, Entries 15, 20, 22). With working conditions established optimization of the temperature was the next step.

Table 4. Optimization of Suzuki coupling reactions and catalyst comparison to Pd-loaded polymer[a]

Entry	Aryl Halide	Base	Solvent	[Pd] (1.5 mol%)	Ligand (3.6 mol%)	Conversion
1	Cl	Cs_2CO_3	Dioxane	$PdCl_2$	PCy_3	0
2[b]	Cl	Cs_2CO_3	Dioxane	$PdCl_2$	PCy_3	0
3	I	Cs_2CO_3	Dioxane	$PdCl_2$	PCy_3	0
4	Br	KO^tBu	Dioxane	$PdCl_2$	PCy_3	0
5	Br	KO^tBu	DMF	$PdCl_2$	PCy_3	0
6[c]	Br	KO^tBu	DMF	$PdCl_2$	PCy_3	0
7[c]	Br	KO^tBu	DMF	$PdCl_2$	PCy_3	0
8[d]	Br	KO^tBu	DMF	$PdCl_2$	PCy_3	0
9	Br	KO^tBu	DMF/H_2O	$PdCl_2$	PCy_3	0
10	Br	K_2CO_3	DMF	$PdCl_2$	PCy_3	0
11	Br	Na_2CO_3	DMF	$PdCl_2$	PCy_3	0
12	Br	K_2CO_3	DMF/H_2O	$PdCl_2$	PCy_3	0
13	Br	Na_2CO_3	DMF/H_2O	$PdCl_2$	PCy_3	0
14	Br	KO^tBu	DMF	$Pd(OAc)_2$	PCy_3	0
15	Br	K_2CO_3	DMF	$Pd(OAc)_2$	PCy_3	26
16	Br	Na_2CO_3	DMF	$Pd(OAc)_2$	PCy_3	12
17	Br	KO^tBu	DMF/H_2O	$Pd(OAc)_2$	PCy_3	0
18	Br	K_2CO_3	DMF/H_2O	$Pd(OAc)_2$	PCy_3	0
19	Br	Na_2CO_3	DMF/H_2O	$Pd(OAc)_2$	PCy_3	0
20	Br	K_2CO_3	DMF	$PdCl_2$ Polymer	None	34
21	Br	Na_2CO_3	DMF	$PdCl_2$ Polymer	None	15

22	Br	K_2CO_3	DMF	$Pd(OAc)_2$ Polymer	None	37
23	Br	Na_2CO_3	DMF	$Pd(OAc)_2$ Polymer	None	18

[a]All reactions were carried out at 80 ˚C with *p*-methylphenyl boronic acid as the standard substrate with the conditions seen in Scheme 4; [b] *p*-methoxyphenyl boronic acid was used as substrate; [c] 7.2 mol%; [d] 120 ˚C

4.1.3 Temperature Optimization for Suzuki Coupling Reactions

Using the conditions established in previous test reaction (Table 4, Entries 15, 20, 22) the temperature was varied to obtain conditions with the highest yield possible. Runs were performed at 50, 80, and 110 ˚C. At 50 ˚C no product was formed indicating that there was not enough energy for the reaction to occur. The reactions at 80 ˚C have some product formation and, unlike the reaction at 50 ˚C, there was also a small amount of black solids formed. The 110 ˚C reactions gave the highest conversion to product and also had the largest amount of black solids. This suggests that the black solids, which are thought to be palladium black, may be mediating the catalytic reaction, instead of the metal on the polymer.

4.1.4 Evaluation of Pd-Loaded Polymers as Catalysts for Suzuki Cross-Coupling

Suzuki coupling of bromobenzene and *p*-methylphenylboronic acid was conducted under the optimized conditions established using 3 mol% of the three catalysts: **A** $Pd(OAc)_2$ with PCy_3; **B** $PdCl_2$-polymer; and **C** $Pd(OAc)_2$-polymer (Scheme 18). Both polymer catalysts **B** and **C** gave a maximum conversion to product of 50% at 5 hours (Figure 11). After 5 hours the reaction reached completion, where further heating to 20 hours gave no additional product. The similarities of the curves and the maximum conversion values indicate that the initial palladium source does not affect the performance of the polymer catalyst. While catalysis did occur using these palladium containing polymers, the standard metal-ligand set of $Pd(OAc)_2$ and PCy_3 showed greater performance with a maximum conversion of 77% after 5 hours. In contrast, the Pd precursor $PdCl_2$ with PCy_3

did not yield any product after 5 hours. This indicates that when the polymer is treated with the metal, some reaction occurs making the $PdCl_2$ as reactive at the $Pd(OAc)_2$ derived polymer. Under the high temperatures required for catalysis, the polymer formed a black solid, which is thought to be palladium nanoparticles.

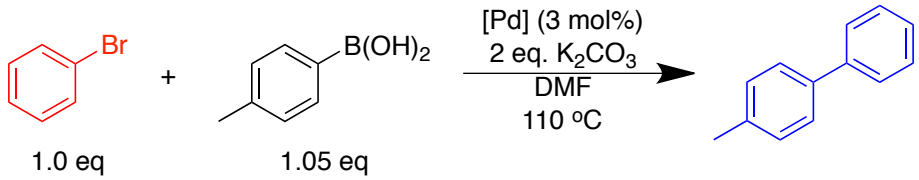

Scheme 18. Catalyst comparison under optimized conditions for the Suzuki Cross-Coupling reaction

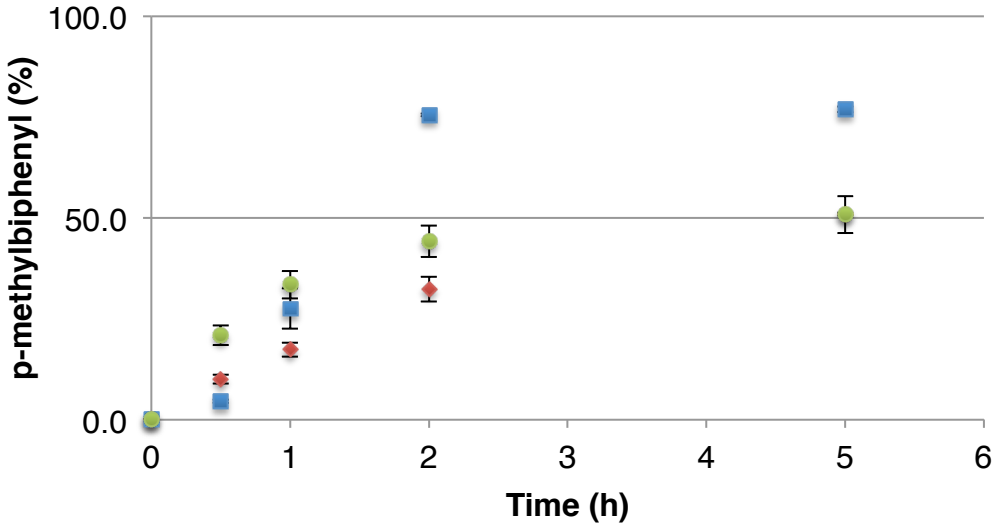

Figure 11. Conversion curves for Suzuki-Coupling reactions of Bromobenzene to 4-methylbiphenyl catalyzed by: **A** $Pd(OAc)_2/PCy_3$ (■), **B** $PdCl_2$-polymer (◆), and **C** $Pd(OAc)_2$-polymer (○).

4.1.5 Filtration of Pd-Loaded Polymers as Catalysts for Suzuki Cross-Coupling

Filtration of both polymer and control catalysts was done to determine if the polymer catalysts were solid-supported as I hypothesized. The reactions were filtered after 0.5 hours and were analyzed at different timepoints following the filtration. If catalysis is arrested following filtration to remove the polymer this indicates that the catalyst is solid-supported. If catalysis does not stop then a soluble solution-based catalyst is present. The filtration of the reaction solutions removes both the polymer catalyst and the base. $Pd(OAc)_2$ with PCy_3 was affected the least with a conversion to product of 70%, which is only 5% less than the standard Suzuki coupling without filtration (Figure 12). This indicates that the $Pd(OAc)_2/PCy_3$ catalyst is mainly homogeneous but there is the possibility that some nanoparticles form and are filtered away. **B** retained a similar conversion to product as well giving a maximum conversion of 45% at 5 hours, which is also only 5% less than the standard reaction. This indicates that the polymer is leeching palladium into solution resulting in catalytic turnover. Upon heating the polymer, black particles formed that could possibly be palladium black. Catalysis still occurs after filtering the particles suggesting that the black particles are not the active catalyst. Pd(0) should be generated during the catalytic cycle and Pd(0) precursors are know to aggregate into nanoparticles. These nanoparticles have been shown to be catalytically active and soluble.[4] It is possible that the palladium from the polymers are forming soluble nanoparticles and is responsible for the catalytic turnover. The filtration had the largest effect on **C,** which gave only 36% conversion after 5 hours, 15% less than the standard cross-coupling reaction. This indicates that at least some part of the catalyst is solid-supported; however, there is still some portion of the catalyst in solution because catalysis was not arrested completely.

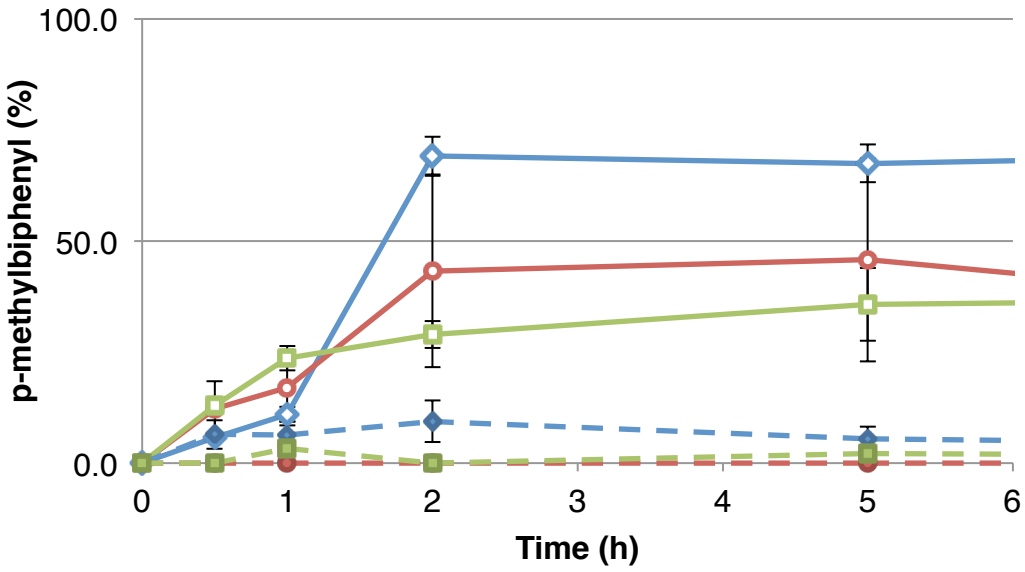

Figure 12. Conversion curves for the filtration at 0.5 hours (solid lines) of: **A** $Pd(OAc)_2$ (◆), **B** $PdCl_2$-polymer (○), and **C** $Pd(OAc)_2$-polymer (■) and mercury test (dotted lines) of **A** $Pd(OAc)_2$ (◆), **B** $PdCl_2$-polymer (○), and **C** $Pd(OAc)_2$-polymer (■).

4.1.6 Mercury Poisoning Test of Pd-Loaded Polymers as Catalysts for Suzuki Cross-Coupling

The mercury test was conducted to determine if there was a heterogeneous catalyst in solution.[2] If catalysis is halted on addition of mercury this indicates that the catalyst is heterogeneous, but if catalysis continues the catalyst is a homogenous molecular species. Suzuki coupling reactions were conducted under the optimized conditions in the presence of 10 molar eq. of mercury relative to palladium (Scheme 19).

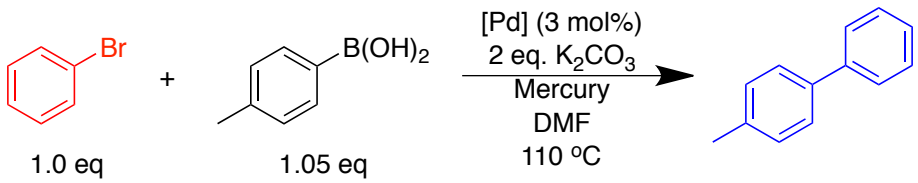

Scheme 19. Mercury poisoning test of Pd-loaded polymers as catalysts in Suzuki Coupling

Analysis of the reaction solutions for the polymer catalysts **B** ($PdCl_2$) and **C** ($Pd(OAc)_2$) indicated <5% conversion to product (Figure 12). This indicates that the polymer catalysts are heterogeneous but not solid-supported. Catalysis was halted with the addition of mercury but not when filtered through a glass microfiber plug; this is indicative of a small heterogeneous catalyst, which is thought to be nanoparticulate. $Pd(OAc)_2$ gave the highest conversions to product at >10% indicating that there is homogeneous catalysis occurring. However, because there was a 66% decrease in product formed this indicates that it is mainly heterogeneous and the particles are too small to be filtered because of the high conversion seen in the filtration results.

4.1.7 SEM Analysis of Polymer Samples

The filtration and mercury tests provided some evidence for the presence of nanoparticles. SEM analysis was performed on the solids filtered from the catalytic reaction of **C** after 2 hours of heating (Figure 13). Elemental mapping analysis was performed on the **C** that was removed from a Suzuki cross coupling reaction conducted under optimized conditions. This was done on **C** only because the Pt-coating required for SEM analysis on **B** did not adhere properly. The polymer had higher concentrations of palladium than the rest of the sample area. The area was identified as a polymer because of the higher concentrations of carbon, oxygen, sulfur, and phosphorus. Upon further inspection of the sample no nanoparticles were observed. The absence of nanoparticles is not thought to be due to insufficient resolution because typical palladium nanoparticles are 10-200 nm[4] and the SEM used is capable of <2 nm resolution. The absence of nanoparticles suggests that they are in solution, which would be consistent with the filtration data. SEM analysis was performed on the native palladium-loaded polymers and no changes between native polymer and polymers that were subjected to catalytic conditions were observed. Further analysis by TEM could be performed on the liquid portion of the catalytic reactions to determine if nanoparticles are present in solution, but this was not done because leeching of palladium from the polymer renders them insufficient catalysts.

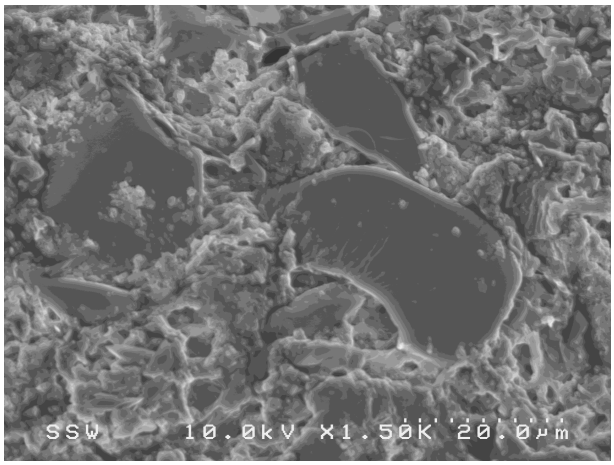

Figure 13. SEM image of **C** under catalytic conditions at magnification level of ×1.50k, the large dark spots in the image is the Polymer **C**

4.2 Metal Scavenging

From the previous studies it was determined that the metal-loaded polymers were not sufficiently active to be effective catalysts. However, the ability to bind to metals effectively and their insolubility makes them good candidates as metal scavengers.

4.2.1 Quenching and Sequestration of Wilkinson's Catalyst

The hydrogenation of styrene using Wilkinson's catalyst, $RhCl(PPh_3)_3$, (Scheme 20) was used as a proof of principle for the quenching and sequestration ability of the alkylphosphine polymer designed by Ragogna *et al.*[1] Polymer was present from the outset of the hydrogenation reaction and after 10 minutes catalytic performance was assessed at different timepoints.

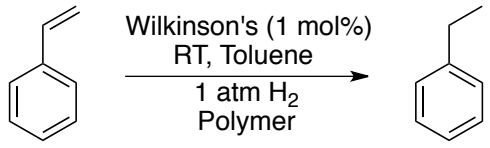

Scheme 20. Reaction conditions of the hydrogenation of styrene using Wilkinson's Catalyst, $RhCl(PPh_3)_3$

Analysis of the hydrogenation with polymer present indicates that the catalyst is quenched almost instantaneously from the time of addition. However, without the polymer the reaction continues to turnover and consumes ca. 90% of the styrene after 80 minutes (Figure 14). This shows that the catalyst is effectively quenched upon addition of polymer; however, it is not known if quenching of the catalyst equals complete sequestration.

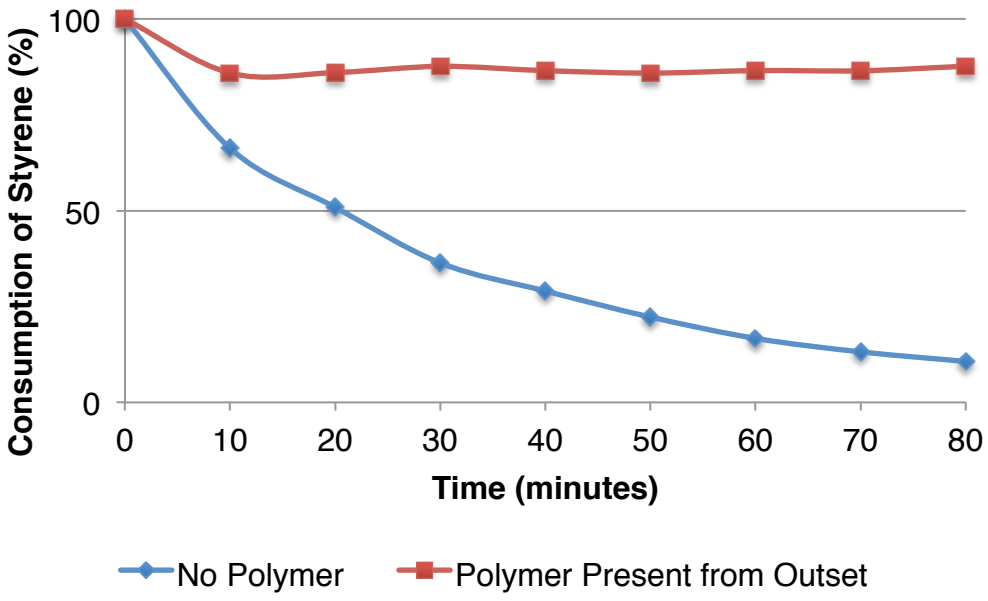

Figure 14. Consumption of styrene over time with and without polymer present

4.2.2 Incubation Time

Using hydrogenation of styrene by Wilkinson's catalyst as the benchmark reaction, the time needed for scavenging with the polymer was probed. This experiment tested three things: 1) how long it takes for catalysis to be halted by the polymer 2) to assess if the maximum sequestration is reached in the same period of time needed for catalyst quenching (i.e. <20 minutes) and 3) if extending the incubation time of the polymer in the catalytic reaction (to 24 h) increases metal removal. Reactions were conducted with polymer present from the outset and the organics were separated by filtration after 20 minutes or 24 hours. The remaining Rh metal in the organic residue was quantified by

ICP-MS analysis (Table 5). The sample incubated for 20 minutes gave a value of 236 ppm of rhodium whereas the 24 hour incubation time sample had 11 ppm of rhodium (Table 5, Entries 1 and 2). From the ICP-MS data of the residue it can be seen that the polymer removed an order of magnitude more rhodium with an incubation time of 24 hours compared to the 20 minute reaction.

Table 5. Conditions Screened for the Sequestration of Rh with Polymer[a]

Entry	Polymer Loading	Incubation Time	Phase	ppm of Rh[b]	% Rh Removed
1	1.5	20 minutes	Liquid	236	95.8
2	1.5	24 hours	Liquid	11.0	99.8
3	0[c]	24 hours	Liquid	3,190	43.2
4	1/10	24 hours	Liquid	586	89.6
5	1	24 hours	Liquid	135	97.6
6	2	24 hours	Liquid	94.3	98.3
7	4	24 hours	Liquid	26.4	99.5

[a] All reactions were carried out using 1 mol% Wilkinson's Catalyst with styrene as the substrate and polymer present from the outset (Scheme 20); [b] ICP-MS analysis; [c] No polymer was present however the reaction was filtered through a 0.22 μm syringe filter

4.2.3 Minimum Amount of Polymer

To establish the minimal amount of polymer required to sequester all of the rhodium in a reaction, an array of reactions were prepared containing different amounts of polymer ranging from 0 to 4 equivalents of phosphine in the polymer relative to rhodium. A control reaction, without added polymer, was filtered and analyzed in an analogous procedure. In this case, simple filtration through a 0.22 μm syringe filter give a residue with 3190 ppm of rhodium, which equates to 43% metal removal (Table 5, Entry 3). This percentage was calculated based on the amount of rhodium that was added to the reaction

(1.0 mol%, 5608 ppm). Addition of a 1/10 an equivalent of polymer to rhodium reduced the amount of rhodium remaining in the liquid phase to 586 ppm (Table 5, Entry 4). The minimum amount of rhodium present in the reaction with 4 equivalents of polymer gave a final value of 26 ppm (Table 5, Entry 7). This value is 2 orders of magnitude smaller than that of the control reaction with no polymer added. This indicates that the polymer is adsorbing the metal present in the reaction and being removed upon filtration.

4.3 References

(1) Guterman, R.; Rabiee Kenaree, A.; Gilroy, J. B.; Gillies, E. R.; Ragogna, P. *J. Chem. Mater.* **2015**, *27*, 1412–1419.

(2) Whitesides, G. M.; Hackett, M.; Brainard, R. L.; Lavalleye, J. P. M.; Sowinski, A. F.; Izumi, A. N.; Moore, S. S.; Brown, D. W.; Staudts, E. M. *Organometallics* **1985**, *4*, 2569–2579.

(3) Catalytic conditions adapted from (a) Fu, G. C.; Littke, A. F. *Angew. Chem. Int. Ed. Engl.* **1998**, *2*, 3387–3388. (b) Buchwald, S. L.; Old, D. W.; Wolfe, J. P. *Angew. Chem. Int. Ed.* **1998**, 9722–9723. (c) Kudo, N.; Perseghini, M.; Fu, G. C. *Angew. Chem. Int. Ed.* **2006**, *45*, 1282–1284. (d) Littke, A. F.; Dai, C.; Fu, G. C. *J. Am. Chem. Soc.* **2000**, 4020–4028.

(4) Zalesskiy, S. S.; Ananikov, V. P. *Organometallics* **2012**, *31*, 2302–2309.

Chapter 5

5 Conclusions and Future Directions

5.1 Deactivation of [Ru(Cp)($P^{tBu}_2N^{Bn}_2$)MeCN][PF_6] in the Catalytic anti-Markovnikov Hydration of Alkynes

Catalytic hydration of terminal alkynes has been attempted using [Ru(Cp)($P^{tBu}_2N^{Bn}_2$)MeCN][PF_6], **1**, as the catalyst; however, no consumption of starting material or conversion to product was observed in different reaction conditions. A new ruthenium compound [Ru(Cp)($P^{tBu}_2N^{Bn}_2$)(-C=CHC_6H_5)][PF_6], **2**, has been synthesized and characterized by X-Ray crystallography, MALDI-MS, ^{1}H, $^{13}C\{^{1}H\}$, and $^{31}P\{^{1}H\}$ NMR spectroscopy. Reactivity studies have shown that [Ru(Cp)($P^{tBu}_2N^{Bn}_2$)(-C=CHC_6H_5)][PF_6], **2**, is stable to air, nucleophiles, acid, and heat. It is characterized as a deactivation species and is likely formed due to the lack of steric protection of the pendant base. Future work will be explored with bulkier substituents on the pendant amine to help prevent deactivation. These bulkier variants will include the [Ru(Cp)($P^{tBu}_2N^{tBu}_2$)MeCN][PF_6] and [Ru(Cp)($P^{tBu}_2N^{Ph}_2$)MeCN][PF_6] complexes because both the tBu and Ph groups would provide more protection than the Bn variant. However, due to the steric limitation at the base there are only a few possible variants that can be examined limiting the overall applicability of these catalysts in the anti-Markovnikov hydration of alkynes.

5.2 [Ru(Cp)($P^{tBu}_2N^{Bn}_2$)MeCN][PF_6] as a Catalyst for the Cyclization of Alkynyl Alcohols

[Ru(Cp)($P^{tBu}_2N^{Bn}_2$)MeCN][PF_6], **1**, has been shown to successfully catalyze the cyclization of 2-ethynylbenzyl alcohol. Optimal conditions have been established for the cyclization of 2-ethynylbenzyl alcohol with a maximum yield of 82% at a catalyst loading of 5 mol%. Catalysis still occurs when the loading is dropped to 1 mol%. Future directions for this work include screening other variants of the catalyst and to establish the substrate scope. These other variants include both the bulkier

[Ru(Cp)($P^{tBu}_2N^{tBu}_2$)MeCN][PF_6] and [Ru(Cp)($P^{tBu}_2N^{Ph}_2$)MeCN][PF_6] complexes. Using [Ru(Cp)($P^{Me}_2N^{Bn}_2$)MeCN][PF_6] and [Ru(Cp)($P^{Ph}_2N^{Bn}_2$)MeCN][PF_6] the effect of the phosphine's electron donating ability and steric bulk can be assessed. Current work within the group is looking at the effect of the phosphine and pendant amine by assessing catalytic performance with the complexes [Ru(Cp)($P^{Ph}_2N^{Bn}_2$)MeCN][PF_6] and [Ru(Cp)(dppp)MeCN][PF_6]. The substrate scope is being assessed with a variety of electron-donating and withdrawing groups such substrates include: (5-chloro-2-ethynylphenyl)methanol, (2-ethynyl-5-methoxyphenyl)methanol, (2-ethynylphenyl)methanamine, and pent-4-yn-1-ol. If successful, more complex substrates will be assessed in the cyclization reactions. Some of the substrates that have been chosen such as the linear substrate, pent-4-yn-1-ol, are not expected to successfully cyclize. This is to show that the placement of the nucleophile is important and can give insight on the rate-determining step. I have shown that [Ru(Cp)($P^{tBu}_2N^{Bn}_2$)MeCN][PF_6] is a successful catalyst for the cyclization of alkynyl alcohols and that the formation of product is competitive with the deactivation from the pendant amine.

5.3 Palladium Loaded Polymer

The palladium-loaded polymers have been shown to successfully catalyze Suzuki cross-coupling reactions regardless of the palladium source used to load the polymer. However, these polymers leech palladium at the high temperatures required for catalysis making them undesirable for this application. Future work will investigate other polymer frameworks that may give a metal binding site that permits catalysis without leaching metal. These polymer frameworks can be modified to include more phosphines in the backbone and other atoms that could be capable of binding to a metal. The functionalization of the phosphines in the polymer can also be altered to have either a more or less electron-donating capability. With these changes it may be possible to synthesize a polymer that does not leech palladium and give successful catalytic turnover.

5.4 Metal Scavenging Polymer

The phosphine rich polymer was found to be highly effective at scavenging rhodium in a short period of time. The optimal equivalent of phosphine in the polymer to metal in solution was determined to be 1.5 equivalents. In just 20 minutes 95.8% of rhodium was removed from solution and catalysis was completely halted. Leaving the polymer in solution for 24 hours removed up to 99.8% of the rhodium. This shows that a longer incubation time scavenges more metal from the reaction. Future work will test the scavenging ability of the polymer with other metal catalysts and methods for polymer recycling. The other reactions include ring-closing metathesis (RCM), using the Grubbs 1st generation catalyst, $Ru(=CHPh)(PCy_3)_2Cl_2$, will be assessed. Possible regeneration of the scavenger will be done by stirring spent polymer in pyridine and PMe_3 then following excessive rinsing and drying the polymer will be analyzed by solid state NMR, ICP-MS, and added to a reaction for scavenging. This full analysis should show if the metal was removed by this technique and if the regenerated polymer can scavenge afterwards.

Appendices

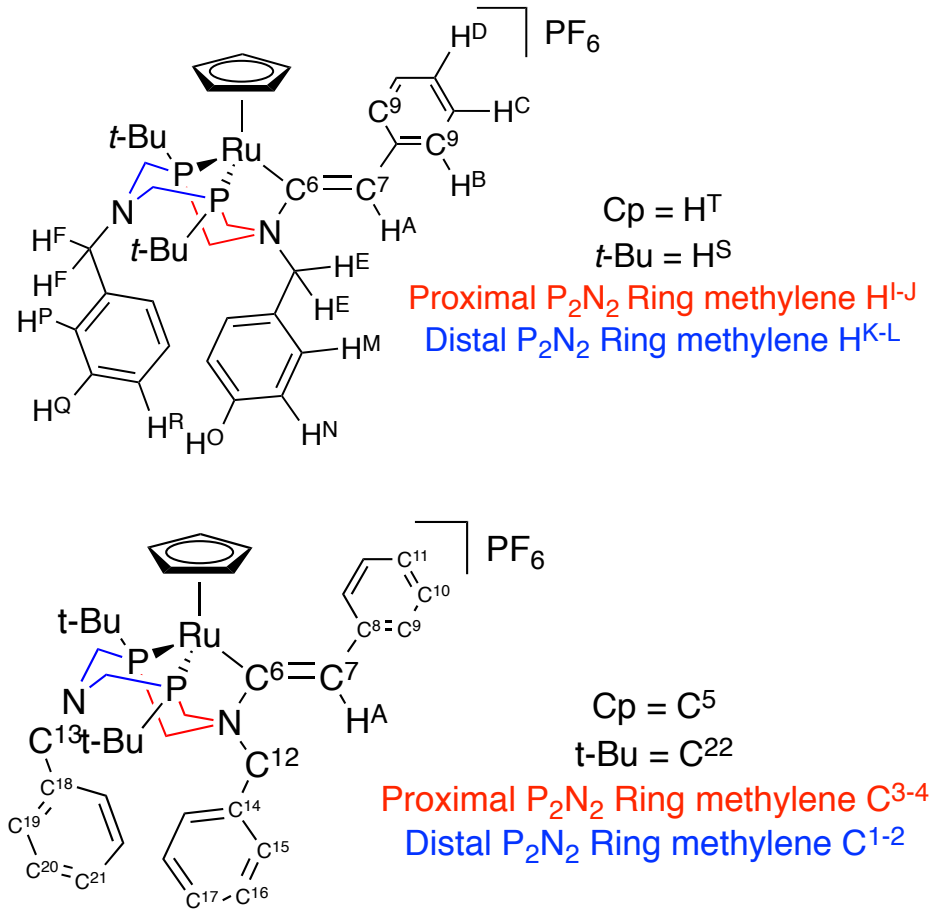

Appendix 1. Full atom labels for complex **2**

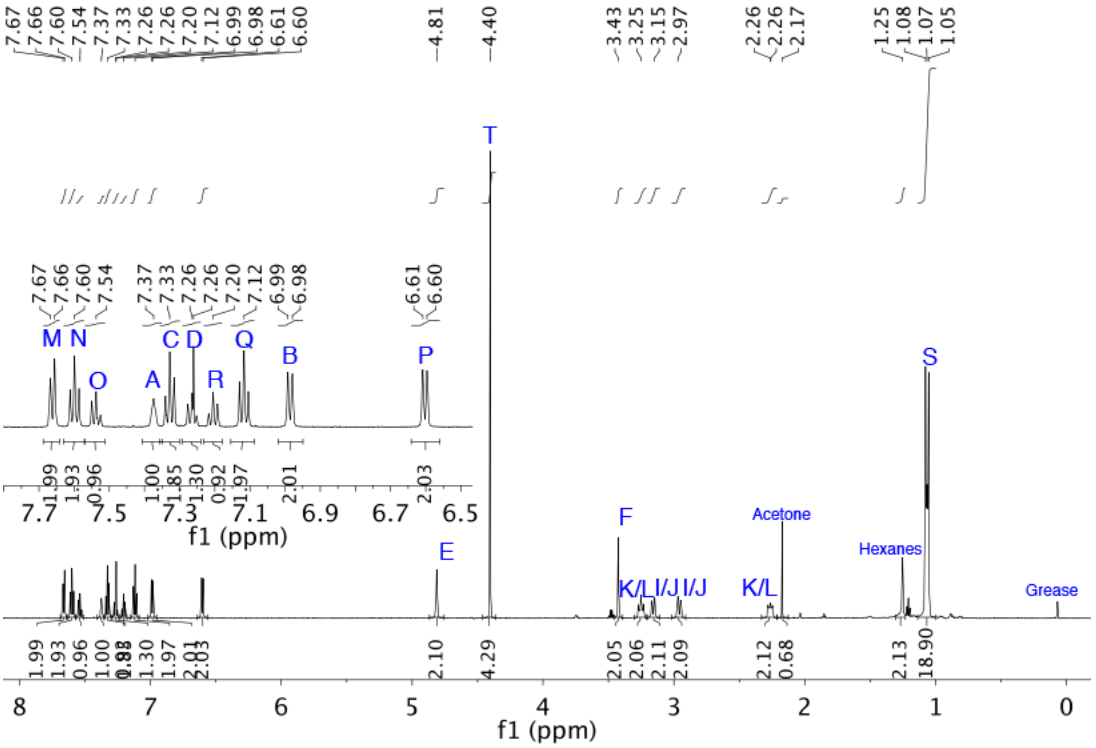

Appendix 2. ^{1}H NMR spectrum of **2** in $CDCl_3$ (600 MHz). See Appendix 1 for proton assignment.

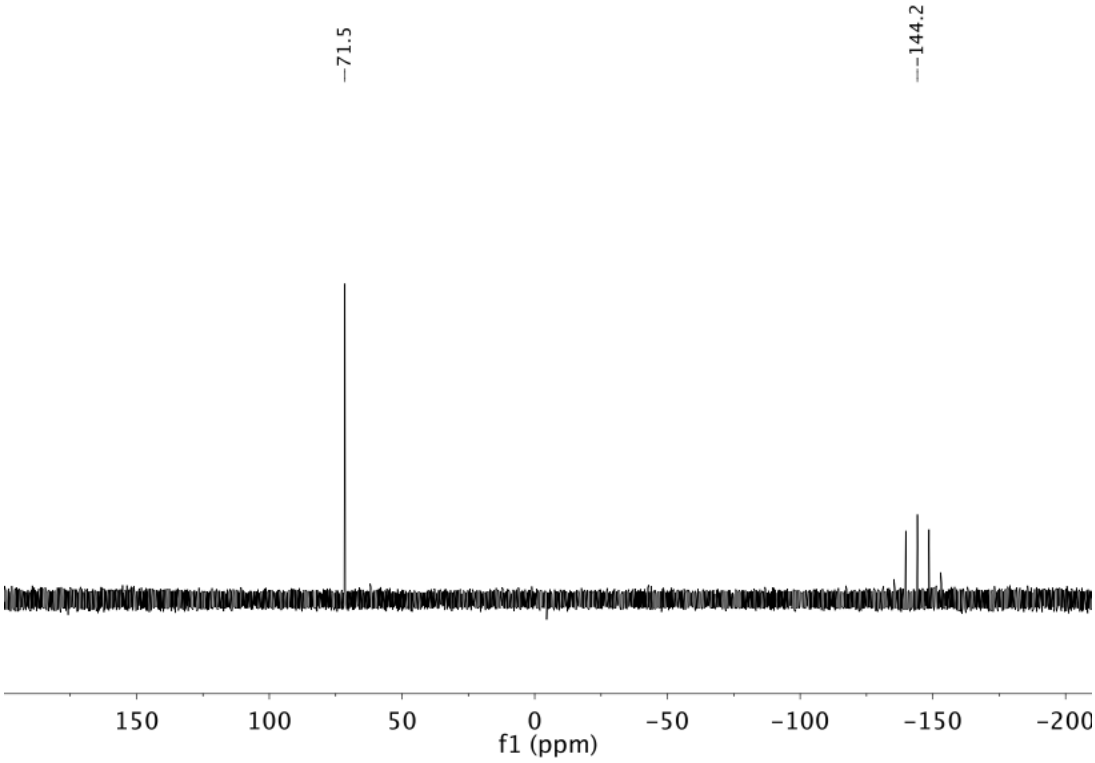

Appendix 3. $^{31}P\{^{1}H\}$ NMR spectrum of **2** in $CDCl_3$ (161.8 MHz)

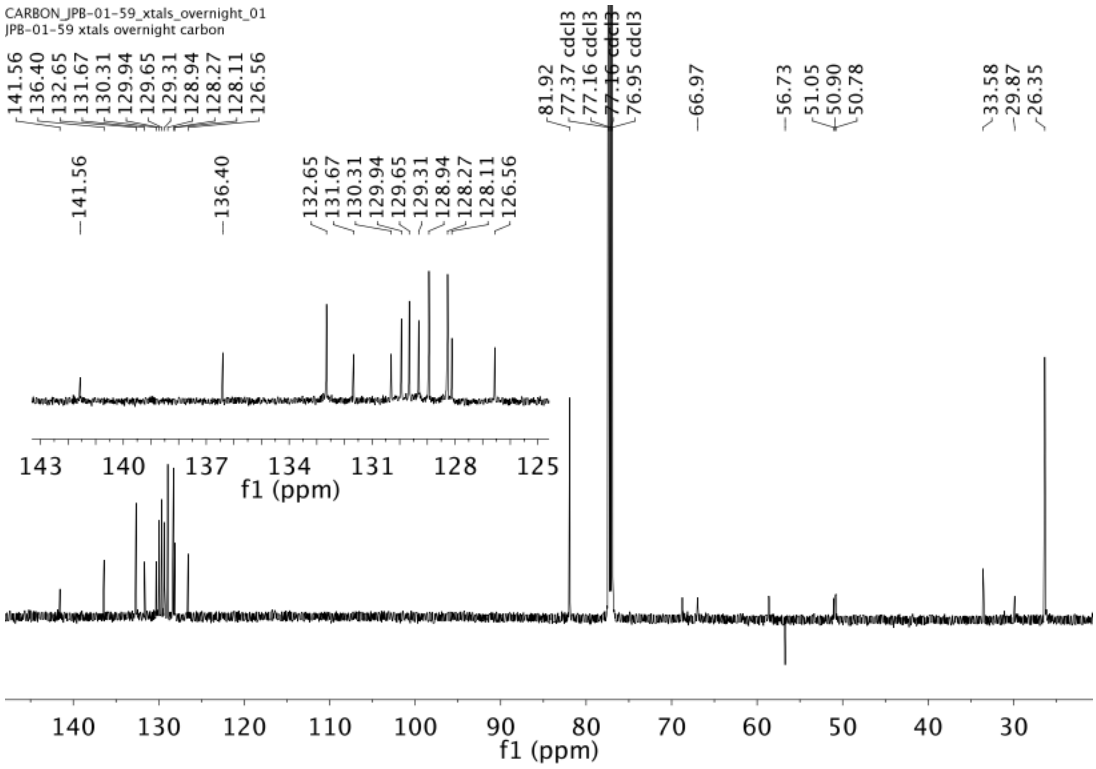

Appendix 4. $^{13}C\{^{1}H\}$ NMR spectrum of **2** in $CDCl_3$ (150.8 MHz)

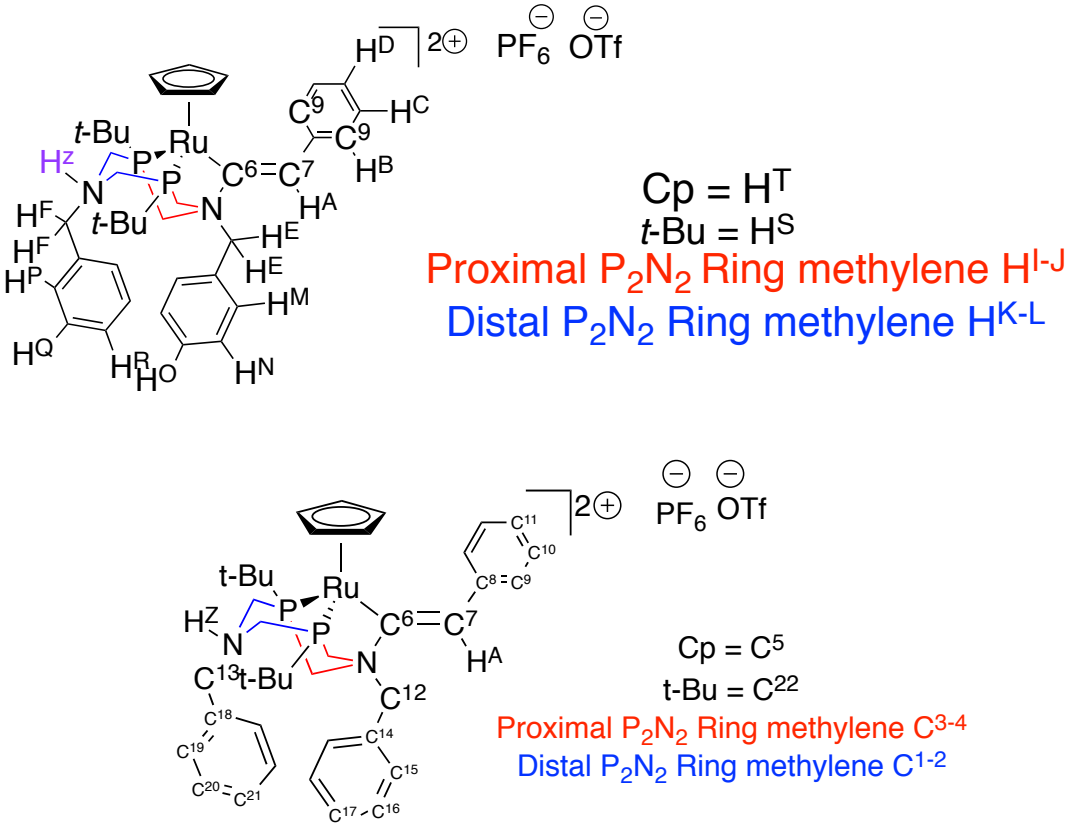

Appendix 5. Full atom labels for complex **3**

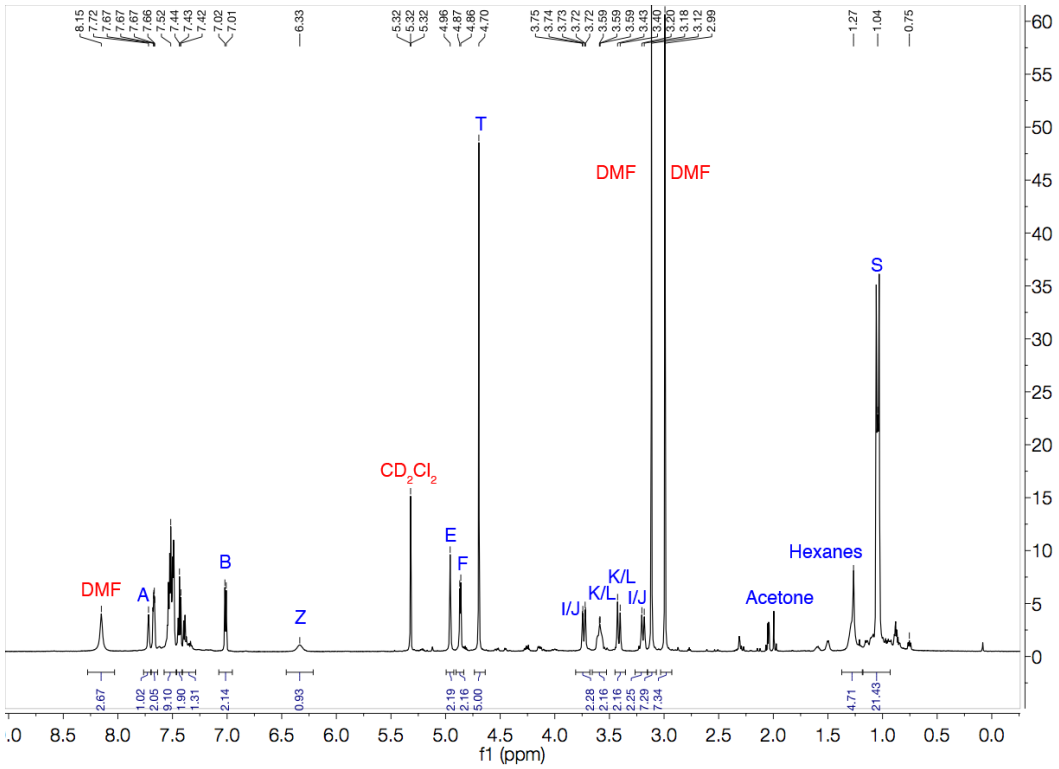

Appendix 6. ^{1}H NMR spectrum of **3** in CD_2Cl_2 (600 MHz). See Appendix 5 for proton assignment.

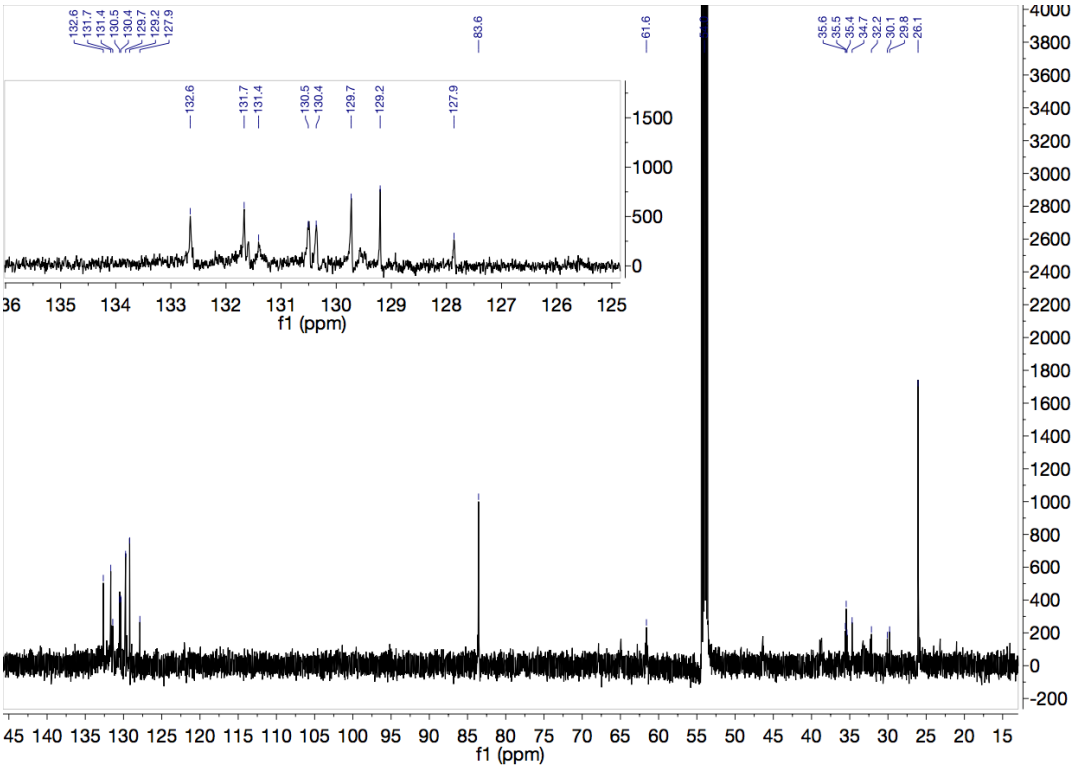

Appendix 7. $^{13}C\{^{1}H\}$ NMR spectrum of **3** in CD_2Cl_2 (150.8 MHz)

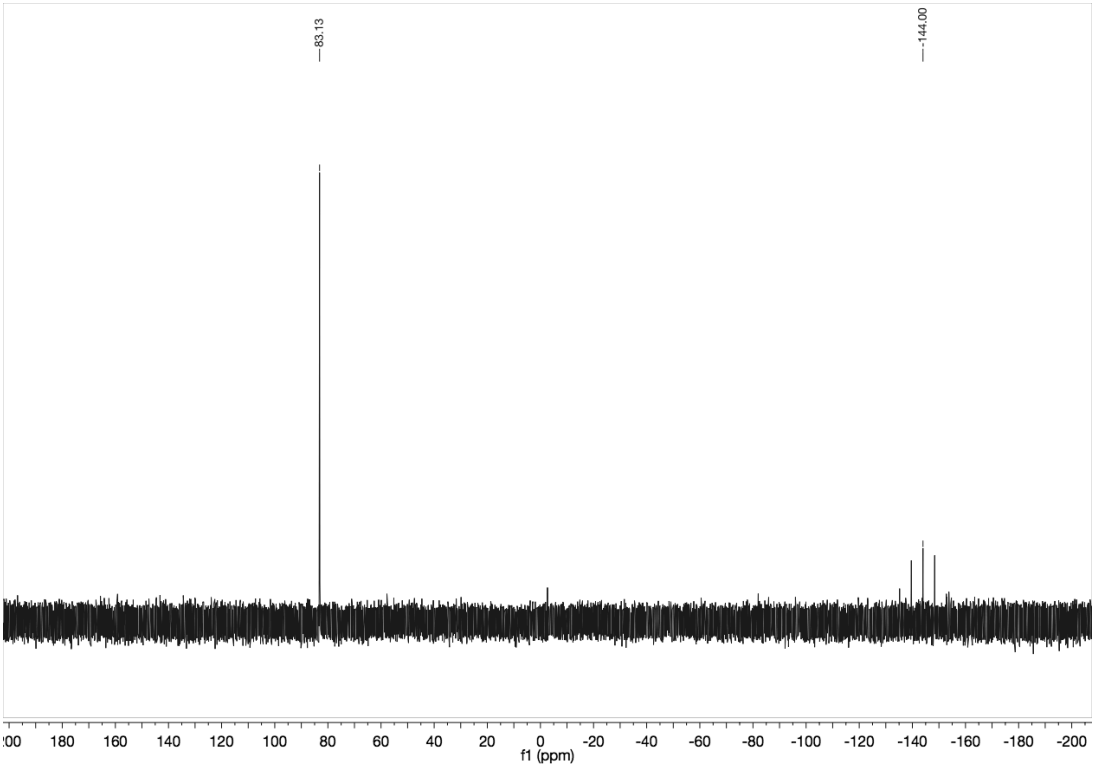

Appendix 8. $^{31}P\{^{1}H\}$ NMR spectrum of **3** in CD_2Cl_2 (161.8 MHz)

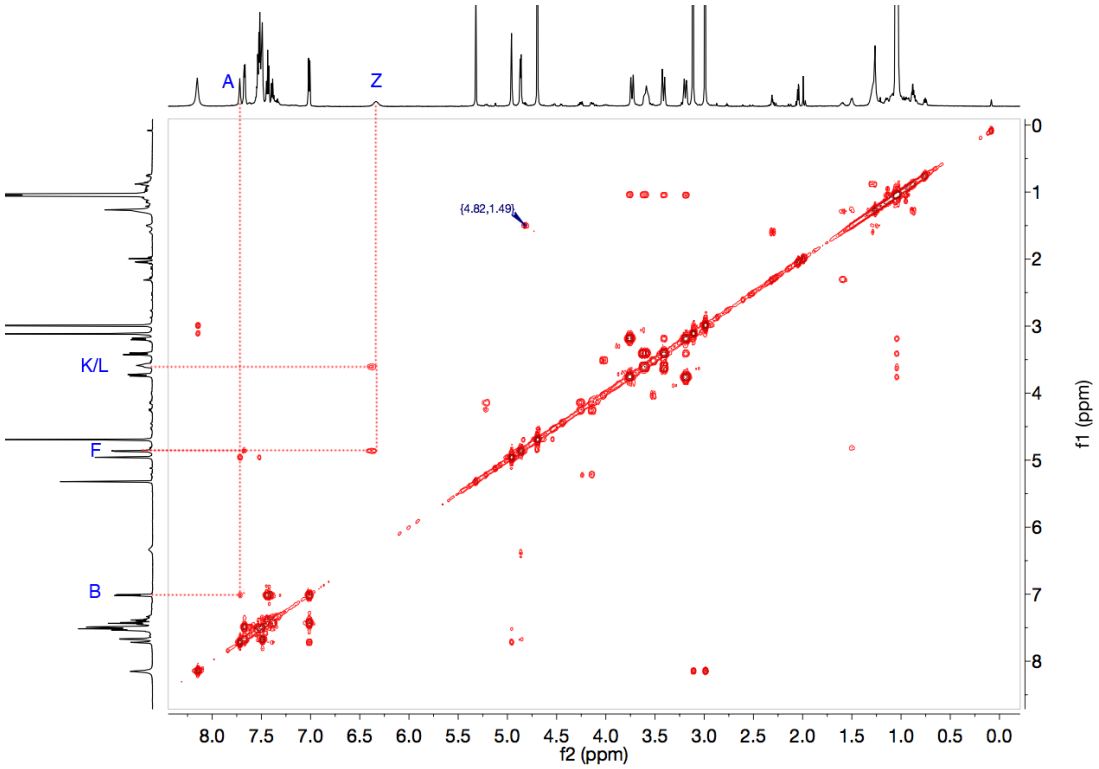

Appendix 9. ^{1}H-^{1}H COSY NMR spectrum of **3** in CD_2Cl_2 (600 MHz). See pg. S4 for proton assignments.

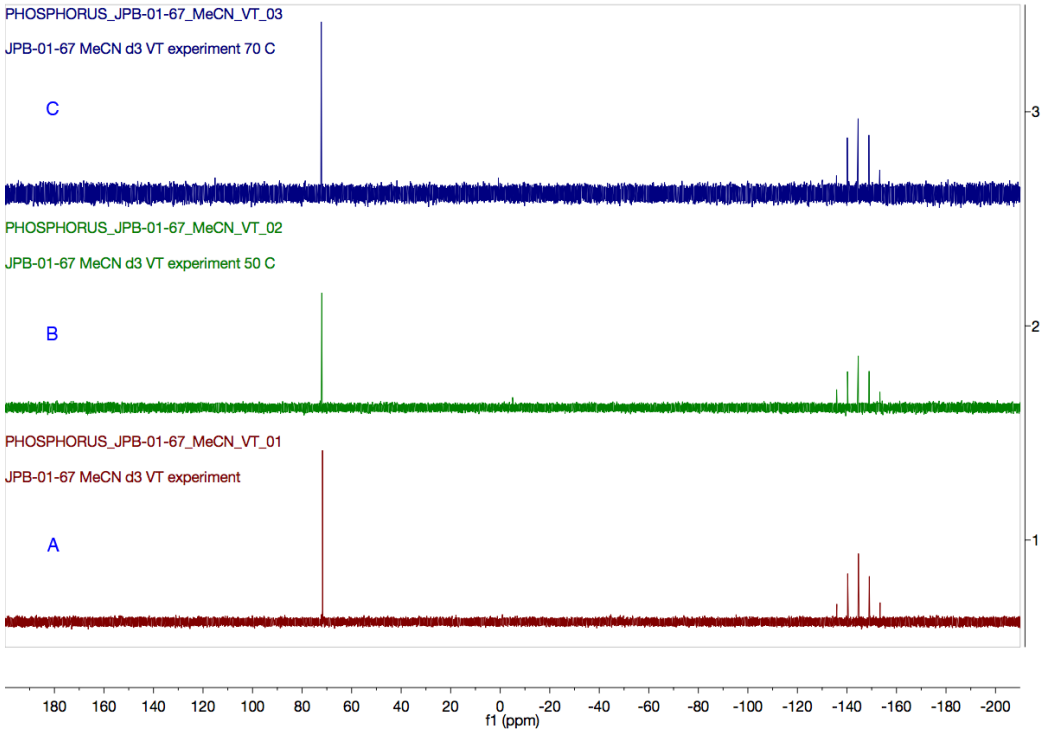

Appendix 10. Variable Temperature $^{31}P\{^{1}H\}$ NMR spectra (161.8 MHz) of **2** in MeCN-d_3 at: A. 25 ˚C, B. 50 ˚C, and C. 70 ˚C

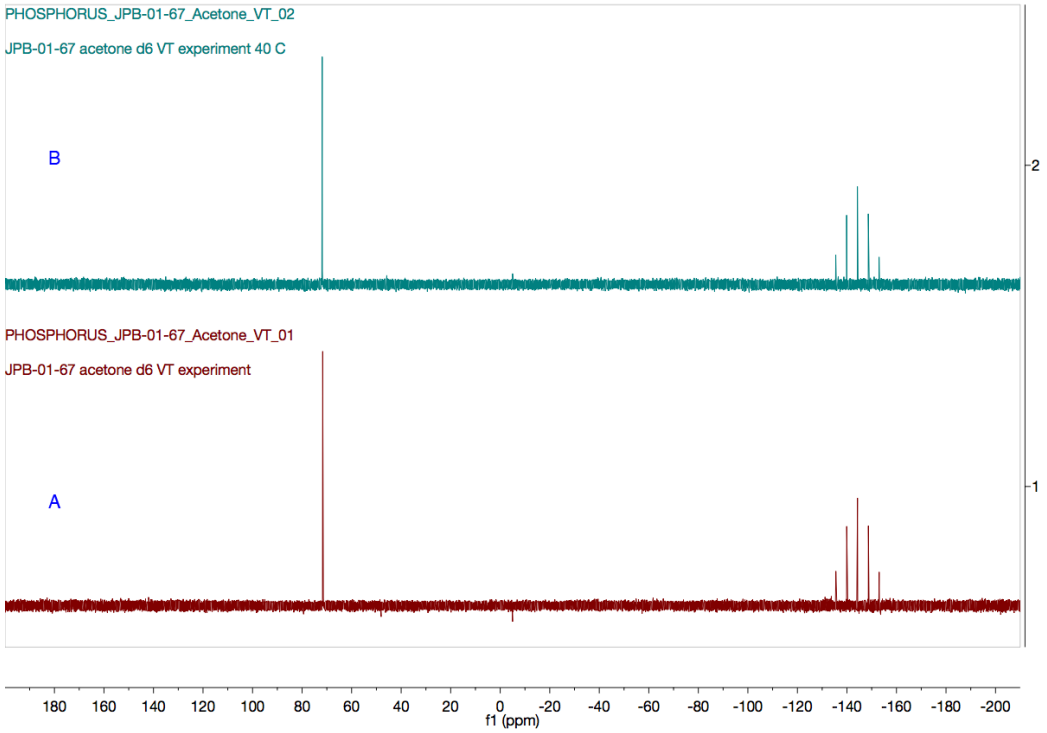

Appendix 11. Variable Temperature $^{31}P\{^{1}H\}$ NMR spectra (161.8 MHz) of **2** in Acetone-d_6 at: A. 25 ˚C and B. 40 ˚C.

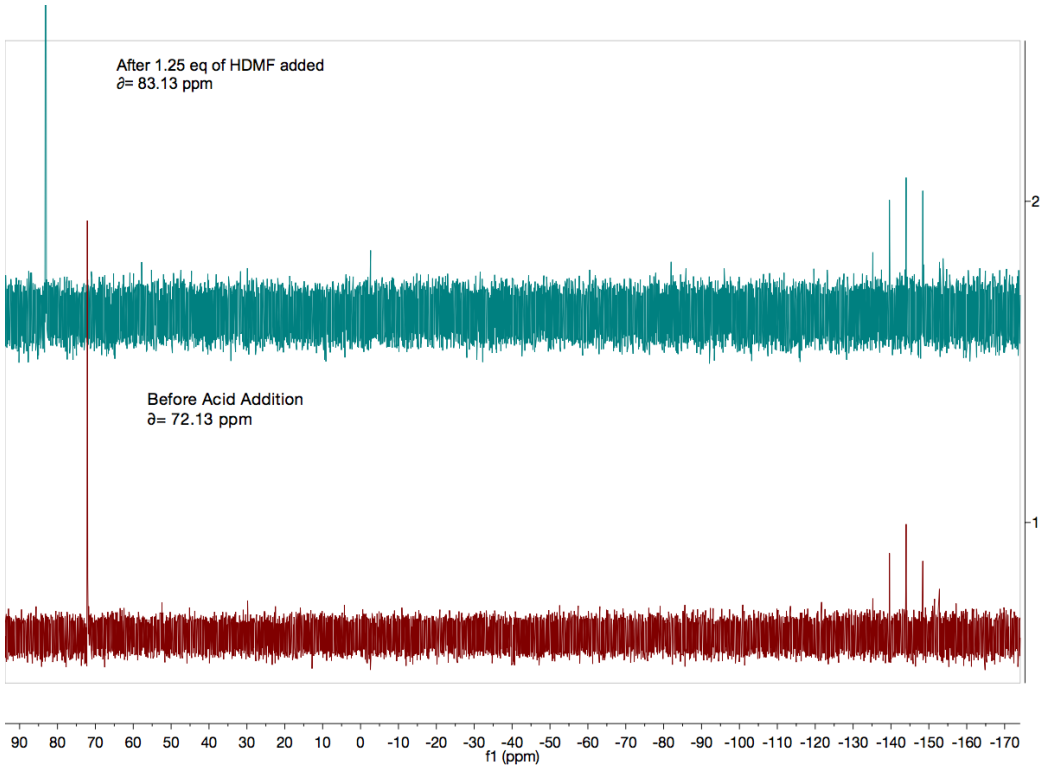

Appendix 12. $^{31}P\{^{1}H\}$ NMR spectra (161.8 MHz), of **2** in CD_2Cl_2 (bottom) and **2** with 1.25 equiv. [HDMF][OTf] in CD_2Cl_2 (top).

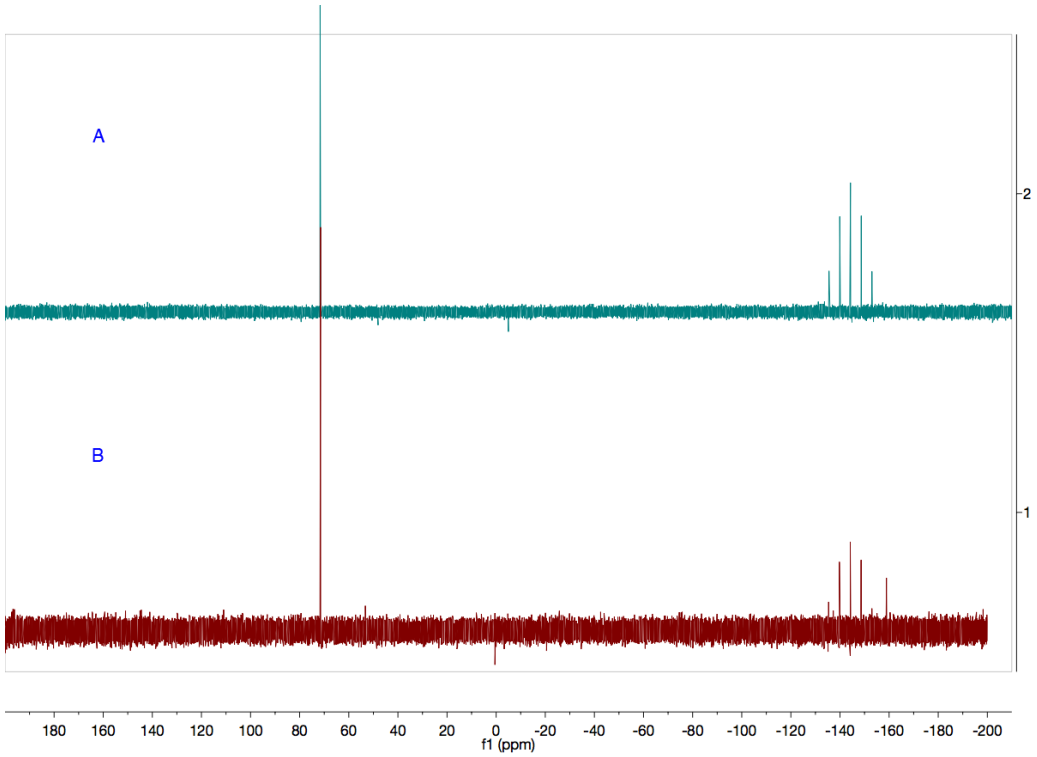

Appendix 13. $^{31}P\{^{1}H\}$ NMR spectra (161.8 MHz) of: A. **2** in $CDCl_3$ and B. **2** + vinylmagnesium bromide in $CDCl_3$

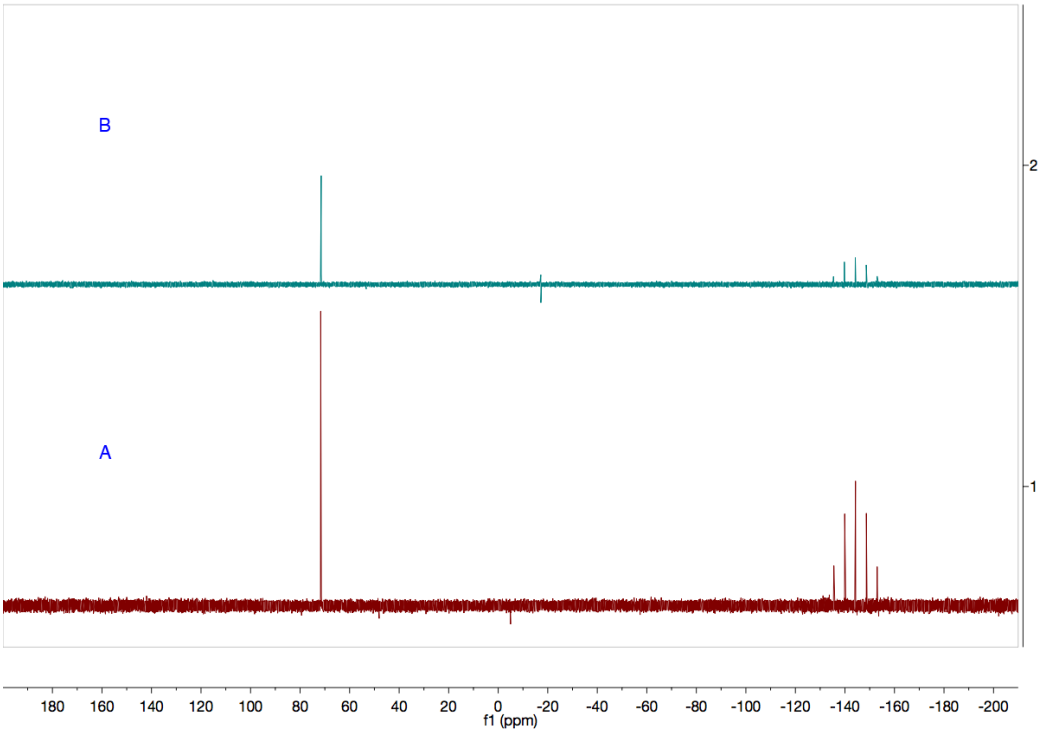

Appendix 14. $^{31}P\{^{1}H\}$ NMR spectra (161.8 MHz) of: A. **2** in $CDCl_3$ and B. **2** + H_2O in $CDCl_3$

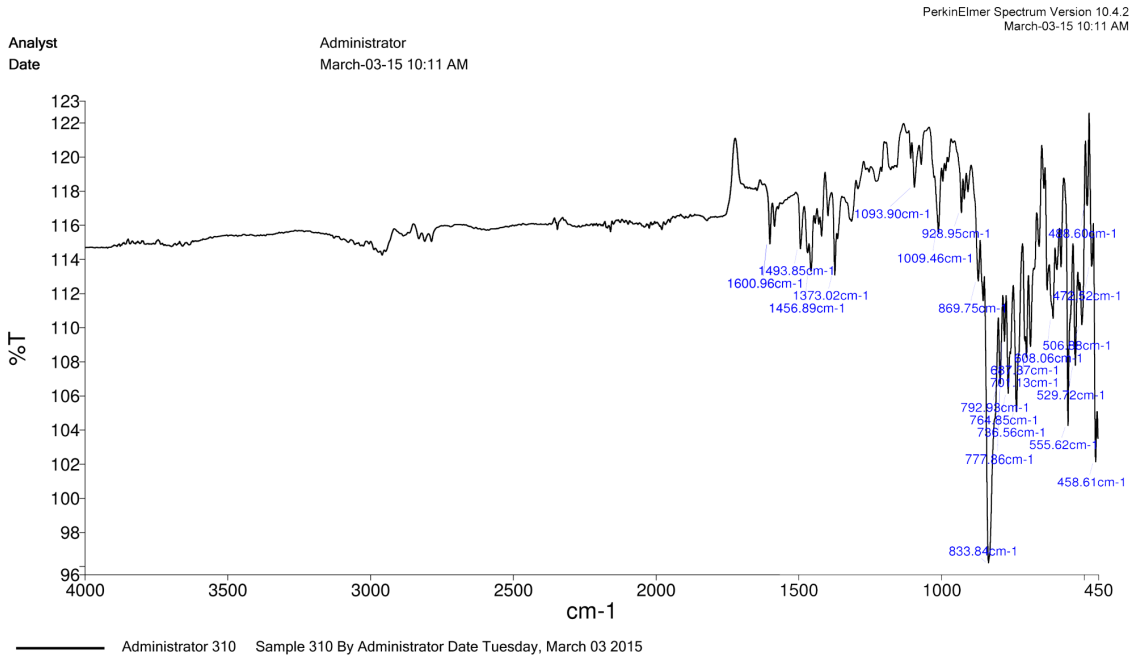

Appendix 15. IR spectrum of solid **2** collected with a PerkinElmer FT-IR Spectrum Two spectrometer with UATR Two attachment

Crystallographic Details for **2**:

Data Collection and Processing. The sample was mounted on a Mitegen polyimide micromount with a small amount of Paratone N oil. All X-ray measurements were made on a Bruker Kappa Axis Apex2 diffractometer at a temperature of 110 K. The unit cell dimensions were determined from a symmetry constrained fit of 9737 reflections with $5.18° < 2\theta < 69.64°$. The data collection strategy was a number of ω and φ scans, which collected data up to 80.826° (2θ). The frame integration was performed using SAINT.[1] The resulting raw data was scaled and absorption corrected using a multi-scan averaging of symmetry equivalent data using SADABS.[2]

Structure Solution and Refinement. The structure was solved by using a dual space methodology using the SHELXT program.[3] All non-hydrogen atoms were obtained from the initial solution. The hydrogen atoms were introduced at idealized positions and were allowed to ride on the parent atom. The structural model was fit to the data using full

matrix least-squares based on *F2*. The calculated structure factors included corrections for anomalous dispersion from the usual tabulation. The structure was refined using the SHELXL-2014 program from the SHELX suite of crystallographic software.[4] Graphic plots were produced using the NRCVAX program suite.[5] Additional information and other relevant literature references can be found in the reference section of this website (http://xray.chem.uwo.ca).

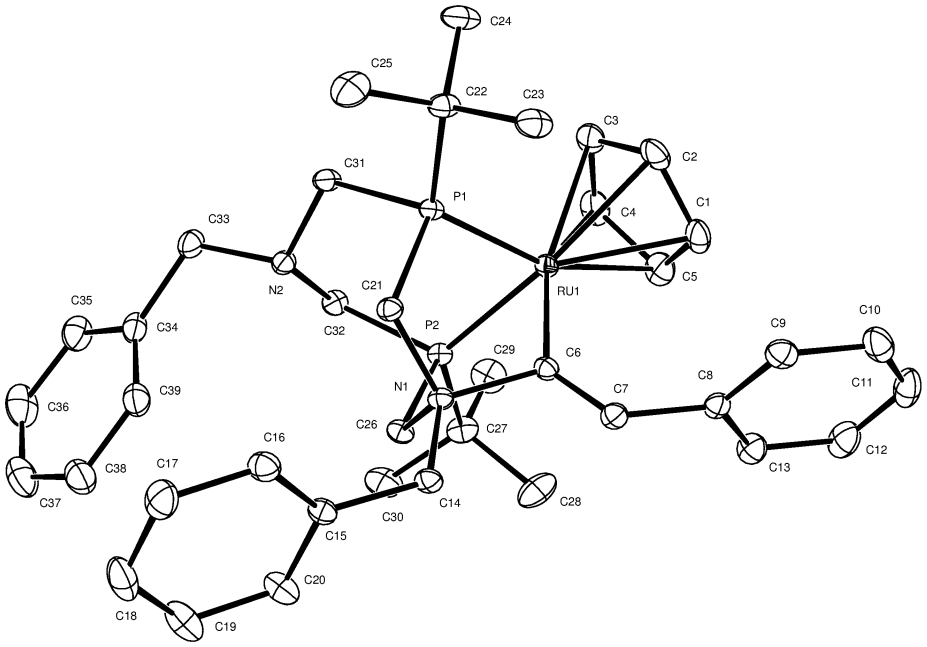

Appendix 16. ORTEP drawing of **2** showing naming and numbering scheme. Ellipsoids are at the 50% probability level and hydrogen atoms and the PF_6^- omitted for clarity

(1) Bruker-AXS, SAINT version 2013.8, **2013**, Bruker-AXS, Madison, WI 53711, USA
(2) Bruker-AXS, SADABS version 2012.1, **2012**, Bruker-AXS, Madison, WI 53711, USA
(3) Sheldrick, G. M., *Acta Cryst.* **2015**, *A71*, 3-8
(4) Sheldrick, G. M., *Acta Cryst.* **2015**, *C71*, 3-8
(5) Bruker-AXS, XP version 2013.1, **2013**, Bruker-AXS, Madison, WI 53711, USA

Appendix 17. Summary of crystal data for **2**

Formula	$C_{39}H_{51}F_6N_2P_3Ru$
CCDC Number	1062815
Formula Weight (*g/mol*)	855.79
Crystal Dimensions (*mm*)	0.267 × 0.225 × 0.083
Crystal Color and Habit	yellow prism
Crystal System	orthorhombic
Space Group	P 21 21 21
Temperature, K	110
a, Å	9.9395(19)
b, Å	15.102(4)
c, Å	25.752(7)
α,°	90
β,°	90
γ,°	90
V, $Å^3$	3865.5(16)
Number of reflections to determine final unit cell	9737
Min and Max 2θ for cell determination, °	5.18, 69.64

Z	4
F(000)	1768
ρ (*g/cm*)	1.471
λ, Å, (MoKα)	0.71073
μ, (cm^{-1})	0.590
Diffractometer Type	Bruker Kappa Axis Apex2
Scan Type(s)	phi and omega scans
Max 2θ for data collection, °	80.826
Measured fraction of data	0.997
Number of reflections measured	187801
Unique reflections measured	22999
R_{merge}	0.0547
Number of reflections included in refinement	22999
Cut off Threshold Expression	$I > 2\sigma(I)$
Structure refined using	full matrix least-squares using F^2
Weighting Scheme	$w=1/[sigma^2(Fo^2)+(0.0286P)^2+0.0322P]$ where $P=(Fo^2+2Fc^2)/3$
Number of parameters in least-squares	467

R_1	0.0346
wR_2	0.0622
R_1 (all data)	0.0498
wR_2 (all data)	0.0662
GOF	1.046
Maximum shift/error	0.005
Min & Max peak heights on final DF Map (*e*-/Å)	-0.545, 0.610

Where:

$R_1 = \Sigma(|F_o| - |F_c|) / \Sigma F_o$

$wR_2 = [\Sigma(w(F_o^2 - F_c^2)^2) / \Sigma(w F_o^4)]^{½}$

GOF = $[\Sigma(w(F_o^2 - F_c^2)^2) / (\text{No. of reflns.} - \text{No. of params.})]^{½}$

Appendix 18. Table of bond lengths for **2**

Ru1-C6	2.0721(16)	C19-C20	1.393(3)
Ru1-P1	2.2303(6)	C19-H19	0.9500
Ru1-P2	2.2315(6)	C20-H20	0.9500
Ru1-C4	2.2426(18)	C21-H21A	0.9900

Ru1-C3	2.2509(18)	C21-H21B	0.9900
Ru1-C5	2.2691(19)	C22-C24	1.528(2)
Ru1-C2	2.2885(18)	C22-C25	1.533(3)
Ru1-C1	2.3014(18)	C22-C23	1.536(2)
P1-C31	1.8450(17)	C23-H23A	0.9800
P1-C21	1.8450(15)	C23-H23B	0.9800
P1-C22	1.8636(17)	C23-H23C	0.9800
P2-C32	1.8488(17)	C24-H24A	0.9800
P2-C26	1.8532(15)	C24-H24B	0.9800
P2-C27	1.8727(17)	C24-H24C	0.9800
N1-C26	1.5077(19)	C25-H25A	0.9800
N1-C21	1.5103(19)	C25-H25B	0.9800
N1-C14	1.5295(19)	C25-H25C	0.9800
N1-C6	1.591(2)	C26-H26A	0.9900
N2-C31	1.461(2)	C26-H26B	0.9900
N2-C32	1.470(2)	C27-C28	1.530(3)
N2-C33	1.472(2)	C27-C30	1.536(3)
C1-C2	1.401(3)	C27-C29	1.537(3)

C1-C5	1.413(3)	C28-H28A	0.9800
C1-H1	0.9500	C28-H28B	0.9800
C2-C3	1.435(3)	C28-H28C	0.9800
C2-H2	0.9500	C29-H29A	0.9800
C3-C4	1.401(3)	C29-H29B	0.9800
C3-H3	0.9500	C29-H29C	0.9800
C4-C5	1.440(3)	C30-H30A	0.9800
C4-H4	0.9500	C30-H30B	0.9800
C5-H5	0.9500	C30-H30C	0.9800
C6-C7	1.340(2)	C31-H31A	0.9900
C7-C8	1.478(2)	C31-H31B	0.9900
C7-H7	0.9500	C32-H32A	0.9900
C8-C13	1.392(2)	C32-H32B	0.9900
C8-C9	1.397(2)	C33-C34	1.510(2)
C9-C10	1.391(3)	C33-H33A	0.9900
C9-H9	0.9500	C33-H33B	0.9900
C10-C11	1.388(3)	C34-C39	1.389(3)
C10-H10	0.9500	C34-C35	1.397(3)

C11-C12	1.384(3)	C35-C36	1.387(3)
C11-H11	0.9500	C35-H35	0.9500
C12-C13	1.391(3)	C36-C37	1.380(3)
C12-H12	0.9500	C36-H36	0.9500
C13-H13	0.9500	C37-C38	1.386(3)
C14-C15	1.506(2)	C37-H37	0.9500
C14-H14A	0.9900	C38-C39	1.389(3)
C14-H14B	0.9900	C38-H38	0.9500
C15-C16	1.393(2)	C39-H39	0.9500
C15-C20	1.396(2)	P3-F6	1.5831(13)
C16-C17	1.394(2)	P3-F2	1.5909(15)
C16-H16	0.9500	P3-F5	1.6028(13)
C17-C18	1.383(3)	P3-F1	1.6057(13)
C17-H17	0.9500	P3-F4	1.6076(13)
C18-C19	1.378(3)	P3-F3	1.6080(14)
C18-H18	0.9500		

Appendix 19. Table of bond angles for **2**

C6-Ru1-P1	80.87(5)	C19-C18-H18	119.9
C6-Ru1-P2	80.38(5)	C17-C18-H18	119.9
P1-Ru1-P2	83.548(19)	C18-C19-C20	120.20(18)
C6-Ru1-C4	152.77(7)	C18-C19-H19	119.9
P1-Ru1-C4	126.35(6)	C20-C19-H19	119.9
P2-Ru1-C4	100.22(6)	C19-C20-C15	120.19(17)
C6-Ru1-C3	154.78(7)	C19-C20-H20	119.9
P1-Ru1-C3	99.01(5)	C15-C20-H20	119.9
P2-Ru1-C3	124.79(5)	N1-C21-P1	108.83(10)
C4-Ru1-C3	36.32(8)	N1-C21-H21A	109.9
C6-Ru1-C5	116.39(7)	P1-C21-H21A	109.9
P1-Ru1-C5	160.10(6)	N1-C21-H21B	109.9
P2-Ru1-C5	108.07(6)	P1-C21-H21B	109.9
C4-Ru1-C5	37.21(7)	H21A-C21-H21B	108.3
C3-Ru1-C5	61.12(7)	C24-C22-C25	109.25(15)
C6-Ru1-C2	118.37(7)	C24-C22-C23	110.30(14)
P1-Ru1-C2	103.63(5)	C25-C22-C23	109.16(15)
P2-Ru1-C2	160.54(5)	C24-C22-P1	107.91(12)

C4-Ru1-C2	60.86(7)	C25-C22-P1	111.63(12)
C3-Ru1-C2	36.84(7)	C23-C22-P1	108.57(11)
C5-Ru1-C2	60.36(8)	C22-C23-H23A	109.5
C6-Ru1-C1	101.95(7)	C22-C23-H23B	109.5
P1-Ru1-C1	135.17(6)	H23A-C23-H23B	109.5
P2-Ru1-C1	141.27(6)	C22-C23-H23C	109.5
C4-Ru1-C1	60.68(7)	H23A-C23-H23C	109.5
C3-Ru1-C1	60.41(7)	H23B-C23-H23C	109.5
C5-Ru1-C1	36.02(7)	C22-C24-H24A	109.5
C2-Ru1-C1	35.55(7)	C22-C24-H24B	109.5
C31-P1-C21	102.67(8)	H24A-C24-H24B	109.5
C31-P1-C22	103.25(7)	C22-C24-H24C	109.5
C21-P1-C22	102.87(7)	H24A-C24-H24C	109.5
C31-P1-Ru1	116.16(6)	H24B-C24-H24C	109.5
C21-P1-Ru1	105.88(5)	C22-C25-H25A	109.5
C22-P1-Ru1	123.44(6)	C22-C25-H25B	109.5
C32-P2-C26	100.67(7)	H25A-C25-H25B	109.5
C32-P2-C27	103.21(8)	C22-C25-H25C	109.5

C26-P2-C27	103.83(7)	H25A-C25-H25C	109.5
C32-P2-Ru1	117.89(5)	H25B-C25-H25C	109.5
C26-P2-Ru1	105.67(5)	N1-C26-P2	108.63(9)
C27-P2-Ru1	122.62(6)	N1-C26-H26A	110.0
C26-N1-C21	111.67(11)	P2-C26-H26A	110.0
C26-N1-C14	108.96(11)	N1-C26-H26B	110.0
C21-N1-C14	108.34(11)	P2-C26-H26B	110.0
C26-N1-C6	105.42(11)	H26A-C26-H26B	108.3
C21-N1-C6	106.64(11)	C28-C27-C30	109.88(16)
C14-N1-C6	115.84(12)	C28-C27-C29	108.89(16)
C31-N2-C32	113.26(13)	C30-C27-C29	109.09(15)
C31-N2-C33	111.06(13)	C28-C27-P2	108.51(12)
C32-N2-C33	110.34(13)	C30-C27-P2	111.77(12)
C2-C1-C5	108.99(17)	C29-C27-P2	108.64(12)
C2-C1-Ru1	71.72(10)	C27-C28-H28A	109.5
C5-C1-Ru1	70.74(10)	C27-C28-H28B	109.5
C2-C1-H1	125.5	H28A-C28-H28B	109.5
C5-C1-H1	125.5	C27-C28-H28C	109.5

Ru1-C1-H1	123.6	H28A-C28-H28C	109.5
C1-C2-C3	107.72(17)	H28B-C28-H28C	109.5
C1-C2-Ru1	72.73(10)	C27-C29-H29A	109.5
C3-C2-Ru1	70.16(10)	C27-C29-H29B	109.5
C1-C2-H2	126.1	H29A-C29-H29B	109.5
C3-C2-H2	126.1	C27-C29-H29C	109.5
Ru1-C2-H2	122.7	H29A-C29-H29C	109.5
C4-C3-C2	108.08(17)	H29B-C29-H29C	109.5
C4-C3-Ru1	71.52(10)	C27-C30-H30A	109.5
C2-C3-Ru1	73.00(10)	C27-C30-H30B	109.5
C4-C3-H3	126.0	H30A-C30-H30B	109.5
C2-C3-H3	126.0	C27-C30-H30C	109.5
Ru1-C3-H3	121.3	H30A-C30-H30C	109.5
C3-C4-C5	108.03(18)	H30B-C30-H30C	109.5
C3-C4-Ru1	72.16(11)	N2-C31-P1	110.69(11)
C5-C4-Ru1	72.39(11)	N2-C31-H31A	109.5
C3-C4-H4	126.0	P1-C31-H31A	109.5
C5-C4-H4	126.0	N2-C31-H31B	109.5

Ru1-C4-H4	121.2	P1-C31-H31B	109.5
C1-C5-C4	107.18(19)	H31A-C31-H31B	108.1
C1-C5-Ru1	73.24(11)	N2-C32-P2	111.96(10)
C4-C5-Ru1	70.40(12)	N2-C32-H32A	109.2
C1-C5-H5	126.4	P2-C32-H32A	109.2
C4-C5-H5	126.4	N2-C32-H32B	109.2
Ru1-C5-H5	121.7	P2-C32-H32B	109.2
C7-C6-N1	113.35(13)	H32A-C32-H32B	107.9
C7-C6-Ru1	135.02(12)	N2-C33-C34	112.93(14)
N1-C6-Ru1	111.56(10)	N2-C33-H33A	109.0
C6-C7-C8	123.40(14)	C34-C33-H33A	109.0
C6-C7-H7	118.3	N2-C33-H33B	109.0
C8-C7-H7	118.3	C34-C33-H33B	109.0
C13-C8-C9	118.74(16)	H33A-C33-H33B	107.8
C13-C8-C7	120.34(15)	C39-C34-C35	118.75(17)
C9-C8-C7	120.88(15)	C39-C34-C33	121.04(16)
C10-C9-C8	120.39(16)	C35-C34-C33	120.12(17)
C10-C9-H9	119.8	C36-C35-C34	120.5(2)

C8-C9-H9	119.8	C36-C35-H35	119.7
C11-C10-C9	120.26(17)	C34-C35-H35	119.7
C11-C10-H10	119.9	C37-C36-C35	120.0(2)
C9-C10-H10	119.9	C37-C36-H36	120.0
C12-C11-C10	119.67(17)	C35-C36-H36	120.0
C12-C11-H11	120.2	C36-C37-C38	120.30(19)
C10-C11-H11	120.2	C36-C37-H37	119.9
C11-C12-C13	120.18(17)	C38-C37-H37	119.9
C11-C12-H12	119.9	C37-C38-C39	119.6(2)
C13-C12-H12	119.9	C37-C38-H38	120.2
C12-C13-C8	120.68(17)	C39-C38-H38	120.2
C12-C13-H13	119.7	C38-C39-C34	120.82(18)
C8-C13-H13	119.7	C38-C39-H39	119.6
C15-C14-N1	115.10(13)	C34-C39-H39	119.6
C15-C14-H14A	108.5	F6-P3-F2	91.15(8)
N1-C14-H14A	108.5	F6-P3-F5	90.86(8)
C15-C14-H14B	108.5	F2-P3-F5	90.53(8)
N1-C14-H14B	108.5	F6-P3-F1	90.52(7)

H14A-C14-H14B	107.5	F2-P3-F1	90.06(8)
C16-C15-C20	119.13(15)	F5-P3-F1	178.48(8)
C16-C15-C14	120.58(15)	F6-P3-F4	178.56(9)
C20-C15-C14	120.10(15)	F2-P3-F4	90.27(8)
C15-C16-C17	120.17(16)	F5-P3-F4	88.87(7)
C15-C16-H16	119.9	F1-P3-F4	89.73(7)
C17-C16-H16	119.9	F6-P3-F3	89.29(8)
C18-C17-C16	120.15(17)	F2-P3-F3	179.41(9)
C18-C17-H17	119.9	F5-P3-F3	89.86(7)
C16-C17-H17	119.9	F1-P3-F3	89.54(7)
C19-C18-C17	120.12(17)	F4-P3-F3	89.29(8)

Curriculum Vitae

Education

University of Western Ontario, Department of Chemistry 2013-2015

London, Ontario, Canada

Masters of Science in Chemistry Supervisor: Johanna M. Blacquiere

Metal-Ligand Cooperative Catalysis and Methods for Metal Removal from Organic Transformations

Dalhousie University, Faculty of Science 2010-2013

Halifax, Nova Scotia, Canada

Bachelor of Science, Major in Chemistry Supervisor: Mark Stradiotto

Design of New N-Heterocyclic Carbene/Phosphine Ligands for use in Palladium-Catalyzed Cross-Coupling Reactions

University of British Columbia, Faculty of Science 2008-2010

Kelowna, British Columbia, Canada

Transferred to Dalhousie University

Publications

2. "Substrate-Mediated Deactivation of a Cooperative $P^{tBu}{}_2N^{Bn}{}_2$ Complex", **John-Paul J. Bow**, Paul D. Boyle, Johanna M. Blacquiere*, *European Journal of Inorganic Chemistry*, Accepted, **2015**.

1. "New Phosphine-Functionalized NHC Ligands: Discovery of an Effective Catalyst for the Room-Temperature Amination of Aryl Chlorides with Primary and Secondary Amines", Craig A. Wheaton, **John-Paul J. Bow**, and Mark Stradiotto*, *Organometallics*, *32*, **2013**, 6148-6161.

Presentations

4. *"Deactivation of a Vinylidene Intermediate by the Cooperative Ligand* $P^{tBu}{}_2N^{Bn}{}_2$*"* (Poster), **John-Paul J. Bow**, Johanna M. Blacquiere, Canadian Chemistry Conference, Ottawa, ON, June 13-17, 2015

3. *"Investigations into the Cooperative Nature of [CpRu($P^R_2N^{R'}_2$)(NCMe)]$^+$ Complexes"* (Poster), James M. Stubbs, John-Paul J. Bow, and Johanna M. Blacquiere, Interdisciplinary Research Showcase, London, ON, December 2, 2014.

2. *"Investigations into the Cooperative Nature of [CpRu($P^R_2N^{R'}_2$)(NCMe)]$^+$ Complexes"* (Poster), James M. Stubbs, John-Paul J. Bow, and Johanna M. Blacquiere. Inorganic Discussion Weekend, Montreal, QC, November 14-16, 2014.

1. "*Design of New NHC/Phosphine Ligands for use in Palladium-Catalyzed Cross-Coupling Reactions*" (Poster), **John-Paul J. Bow**, Craig A. Wheaton, and Mark Stradiotto, Atlantic Inorganic Discussion Weekend, Moncton, New Brunswick, March 22-23, 2013.

Awards

1. CSC 1st Place Inorganic Poster Presentation Award (2015)

Related Experience

Head Laboratory Teaching Assistant

Inorganic Chemistry of the Main Group Elements, Chem 2281, *University of Western Ontario,* Jan 2015-April 2015

Laboratory Teaching Assistant

Transition Metal Chemistry, Chem 3371, *University of Western Ontario*, Sept 2013-Dec 2013 and Sept 2014-Dec 2014.

Inorganic Chemistry of the Main Group Elements, Chem 2281, *University of Western Ontario,* Jan 2014-April 2014

Discover Chemistry Days Demonstrator, *Dalhousie University*, May 2013

Volunteer

Peer Mentor, Dalhousie Peer Partnership Program, *Dalhousie University*, 2012-2013.